Starch Modification for Sustainable and Functional Material Applications

by

Ewomazino Constance Ojogbo

A thesis

presented to the University of Waterloo

in fulfilment of the

thesis requirement for the degree of

Master of Applied Science

in

Chemical Engineering

Waterloo, Ontario, Canada, 2019

Author's Declaration

This thesis consists of materials all of which I authored or co-authored: see Statement of Contributions included in the thesis. This is a true copy of the thesis, including any required final revisions, as accepted by my examiners.

I understand that my thesis may be made electronically available to the public.

Statement of Contributions

Chapter 2 of this thesis has incorporated a literature review paper that I co-authored with a post-doctoral fellow, Dr. Ogunsona, and my supervisor, Prof. Mekonnen. I wrote the introduction and modification of starch. Dr. Ogunsona wrote on the advanced functional applications of starch, while Dr Mekonnen provided overall guidance and review of the paper.

Chapter 3 consists of a paper that I co-authored with an undergraduate co-op student, Rachel Blanchard and my supervisor, Prof. Mekonnen. I designed and conducted the experiments and wrote most of the paper. Rachel assisted with designing and running some experiments and result analysis.

Chapter 4 contains results that is currently submitted for peer-reviewed publication. I co-authored this paper with Prof. Valerie Ward, and my supervisor Prof. Mekonnen. I carried out the lab experiments, analyzed the data, and wrote the paper. Prof. Ward provided me with guidance and training and supplied the facility for antimicrobial testing.

Abstract

Among biodegradable polymers, starch has attracted significant interest and is currently used in numerous industrial applications. This is because of its renewability, biodegradability, abundance, and cohesive film-forming properties. Moreover, the hydroxyl (-OH) groups associated with the anhydroglucose units provide it with several modification possibilities. These features resulted in a substantial interest for its use in several advanced functional material applications in addition to the typical consumer plastic applications. This thesis focuses on modification of starch for functional material applications where starch is used as one of or the major constituent.

The goal is to create polymeric materials based on starch and targeted two material applications: Hydrophobic and melt processable starch esters for possible degradable plastic applications, and antimicrobial polymer surfaces for packaging and biomedical devices where starch is used as the major constituent. The use this biodegradable polymer could potentially complement and replace non-degradable polymers obtained from fossil fuels such as polyethylene and polypropylene. However, its hydrophilicity, limitations in thermal and mechanical properties, rapid degradability, and strong intra- and intermolecular hydrogen bonding in the polymer chains limit its melt processability and subsequently its widespread commercial application as a renewable polymer. It is therefore necessary to modify it to mitigate these limitations and bring about other desirable properties.

To achieve this goal, a controlled modification of starch to replace the -OH moieties was carried out using reagents that target the required applications. The extent of modification which is tunable is estimated based on the degree of substitution or percent grating efficiency. Based on this, the effect of modification can be analyzed using different techniques. In the first study, an

esterification of starch using an activated fatty acid (lauroyl chloride) was carried out in a controlled reaction conditions. An analysis of the modified starch esters revealed melt processable and thermoplastic starch with film forming properties. This implied that the esterified starch could be used in industrial thermoplastic and melt-processable applications without the use of external plasticizers or modifiers.

In a second modification, a systematic study was carried out to investigate the antimicrobial efficacy of starch as an antimicrobial carrier to prevent the leaching out of the antimicrobial agent, to create antimicrobial surfaces for packaging and biomedical surfaces applications. Antimicrobial properties were introduced on starch by grafting with the biocide, polyhexamethylene guanidine hydrochloride, in a two-step homogenous reaction process. The modified starch was then incorporated into PLA films at various concentration and the antimicrobial efficacy is evaluated by testing against a Gram positive bacterium, *Bacillus subtilis* and a Gram negative bacterium, *Escherichia coli* using a shaking flask method and an agar plate assay. The results revealed that the polymer surfaces have high antimicrobial potency and deactivate or reduce the growth rate of bacteria on contact. This material has great potential for use on surfaces requiring minimal to no bacterial contamination such as medical devices and food packaging applications.

Acknowledgements

I would like to thank my supervisor, Prof. Tizazu Mekonnen for his unwavering support, guidance and encouragement throughout my master's program. Thank you for motivating me and always steering me in the right direction as regards my career and personal growth.

I would like to appreciate Prof. Valerie Ward for opening her laboratory to me to perform some experiments, for technical support, and collaboration.

My sincere gratitude goes to my friends Christine Lewis, Ogheneovo Idolor, and Bassey Michael and every member of the Mekonnen Lab team for their friendship, support, encouragement and the memories we created.

My deepest appreciation goes to my family without whose support I wouldn't be where I am today. Thanks for encouraging, motivating, and loving me unconditionally. You have made me confident in my abilities and give me reasons to be a better version of myself. I wish to thank My son Somto Ojogbo for being such a sweet little boy and cooperating when mummy had to work.

Finally, I want to thank Jehovah God for life, good health, grace, and mercies; and the holy spirit for teaching me all things.

Table of Contents

List of Figures

List of Tables

List of Abbreviations

AGU	Anhydroglucose unit
AMS	Antimicrobial starch
CFU	Colony forming unit
DMA	Dynamic mechanical analysis
DMSO	Dimethyl sulpooxide
DS	Degree of substitution
DSC	Differential scanning calorimetry
EA	Elemental Analysis
FA	Fatty acid
IPDI	Isophorone diisocyanate
Kbr	Potassium bromide
NMR	Nuclear magnetic resonance
PC	Positive control
PHGH	Polyhexamethylene guanidine hydrochloride
PLA	Poly lactic acid
SEM	Scanning electron microscopy
Tg	Glass transition temperature
TGA	Thermo gravimetric analysis
TPS	Thermoplastic starch
UV	Ultra violet
XRD	X-ray diffractometry

Chapter 1. Introduction, Objectives, Motivation and Outline

1.1. Introduction and Motivation

Biodegradable polymers obtained from renewable natural resources have recently been receiving increasing attention due to their potential as alternatives to traditional petroleum-based plastics. Among the various sources, polysaccharides stand out as a highly convenient feedstock because they are readily available, renewable, inexpensive and provide great stereochemical diversity. Starch, a renewable polysaccharide polymer, has attracted a lot of attention as a feedstock due to its melt processability after plasticization, renewability, biodegradability, low cost, and abundance of –OH leaving it open to a number of modification possibilities. However, its hydrophilicity, limitations in thermal and mechanical properties, too rapid degradability, and strong intra– and intermolecular hydrogen bonding in the polymer chains limit its melt processability and subsequently its widespread commercial application as a renewable polymer.

In order to use starch as a feedstock for applications, it is necessary to modify it to mitigate these limitations and bring about other desirable properties. The rich –OH groups on the structure of starch allows chemical modification and changes the polymer structure and properties, which can be investigated using different analytical techniques. Starch based polymers are a potential substitute to fossil fuel-based polymers because of the low cost, abundance, renewability and biodegradability. For instance, it is envisaged that using starch as a feedstock for plastics and food packaging applications can reduce the problem caused by plastics pollution. As a result, it is important to modify starch accordingly for material applications.

1.2. Objectives and Motivation

The objective of this thesis was to modify starch for use as a feedstock for material applications. Two modifications were carried out and the properties of the modified material evaluated for specific applications. This was carried out according to the following steps.

Hydrophobic and melt processable starch laurate esters

- The first step was to modify starch using the selected fatty acid in a controlled esterification process. Our target was to replace the hydroxyl groups in starch to instill hydrophobicity and melt processability in the material. The degree of substitution was then evaluated.
- The next step was to analyze the properties of the modified starch and evaluate how the degree of substitution affected the material properties. The changes in morphology, network thermal stability, hydrophobicity, solubility profile, and thermal transition events were studied. The hydrophobicity and melt processability were most important amongst other properties due to their importance for plastics applications. At the end of this stage, the minimum degree of substitution required for the application was established.

Functionalized microparticles for antimicrobial surfaces

- Here, the selected antimicrobial agent was grafted on the backbone of starch. The target was to use starch as a carrier of antimicrobial properties, which can be blended or used as a filler with other polymers for antimicrobial surface applications such as food packaging materials and biomedical devices.
- Polymer films made for the modified starch-polymer blend were then tested against bacteria to elucidate the antimicrobial performance and establish the minimum

concentration of modified starch to inhibit the growth of bacteria. At the end of this study, the minimum inhibitory concentration to prevent the growth of bacteria was established.

- Due to the low molecular weight of PHGH, it has been reported to leach out of polymer systems. Attaching it to the backbone of high molecular weight starch and using the modified starch with other polymers systems can prevent leaching.

A summary of the discussed research objectives and stages are shown in Figure 1-1.

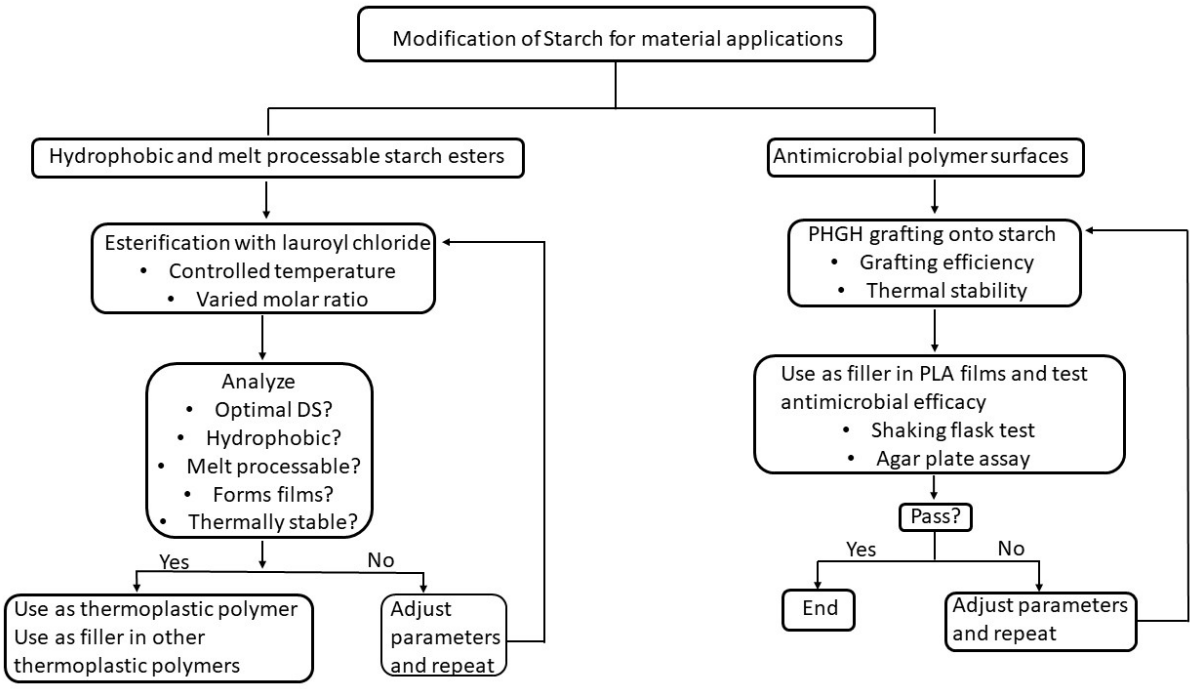

Figure 0.1. Overall research goals and objectives

1.3. Thesis Outline

This thesis is presented in 5 chapters as described below:

The first chapter is an introduction of this work. It covers the motivation, research objectives and outline.

The second chapter provides detailed background and literature review. It discusses the physical and chemical properties of starch, modification types and application of starch and its derivatives for functional applications.

The third chapter investigates a facile, one-step hydrophobic esterification of starch and structure-property correlations of the modified starch for melt-processable applications. It presents a short introduction into the topic, materials and experimental methods, experimental results and discussion, and concluding remarks.

The fourth chapter investigates functionalized starch microparticles for antimicrobial surfaces. It presents a short introduction into the topic, materials and experimental methods, experimental results and discussion, and concluding remarks.

Chapter 5 presents the overall thesis conclusions and recommendations for future work.

Chapter 2. Literature Review: Modification of starch for renewable polymer and advanced material applications[1]

2.1. Introduction

Polymers are key materials to mitigate society challenges in the areas of transportation, construction, consumer plastics (e.g. packaging, shopping bags, and cutlery), architectural and industrial coatings, sustainable energy generation, clean water and defense and security. The continuously increasing demand for polymers driven by global population growth, and concerns associated with environmental pollution from solid polymers (e.g. consumer plastics), and the threat of global warming related to the production of polymer feedstock necessitates the development of sustainable and innovative strategies for the polymer industry [1,2]. The use of biomass such as plant fibers, biopolymers produced from natural resources or microorganisms is being explored in numerous applications and across industries [3–5]. While there are some successes in some niche application markets, renewable polymers that are currently produced at a large scale often are costly and have inferior performance compared to their petroleum-derived counterparts.

Among the natural materials, starch is one of the least expensive polysaccharides with a huge potential for solid plastic and other functional polymer applications. Starch, the focus of this work, is a polysaccharide synthesized by plants and found mainly in cereals, roots tubers, fruits and legumes in the range of 25-90% [6,7]. It is a semi-crystalline polymer comprised of about 1,000-2,000,000 anhydroglucose units (AGU) linked by α-1,4 glycosidic bonds[8]. The AGU units in the starch chain have three reactive hydroxyl groups, in most cases one primary and two

[1] A version of this chapter has been published. E. Ogunsona, E. Ojogbo, T. Mekonnen, Advanced material applications of starch and its derivatives, Eur. Polym. J. 108 (2018) 570–581. doi:10.1016/j.eurpolymj.2018.09.039.

secondary hydroxyl groups making it amenable to various modification chemistries. Several review articles and books have been published on the physical properties, chemical structures, characteristics, and modification of starch [9–11]. Thus, this review will selectively focus on the recent progress in the application of starch as a feedstock for advanced and functional material applications of starch.

2.1.1. Starch as a renewable material feedstock

A starch granule is synthesized via the polymerization of glucose that is produced via photosynthesis of carbon dioxide in plants. It is mainly used as food and finds use in a variety of industrial applications [12]. The major industrial use of starch besides food is as a composition in adhesives and paper binders, textiles, chemical production, a feedstock for fermentation and other industrial products [13]. The interest in starch for use in advanced materials applications is accrued from its widespread geographic distribution from various plants, low cost, and abundance. Starch as a macromolecule is also appealing because of its physical, chemical and functional properties such as ease of water dissolution, water retention properties, gelatinization, pasting behavior when subjected to temperature and ease of modification to optimize functional properties [14]. Unfortunately, the hydrophilic nature of starch alongside its brittleness, retrogradation and thermal degradation has limited its extensive use for industrial polymer applications that require mechanical integrity. Therefore, in most cases, the functional group of starch, i.e -OH group, is modified to mitigate the aforementioned limitations and obtain desirable properties for its success in industrial materials application.

Native starch granule is composed of amylose, a linear glucose chain attached by α-1,4 glucosidase bond, and amylopectin, a branched glucose chain with branching at α-1,6 postition[6]. Many studies have shown that the amylose-amylopectin ratio affects the functionality and chemical properties

of starch as a biopolymer [8,14]. Table 2.1 shows various botanical sources of starch and the amylose-amylopectin ratio.

Table 0.1. Botanical sources of starch and their corresponding amylose/amylopevctin ratio, and crystallinity

Source	Crystallinity (%)	Amylose (%)	Amylopectin (%)	Reference
Rice	38[15]	20-30	80-70	[16]
Potato	23-53[15]	23-31	77-69	[17]
Cassava	31-59[18]	16-25	84-75	[19]
Waxy cassava	N/A	0	100	[19]
Wheat	36-39[15]	30	70	[16]
Corn	43-48[15]	28	72	[20]
Sorghum	22-28[21]	24-27	76-73	[22]

The structure and composition of starch are responsible for both its physical and chemical properties. The ratio of amylose to amylopectin and the overall structure of starch varies based on the botanical sources, growing climate conditions, geographic location for cultivation and soil type[17]. Starch has A, B and C crystal structures, which is a function of its origin. In general, it has a small granule size and comes in various shapes based on the source[6]. The granule is composed of anhydroglucose units linked by α-1,4 glycosidic bonds to form amylose and amylopectin polymer entities. Amylose is a linear polymer with α-1,4 glycosidic bonds linking the anhydroglucose units with an average molecular weight of 1 x 10^6 g/mol. It accounts for the amorphous structure in the starch granule. Amylopectin, on the other hand, has a higher molecular weight averaging about 1 x 10^8 g/mol and linked by short α-1,4 glycosidic bonds with high branching at the α-1,6 positions that account for the crystallinity in starch[6,23]. The branching of amylopectin polymer creates double helix of approximately 5nm length in the starch granule that aligns in the crystalline region[24]. The crystalline region is represented by double helices as shown in Figure 2.1.

X-ray diffraction of the macroscopic view of starch under illuminated light showed a positive birefringence indicated by a maltese cross, demonstrating an arrangement of the macromolecular units represented by a helix in the starch morphology, which disappears upon disruption of the starch granule[8]. This interchanging arrangement of amorphous and crystalline lamellae in the starch granule is responsible for the semi-crystalline nature of starch with a crystallinity ranging from 20 to 45%[24].

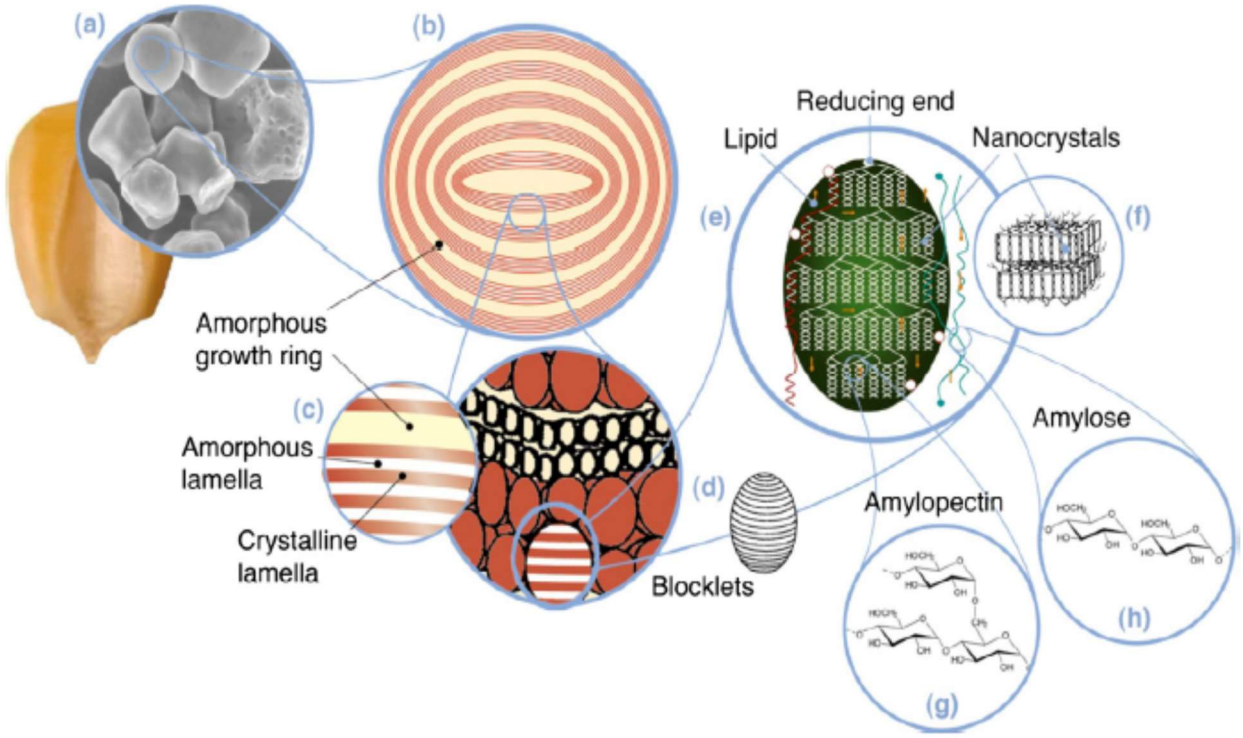

Figure 0.1. Representation of starch structure (a) Corn starch granules (30 µm), (b) semicrystalline and amorphous starch growth rings (120–500 nm), (c) crystalline and amorphous lamellae (9 nm), (d) growth rings and blocklets internal structures (20–50 nm), (e) Double helices of amylopectin, (f) starch nanocrystals or called crystalline lamellae when starch nanocrystal is prodced via acid hydrolysis, (g) molecular structure of amylopectin (0.1- 1 nm), (h) molecular structure of amylose (0.1–1 nm). Adapted from Le Corre *et al* [25]. Elsevier copyright © 2014.

Another important component found in starch is phosphorus, a non-carbohydrate component. Phosphorus exists as monoesters of phosphate and phospholipids. Its presence in the starch granule

influences the gel strength, lucidity and solubility depending on the macro-polymer with which it bonds[6].

2.2. Modifications of starch

Native starch is hydrophilic in nature, insoluble in water at room temperature, and suffers from retrogradation. Furthermore, it cannot be melt-processed as it degrades under relatively low temperature and lacks mechanical integrity. These shortcomings have limited its use for polymer applications requiring mechanical strength and thermal stability, especially in the plastic industry where starch needs to be melt processed in most cases. Also, the poor solubility of starch in cold water limits its potential application as an additive in some applications such as enhanced oil recovery (EOR) and drilling fluid additives. Thus, starch modification is desirable not only to mitigate these challenges but also to bring about other functional properties. Some of the properties that can be achieved via starch modification include thermal stability, hydrophobicity, amphiphilicity, paste clarity, mechanical strength, freeze-thaw stability retrogradation resistances amongst others [26–31]. Several starch modification processes are reported in literature including, physical processes [32,33], chemical modifications [34–37], enzymatic [38–40], and biotechnological approaches [16] or combinations.

2.2.1. Chemical Modifications

Chemical modification of starch is an important modification route that involves the blocking or introduction of functional groups to impart desirable physical and chemical properties while maintaining chain integrity, thereby extending its application. Because of the intrinsic advantage of an abundance of hydroxyl groups on the structure of starch, different chemical modifications have been studied, including etherification [41–43], oxidation [34,44,45], acetylation [28,46–48], esterification

[49–52], polymer grafting [53–55], crosslinking [56,57], silyation [58–60], hydrolysis [61–63] etc. A combination of physical and chemical modifications can also be conducted. The physicochemical properties that can be modified include gelatinization, retrogradation, viscosity and pasting properties, thermal stability, solubility, hydrophilicity, and compositions. The extent of modification depends on the crystallinity of starch, amylose to amylopectin ratio, reaction conditions, and molecular distribution of starch [64]. Some of the common chemical modification of starch as applied to material application are reviewed in the following sections.

2.3. Starch and its Derivatives for Advanced Functional Applications

2.3.1. Application of Starch in Self-Healing Polymeric Materials

Hard and brittle polymers and their composites such as thermosets fail catastrophically when cracks develop and grow in their structure. Rapid failure occurs as the crack grows and propagates through the polymer leaving it with the inability to transfer stress efficiently. Elastomers and very low modulus phases can be introduced into the polymer to tackle this problem; they can absorb, deflect or stop these cracks from further propagation when introduced in very small and well dispersed phases[65,66]. However, the inclusion of this type of phase typically deteriorates the mechanical properties of the polymer such as the tensile and flexural strengths and moduli. Mitigating this problem without diminishing the physical properties of the polymer has led to the development of self-healing polymers. Self-healing polymers typically contain hard crosslinked formaldehyde-based microcapsules shells which are well dispersed within them[67]. This is carried out to allow the microcapsules survive the process of dispersion within the polymer phase without rupture. These microcapsules usually contain highly reactive liquids (healant) such as epoxies, glycidyl methacrylate (GMA) and isocyanates. These liquids, typically monomers can readily react with multiple functional groups on polymer chains because of the presence of reactive groups on

their chains. The self-healing mechanism occurs when the microcracks within the polymer propagate, meet and, rupture one or multiple microcapsules containing the healant. The healant flows into the cracks, bridges the gaps and crosslinks over time depending on its surrounding temperature and the type of crosslinking agent present within the polymer phase. Figure 2.2A shows a schematic of the mechanism by which self-healing polymers repair microcracks.

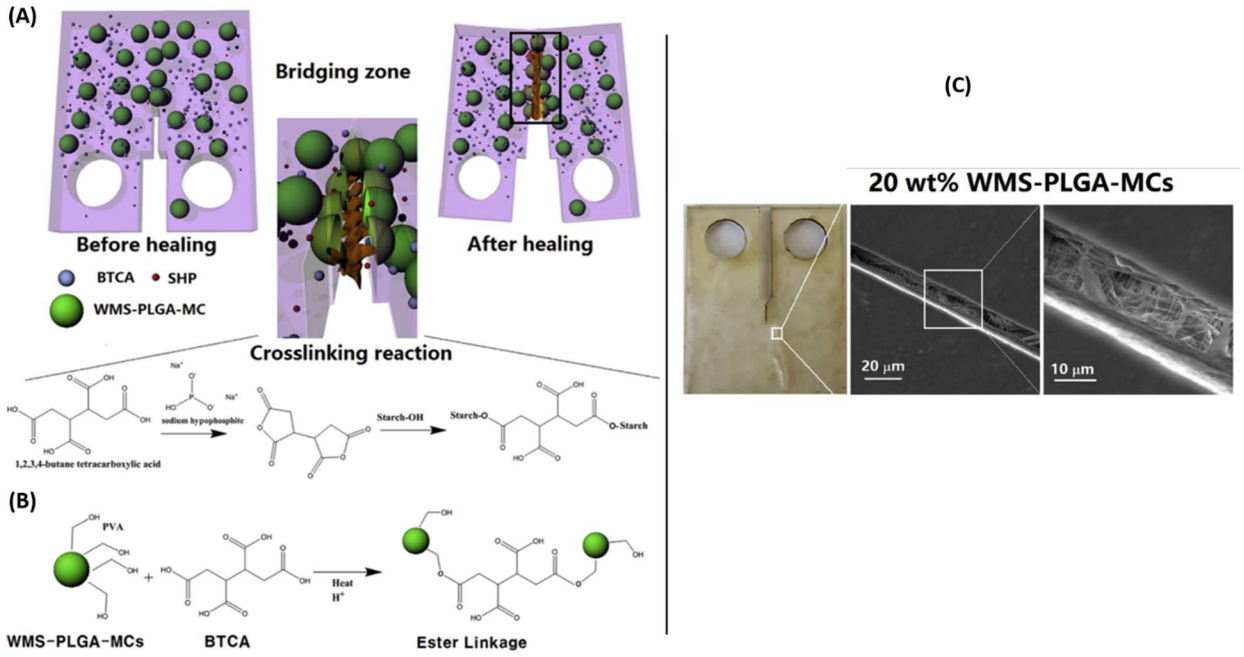

Figure 0.2 . Schematic representing (A) typical mechanism in self-healing polymer with specific reference to start as healant in WMS resin and (B) the esterification reaction occurring between BTCA and WMS. (C) Morphology of WMS resin revealing self-healed WMS resin after fracture with ligaments of crosslinking WMS as healant. Adapted from Kim *et al*.[68]. Elsevier copyright © 2017.

Most self-healing polymers and their healants are petroleum based. However, the utilization of biobased derivatives as healants in polymers have been developed[68,69]. However, only one study has utilized starch as healant in self-healing polymers to the best of our knowledge. Waxy maize starch (WMS) otherwise known as waxy corn starch was used both as the healant and polymer[68]. The WMS was gelatinized to activate the hydroxyl groups on the starch and then encapsulated

with poly(d,1-lactide-co-glycolide) (PLGA) by double emulsion solvent evaporation technique. These microcapsules were then incorporated into gelatinized WMS alongside butanetetracarboxylic acid (BTCA) and sodium hypophosphite monohydrate (SHP) as cross-linking agent and catalyst respectively, then cast into a mold to produce sheets, which were cured and cut into test samples. Figure 2.2A is a representation of the mechanism through which self-healing occurs when the crack ruptures the microcapsule and exposes the WMS. The catalyst and crosslinking agent were added in excess to ensure good dispersion and contact with the WMS liquid when exposed due to rupture of the microcapsule. The self-heal mechanism occurs through SHP catalyzed esterification reaction between the carboxyl groups of the BTCA in the matrix and the hydroxyl groups of gelatinized starch as represented in the schematic in Figure 2.2B. The results showed that the healing efficiency increased with increasing microcapsule concentration up to 20 wt. %. It is conceivable that the higher the microcapsule concentration, the greater the probability of the crack rupturing more of these capsules and exposing the healant resulting in better crack bridging. Figure 2.2C shows the micrograph of a bridged crack after 24 hours of healing of WMS resin with 20 wt.% of microcapsules. The disadvantage to having high concentrations of microcapsules especially in thermoset resins is the potential reduction in the strength of the matrix especially if the interfacial bond between the shell and the matrix is poor as observed in the aforementioned study. This can be alleviated by introducing a compatibilizer to improve the interfacial adhesion between the matrix and capsules. In the aforementioned study, polyvinyl alcohol was used as an interface to improve bonding between the WMS resin and the microcapsule. Micromechanics of polymer reinforcement has shown that spherical particles are most efficient for improving the impact strength or toughness of a polymer while fibrous or platelet particles can drastically improve the strength[65]. Therefore, it will be of great advantage to develop

a method of producing microcapsules which are elongated to have an elliptical or fibrous shape. This will not only act as reinforcement for the matrix but will greatly increase the efficiency of the self-healing mechanism as there will be high probability of rupturing these fibrous capsules due to it greater aspect ratio.

In Table 2.2, a comparison between close or comparable healing parameters such as healing efficiencies, healant, curing temperatures and mode of evaluation of self-healing polymers are summarized. Starch based healant showed a tremendous healing efficiency of 51 and 66 % in comparison to other healants used. Starch being a biodegradable and green material with low cost gives it great advantage to be further explored as a healant with other polymeric materials as well.

Table 0.2. Self-healing polymers with similar healing parameters and mode of evaluation.

Self-Healing Material	**Mode of Evaluation**	**Healant**	**Healing Parameters**				**Ref**
			Healant Concentration (wt. %)	**Curing Temperature (C)**	**Curing Time (h)**	**Healing Efficiency (%)**	
Corn Starch Resin	Tensile Fracture Stress	Gelatinized corn Starch	20	21	24	51	[68]
	Tensile Fracture Toughness		20	21	24	66	
Epoxy	Tensile Fracture	Dicyclopentadiene	20	25	48	45	[70]
			20	25-30	48	80	
	Toughness		10	Room temperature	N/A	75	[71]
	Tensile Fracture		40	N/A	48	14	[72]
Poly (dimethyl siloxane) elastomer	Tensile Tear Strength	Vinyl functionalized poly (dimethyl siloxane)/ platinum catalyst	20	N/A	N/A	120	[73]

2.3.2. Application of Starch in Porous Foam Structures

The bind ability of starch has given rise to its use as a binder, pore former for metallic and ceramic porous foam structures[74–79]. Applications requiring environments with elevated temperatures and pressures or materials that are inert and biocompatible typically use ceramic or metallic foam structures. These structures have typically been manufactured using other methods such as replication method[80,81] where the ceramic for example fills the empty space of polymer foam structure, is solidified and then the polymeric foam is burned out to reveal the porous ceramic structure. Use of additives as pore formers in coagulating the ceramic particles is another method used in porous ceramic foam structures[82,83]. However, the disadvantage to this is, the ceramic structure is always dependent on the empty structure of the polymeric foam used. Another method used is the agitation of a suspension containing the ceramic particles and foaming agent, which results in closed cell foam generation. A porous structure is formed with the removal of the liquid and sintering of the formed structure. However, these methods have disadvantages as the formation of the pores cannot be controlled. This subsequently results in physical properties and dimensions of part produced which are dependent on the process. Likewise, dispersion agents and chemicals used in the process are typically expensive and not environmentally friendly.

Starch can provide a lending hand to be used as a pore former in the creation of porous ceramic and metallic structures[77,84]. The manufacturing of the porous structures with starch is done by starch consolidation[74]. The process occurs when a specific amount of starch (the pore former) is added to a specific amount of ceramic slip, which is a suspension of ceramic powder in water (the solids) and heated under constant stirring[85]. The starch granules swell resulting from water intake when the hydroxyl groups are exposed under elevated temperature. This causes water to be drawn from the slip and forces the ceramic powder to consolidate into a solid porous structure. The pore

size of this structure is controlled by the swelling of the starch granules; the more it swells, the larger the pore size of the structure is. The swelling or gelation of the starch also act as a binder for the newly formed structure. The structure is dried; starch burned out and then sintered. A study investigating the use native and etherified potato starches for the manufacture of alumina foams was conducted by Lyckfeldt and Ferreira[74]. In this work, the effectiveness of using modified starch (trade name of Trecomex) in comparison to native starch was examined. It was found that gellability and dispersibility of starch in water played a huge role in the production of the porous ceramics structure without critical deformation to its structure. Subsequently, it was also found that the modified starch was better at consolidating the alumina particles. Likewise, it was found that the higher the starch content, the greater the pore size was. Similar result was obtained when 5 and 40 wt. % starch concentrations were used as pore former in the manufacture of cordierite ceramic foam structures[77].

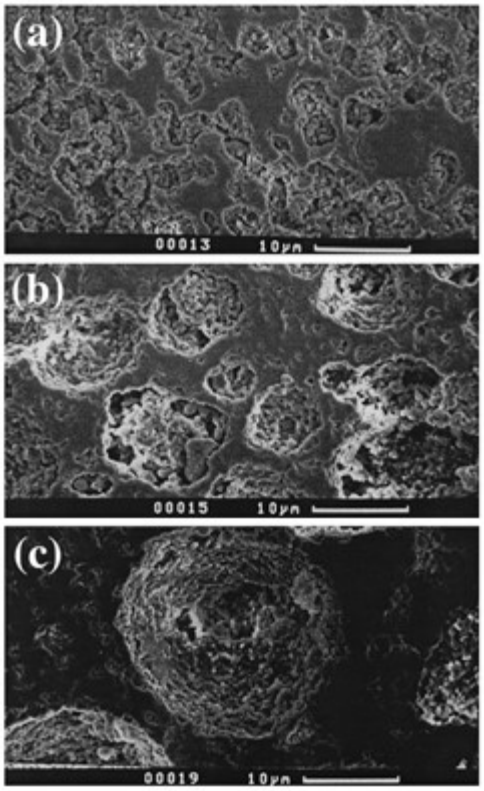

Figure 0.3. Structures of porous alumina made using a 55% volume fraction of starch that are from (a) rice starch (b) corn starch, and (c) potato starches. Adapted from Davis *et al*.[75]. Wiley copyright © 2000.

Similarly, the pore structure and size are dependent on the type of starch used[75]. The larger the granular particle size of the starch is, the larger the porosity of the structure. Figure 2.3 shows the porous structure of alumina porous structures formed using (a) rice, (b) corn and (c) potato starches as pore formers. The granular particle size of these starches increases in the following order; rice < corn < potato. It can be observed that the rice starch showed smaller but somewhat interconnected and co-continuous pore structures (Figure 2.3a). As the particle size is increased, the pores begin to segregate (Figure 2.3b) and finally separate when the particle size is the largest (Figure 2.3c). This suggests that the pore size not only can be engineered by selecting pore formers with desired particle size, but the networking or open porosity of the structure can be controlled as well. The use of starch as pore former has also been applied using the consolidation method in the production of titanium foams with open cell structures[84]. Figure 2.4 shows the effect of the modified starch (Trecomex) on the storage modulus of the starch, alumina slip mixture (slurry) obtained from rheological analysis. It was observed that at higher temperatures, the slurry containing modified starch exhibited better storage modulus than that containing natural starch. Due to the initial gelation process required to modify the starch, the modified starch is susceptible to gelation at lower temperatures than the natural starch is. Therefore, it swells faster resulting in consolidation and reduced segregation of the alumina particles and higher storage modulus of the slurry approximately above 55°C.

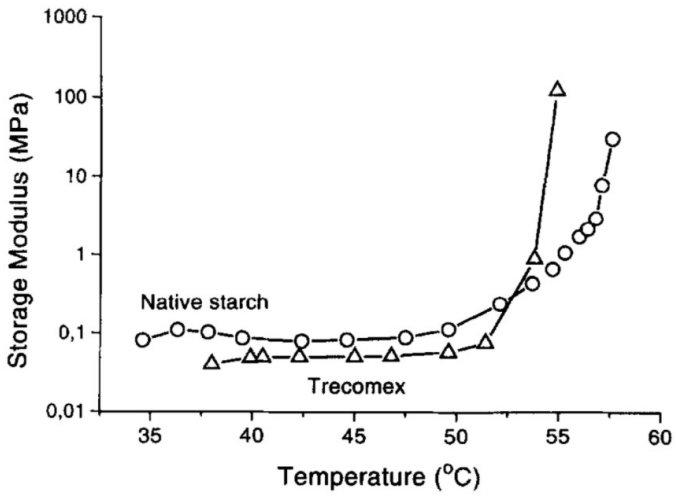

Figure 0.4. Effect of modified and unmodified starch on the storage modulus of alumina/starch slurry for porous structure manufacture. Adapted from Lyckfeldt *et al.*[74]. Elsevier copyright © 1998.

2.3.3. Applications of Starch in Water Treatment

Water treatment has been one of the greatest challenges for environmental science because of the ever-increasing amounts and types of contaminants found in it. As technology evolves, the use of various chemicals which are toxic to both humans and the environment are also evolving. Filtration using micro and nano membranes have been employed to remove solid contaminants[86,87]. However, soluble contaminants are sometimes notorious to get rid of. Most research have been able to remove these contaminants, however, at the cost of using other chemicals (e.g. polyacrylamide) which could potentially be harmful if trace amounts are left behind. Therefore, a substantial research focus is in place to utilize green or environmentally friendly materials and approaches to decontaminate water. Starch has an abundant potential for use as a substitute of other potentially toxic polymers used in in water treatment. This is because starch is non-toxic, sustainable, relatively low cost, and amenable to various chemical modifications that are of interest to water treatment applications. Furthermore, the -OH functional groups on starch structure could

be used as anchor points of contaminant particles[88] in water treatment. Starch as a sorbent or functional material in wastewater treatment has numerous advantages such as it availability across the world and renewability, which makes it feasible and attractive economically. In terms of its properties in relation to water, it has excellent swelling capacity which in turn makes gives it fast kinetics and excellence at removing a wide range of pollutants. Due to its functional groups, it can easily be modified and tailored to target specific pollutants. The gelation characteristics of starch allows it to be soluble in water at elevated temperatures has made it a suitable choice to be used as a dispersant for nanoparticles used in water decontamination[89]. Better dispersion of these nanoparticles will result in improved reactivity to efficiently decontaminate water.

A study by He and Zhao prepared Fe-Pd nanoparticles with and without the use of starch as the dispersing agent or stabilizer for the dechlorination of trichloroethene (TCE) hydrocarbon[89]. Morphological analysis through transmission electron microscopy showed that Fe-Pd nanoparticles without starch were agglomerated and formed a network or dendritic floc with varying densities (Figure 2.5a). Contrarily, starch-Fe-Pd nanoparticles exhibited remarkable dispersion (Figure 2.5b).

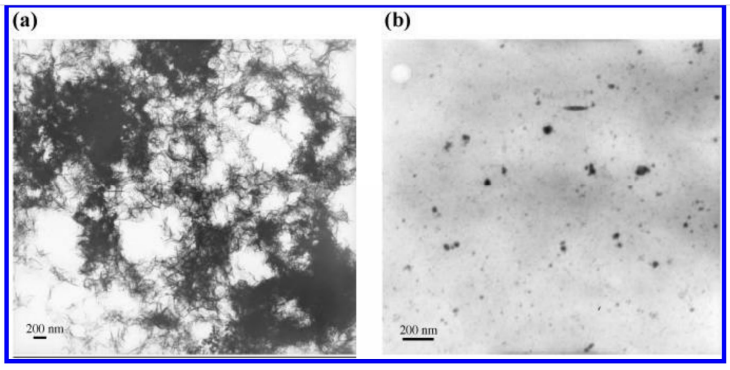

Figure 0.5. Transmission electron microscopy of Fe-Pd nanoparticles prepared (a) without and (b) with starch as stabilizing agent. Adapted from He *et al.*[89]. ACS copyright © 2005.

It was found that iron-starch interactions and development of intra-starch Fe clusters contribute a crucial part in dispersing and stabilizing the iron nanoparticles. These nanoparticles were tested for their efficiency in the dichlorination of TCE. The dichlorination rate of starch-Fe-Pd was found to be significantly greater than particles not stabilized with starch. This is because the exposure of the particles to reactivity was far greater when starch was used as a stabilizer in comparison to agglomerated particles, which only reacted with particles that were exposed. To understand the efficiency of starch as a stabilizer, another research has reported similar dichlorination rate but with a concentration of 200 times the amount of Fe particles[90]. A summary of starch derivatives used in the removal of pollutant from water are presented in Table 2.3. One major drawback of starch use in water decontamination is that the particle size varies with plant source and therefore might perform differently due to difference in surface area.

Table 0.3. Starch based materials used in water decontamination.

Material	**Contaminant**	**Ref.**
Starch-Fe-Pd	Trichloroethene	[89]
Starch xanthate	Ni^{2+}, Cu^{2+}, Cr^{3+}	[91]
carboxymethyl starch	Pb^{2+}, Cd^{2+}, Cu^{2+}	[92]
Polymerized starch with epichlorohydrin	Dyes	[93]

2.3.4. Applications of Starch as Excipient in the pharmaceutical Industry

An excipient is defined by the international pharmaceutical excipient council (IPEC) as “any substance other than active drug or pro-drug that is included in the manufacturing process or is contained in finished pharmaceutical dosage forms”. Other entities categorize them according to their functions in the final manufacture drug such as binders, dis-integrants, diluents and

lubricants[94,95]. The application of starch in the pharmaceutical industry spans from its use as non-active ingredient, drug delivery to coating and binders in drugs. It is also an important excipient, which the industry uses extensively[95]. This is because of its physical characteristics and properties such as smoothness and ability to be molded, gellability and binding capacity. Moreover, its abundance and availability coupled with low cost, biodegradability and biocompatibility makes it an attractive material to the industry.

The ability of starch to gel has found use as a binding agent in the production of capsules and tablets through the process of wet granulation[96]. Starch is especially suitable in this process as it can act as a dispersing agent to uniformly distribute the drug particles in either high or low concentrations and binds the particles to form loose agglomerates while allowing for easy compression thereafter, to form compacted tablets typically for oral ingestion[97]. It is typically used at low concentrations of about 3 to 20 wt. % with respect to the weight of the compacted tablets[30]. This range of starch concentration is due to the variance in the type and concentrations of other materials used in the formulation as well as parameters in the production of the tablets.

Although starch has been applied as a binder in tablet and capsule production, it also functions as a disintegrant[98]; it aids the break up capsules shells and tablets for quick release and assimilation of the active components of the drug into the body[95]. Starch is one of the most commonly used disintegrant in the drug industry for tablet and capsule manufacture. The hydrogen bonds between the starch molecule and the other constituents of the tablet after compaction of the drug help bind the tablet. However, when the drug encounters an aqueous medium (water), the starch granules absorb it; this results in the disruption of hydrogen bonding, swelling of the granules which then elastically deforms[98,99]. This process loosens up the compacted tablet particles, which eventually breaks apart. Figure 2.6 shows a schematic of the process of drug disintegration into particles,

which are then absorbed by the body. Depending on the type of starch used and its position as either indo, exo, or indo-exo-disintegrants, drug composition and parameter used in the manufacture just to mention a few, the rate of disintergration varies significantly[98].

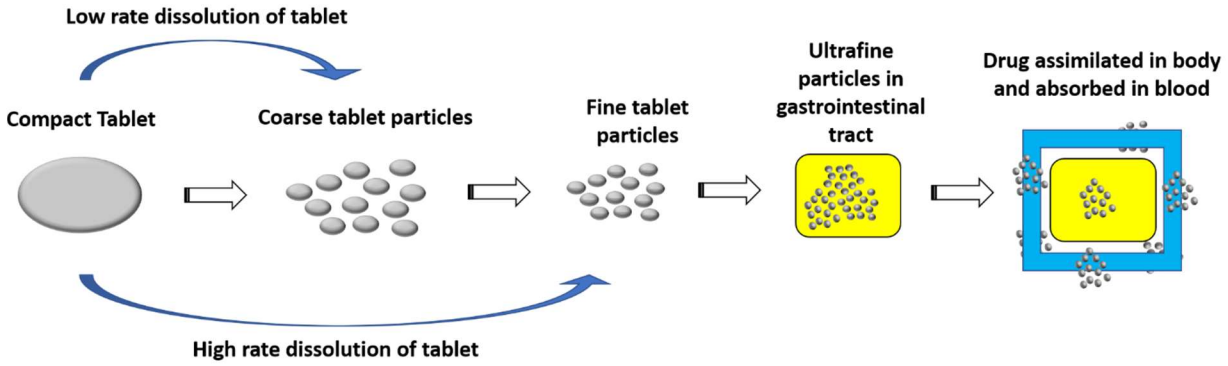

Figure 0.6. Schematic representation of tablet disintegration and assimilation into the body [94].

Starch is widely used as a disintegrant because it is required at a relatively low concentration ranging from 3-15 wt. % of the total drug weight[30,100]. Native starch in comparison to modified starch, such as regelatinized starch perform not as well as modified starch in its binding and disintegrant applications in drugs[95]. This is due to the partial opening of the starch granules after pregelatinization, thereby allowing the exposed hydroxyl groups form hydrogen bonds with other starch molecules and active drug particles in the tablet. This results in better dispersion of the starch within the drug. Hence, bonding is improved and render the disintegration of the drug more efficient.

2.3.5. Advances in Drug Delivery using Starch

Starch as a green and biocompatible material has currently attracted a substantial interest as a potential drug delivery agent as well as in controlling the rate of active drug release over periods of time. The drug release over time of tablets can be controlled through the modification of the

dual functional native starch used as binder and disintegrant. Odeku *et al* [101–105] studied various starches from various sources in tablet manufacture and found that the rate of disintegration, which is also related to the rate of active drug component release was greatly affected by the source of the starch and the modification type done to the native starches. Depending on the type of modification carried out to starches such as acid modified, pregelatinized, freeze-dried, crosslinked and hydroxypropylation, the disintegration and binding properties are significantly affected which consequently affects the rate of drug release. Similarly, the source of the starch is also great influencing factor of these properties as well. Therefore, it is important that the right source of starch and modification be chosen to target specific drug release.

Alexiou *et al*[106] conducted a study to explore the biocompatibility and reactivity of starch as a carrier for targeting cancer cells. In this study, iron oxide nanoparticles were sized with modified starch containing phosphate groups, which were then infused with mitoxantrone as chemotherapeutic drug [106]. It was shown that by applying a magnetic field over the cancer tissues in the subject, these nanoparticles concentrate in these areas and destroy the cancer cells by penetrating them.

Ahmad *et al*[107,108] developed a novel method of drug delivery in the gastrointestinal tract (GIT) using bioadhesive microspheres (BAM) synthesized from rice starch by double emulsion evaporation method. In this study, BAM was used as a carrier for metronidazole for colon and intestinal disease treatment. It was shown that these microspheres were able to withstand microbial degradation and hydrolysis from enzymes, acids and alkalis, thereby resulting in slow drug release for a prolonged period. It was also suggested that this novel application of starch can be used as a carrier for other types of effective drugs to combat gastrointestinal tract infections. Using the same rice starch but modified by carboxylation and oxidation, Ahmad *et al*[109] studied the drug release

rate of tablets containing metronidazole. It was found that the modified starches were effective in the release rate and varied depending on what environment the tablet was in within the GIT.

The thermo-sensitivity of starch derivatives has recently been geared towards drug delivery[110]. This novel research is based on previous technology where thermo-sensitive polymers have been used in drug delivery[111]. The swelling and expansion, which occur when starch is exposed to moisture at elevated temperatures has been used to control the release of drugs. This mechanism was applied to corn where it was degraded using acid to expose functional groups on the starch granules[110]. This treated starch was then reacted with butyl glycidyl ether under controlled parameters to yield micelles of 2-hydroxy-3-butoxypropyl starch polymers. Prednisone as the choice of drug was then loaded into the modified starch through a dialysis process. The results showed that the modified starch carrying hydrophilic alkyl groups can form micelles and the lower critical solution temperatures (LCST) of this starch was a function of the degree of molar substitution (MS) of butyl glycidyl ether to the anhydroglucose units of the starch molecules. By doubling the MS from 0.32, the LCST was decreased from 32.5 to 4 °C. This indicates that the micelles can be designed to swell and control the rate of drug release at different temperatures. With the LCST of the modified starch micelles determined to be 32.5 °C, they were tested for their drug release in distilled water at 20 and 40 °C. It was found that 38 % of the drug was released at 20 °C while 90 % was released at 40 °C. In both cases, the duration of the study was 100 h. At temperatures above the LCST, the micelle structure was less stable and resulted in a failure to confine the drug and therefore caused it to leach out of the structure. Starch in combination with polymers for porous media and drug infusion is another area that has also been investigated. Microcapsules, where starch is utilized in drug delivery has also been investigated. These applications of starch in drug delivery systems have been summarized in Table 2.4.

Table 0.4. Modified starch and their application towards drug delivery systems

Material	Delivery Method	Preparation Technique	Result/Summary	Ref.
Corn starch-Polycaprolactone blend	Porous microparticles	Emulsion solvent extraction/ evaporation	This study was able to produce microparticles ranging in sizes from 5 to 900 µm with both smooth and porous surface morphologies. In-vitro studies also showed that there was a steady release of the drug of choice over a 30-day period, indicating its potential as a carrier for other active drug ingredients	[112]
Sweet potato starch	Microparticles	Spray-drying of gelatinized starch	This studied produced heterogeneously shaped particles which showed a drug release sustainability of over 6 h. it also showed that the concentration of starch used in the production of the particles as well as that of the model drug affect the release rate.	[113]
Corn and potato starches	Hydrogel	Isostatic ultra-high pressure	The result from this study showed that corn starch-based hydrogel carrier exhibited sustained drug release while potato starch-based hydrogel exhibited fast drug release. This study showed that the source of the starch can significantly affect the developed drug carrier properties.	[114]
Hydrolyzed potato starch	Microspheres	Single emulsion crosslinking	This study produced microspheres with diameters ranging from 3 to 540 µm. Particle size was shown to be dependent on the crosslinking reaction while the release of the drug was rapid within the first 2 h regardless of medium used.	[57]
Glutinous rice starch and polyvinyl alcohol blend	Microfibers	Electrospinning	Changing the ratio of starch to PVA ratio showed an effect on the type of fibers produced; either beaded or smooth cylindrical fiber. The study also showed that the fibers had high water-soluble index which was excellent to be used as a drug carrier. Drug release test showed that the initial release was from the PVA phase while the sustained release was from the starch phase. This	[115]

			indicates that a quick and sustained dose can be applied when using a model drug.	
Crosslinked starch	Mucoadhesive starch nanoparticles		The results showed that the nanoparticles were effective in rapid drug release and dependent on the particle size. Likewise, the degree of crosslinking was observed to have an effect on the drug release rate as well.	[116]

2.3.6. Antimicrobial Films and Coatings based on Starch

The proliferation of antibiotics resistant bacteria has posed a substantial demand for innovative strategies to fight pathogenic bacterial infection in the health and personal care as well as food contamination. Polymers that have antimicrobial properties represent a valuable alternative to conventional antibiotics and is currently gaining interest in coatings, personal care and active food packaging, and biomedical applications. Typical antimicrobial agents used with polymers are organic or inorganic acids, metals, alcohols ammonium compounds or amines [117]. However, due to the low molecular weight of these antimicrobial agents, their retention capacity has been reported to be poor causing them to leach out when applied directly to a substrate or polymer system, thereby inhibiting their antimicrobial performance. The interest in starch as an antimicrobial agent carrier is accrued from its film-forming properties, and high molecular weight. The use of such high molecular weight polymer as a carrier of antimicrobial polymer eliminates the problem of leaching via entanglement and other interactions with the baseline plastic making polymer [118,119]. In addition, starch is economical, environmentally friendly, and non-toxic making it appealing in food packaging and biomedical applications. Typically, the antimicrobial agent is covalently bonded to starch via a synthetic strategy to improve its retention in polymers.

Guan *et al* [119] synthesized antimicrobial modified starch by covalently bonding polyhexamethylene guanidine hydrochloride (PHGH) with potato starch through a coupling reaction using glycerol diglycicyl ether (GDE) to improve its adsorption on cellulose fibers. A shaking flask method was used to evaluate the biocidal activity against *E. coli* and *S. aureus* while atomic force microscopy was used to monitor the antimicrobial mechanism. Their results revealed that 1 wt.% PHGH modified starch in cellulose fibers inhibited the growth of the studied bacteria by almost 100 % [119]. A similar study carried out by Ziaee *et al* [118] using modified starch containing 12 wt.% PHGH with as low as 20 mg/g PHGH modified starch dosage on cellulose fibers revealed excellent antimicrobial activities against *E. coli* bacteria as indicated by the collapse of bacteria membrane investigated by AFM and the growth of *C. globosum* fungi investigated by SEM. In this studies, introducing the modified starch in fibers increased the tensile index and decreased the tear index simultaneously [118]. Several other authors have also researched and reported positive antimicrobial outcomes by using guanidine hydrochloride based modified starch [120,121].

Pelissari *et al* prepared a film from plasticized starch-chitosan modified with oregano essential oil (OEO) at concentrations of 0, 0.1, 0.5 and 1 % and investigated the antimicrobial properties against *Bacillus cereus*, *Escherichia coli*, *Samonella enteritidis* and *Staphylococus aureus* using the disk inhibition zone method. From their results, although a higher inhibition halo was observed for *B. cereus* and *S. aureus* (gram positive) and a smaller inhibition halo for *S. enteritidis* and *E. coli* (gram negative), all OEO modified films exhibited inhibition zones, which increased with an increase in OEO concentration. The presence of OEO in starch films not only improved the biocidal activity but also improved hydrophobicity and water vapor barrier properties [122].

Shen *et al* plasticized potato starch and prepared antimicrobial starch films modified by incorporating potassium sorbate or chitosan at concentrations of 0, 5, 10, 15 g/100 g starch and observed the biocidal activity of modified films against *E. coli* and *S. aureus*. Films prepared with 10% or less potassium sorbate could not suppress the growth of *E.coli* and showed no inhibition zones. They suggested an interaction between the hydroxyl group in starch and the carboxyl group in potassium sorbate limited the release of potassium sorbate responsible for inhibiting the growth of bacteria from the film; hence limiting the biocidal activity. On the other hand, significant inhibition zones were observed when the concentration was increased to 15 % resulting from the release of sorbic acid from the starch films. The films prepared with chitosan revealed inhibition zones at 5 % with an increase in the inhibition zone diameter as the concentration increased to 15 %. Potassium sorbate starch films tested against *S. aureus* revealed no inhibitory zones as compared to chitosan-starch films which inhibited the growth of *S. aureus* at 10 % concentration; with no change in activity with an increase in concentration. The films that revealed inhibition zones in both cases showed no contamination, which suggests that these antimicrobial agents inhibited the growth of other microorganisms as well. In addition to the biocidal activity, the presence of these antimicrobial agents impacted the mechanical properties, water vapor and oxygen permeability, and solubility of films [123]. Other examples of starch utilization in antimicrobial polymer applications are presented in Table 2.5.

Table 0.5. Antimicrobial modified starch and its activities.

Starch Source	Antimicrobial Agent	Concentration	Microorganism	Remarks	Reference
Potato	PHGH	1 %	*E. coli* *S. aereus*	100 % inhibition	[119]

		12 %	*E. coli* *C. globosum*	Excellent antimicrobial activities	[118]
Cassava	Chitostan-oregano	0.1, 0.5, 1 %	*B. cereus, E. coli, S. enteridites,* and *S. aereus*	Increased biocidial activity against gram positive than gram negative bacteria	[122]
Sweet Potato	Potassium Sorbate	5, 10, 15 %	*E. coli*	No inbibition zones at ≤ 10 %	[123]
			S. aereus	No inhibition zones	
	Chitostan	5, 10, 15 %	*E. coli*	Inhibition began at 5 % concentration; increased with concentration	
			S. aereus	Inhibition at 10 %, no increase with concentration	
Tapioca	Chitostan	1 %	*Lactobacillus spp*	Low effectiveness	[124]
			Zygosaccharomyces bailii	Effective	
		3 %	*Zygosaccharomyces bailii*		

	Chitostan-Potassium sorbate		*Lactobacillus spp*	No inhibition	
Wheat	Chitostan	Various	*B. subtilis* *E. coli*	Low inhibition	[125]
	Chitostan-lauric acid	8 %	*B. subtilis* *E. coli*	Efficient inhibitory effect	
Potato starch	Guanidine hydrochloride	4,8,12,16 mol % compared to starch	*E. coli* *S. aereus*	Excellent antimicrobial properties	[120]

2.3.7. Other advanced applications of starch and its derivative materials

Technological advances and research have certainly focused on the use of starch in various applications such as electronics, photonics, energy, sensors and superhydrophobic surfaces. The property and ability for the starch to form thin films when gelatinized and cast on a substrate have lent itself as a moisture barrier in the application of superhydrophobic papers. In a study by Chen *et al*, a superhydrophobic paper was fabricated by the casting of two layers of solutions on the surface of paper [126]. The first layer comprised of a gelatinized starch composite containing enzyme, sizing agent, crosslinker and aluminum sulfate as a pH adjuster and was rolled on while the second layer was a suspension of hexamethyldisilazane treated silica nanoparticles (HMDS-SiNPs) in ethanol. This layer was immediately sprayed on after the application of the gelatinized starch and allowed for the ethanol to evaporate. This allowed for the bonding of the HMDS-SiNPs to the starch layer while it was curing. Results from the contact angle test showed that the

treated paper was superhydrophobic with a contact angle of 162 degrees as shown in figure 2.7a. The presence of the HMDS-SiNPs on the surface acted to repel the water molecules. In a submersion test, both treat papers with and without the first layer of gelatinized starch were completely submerged in water for a period of 2 mins. The paper without the starch layer was completely soaked and allowed water to penetrate through its fibers. However, the paper with both layers treated was dry after the 2 mins water immersion. For this, it was suggested that the thin film formed from the crosslinked and gelatinized starch clogged the porous structure of the paper fibers and prevented water from penetrating through it. Other significant improvements noticed were increased mechanical durability of the treated paper. Likewise, the visual appearance of the paper after treatment was not affected since very thin layers were applied. It can be observed that the tailoring of starch with other materials can provide several interesting attributes with numerous applications; one such feature is hydrophobicity of starch that is inherently hydrophilic.

Starch has been shown to have comparatively good optical properties, which can be channeled for use in various applications. The application of starch as a substrate in photonics in comparison to other biopolymer substrates has been investigated by Cyprych *et al* [127] and shown to have greater photostability due to its low oxygen permeability. In this study, starch was gelatinized using water and then doped with rhodamine 6G water solution, which acted as a light amplification medium. This mixture was casted on a glass substrate and allowed to air dry, forming a layer of rhodamine 6G doped modified starch. When the doped starch was photoexcited, a generation of random lasing effects was observed due to the formation of a random roughness of the starch granules deposited on the substrate. In comparison to other biomaterials such as DNA, and proteins, starch could exhibit better photonic properties. Figure

2.7b shows a schematic of the mechanism of random lasing due to the random formation of starch granules on a glass substrate. This work showed that starch has the potential to be used in photonic applications such as light emitting diodes and color imaging. With further research and development, the future of and applications of starch-based phonic materials seems promising.

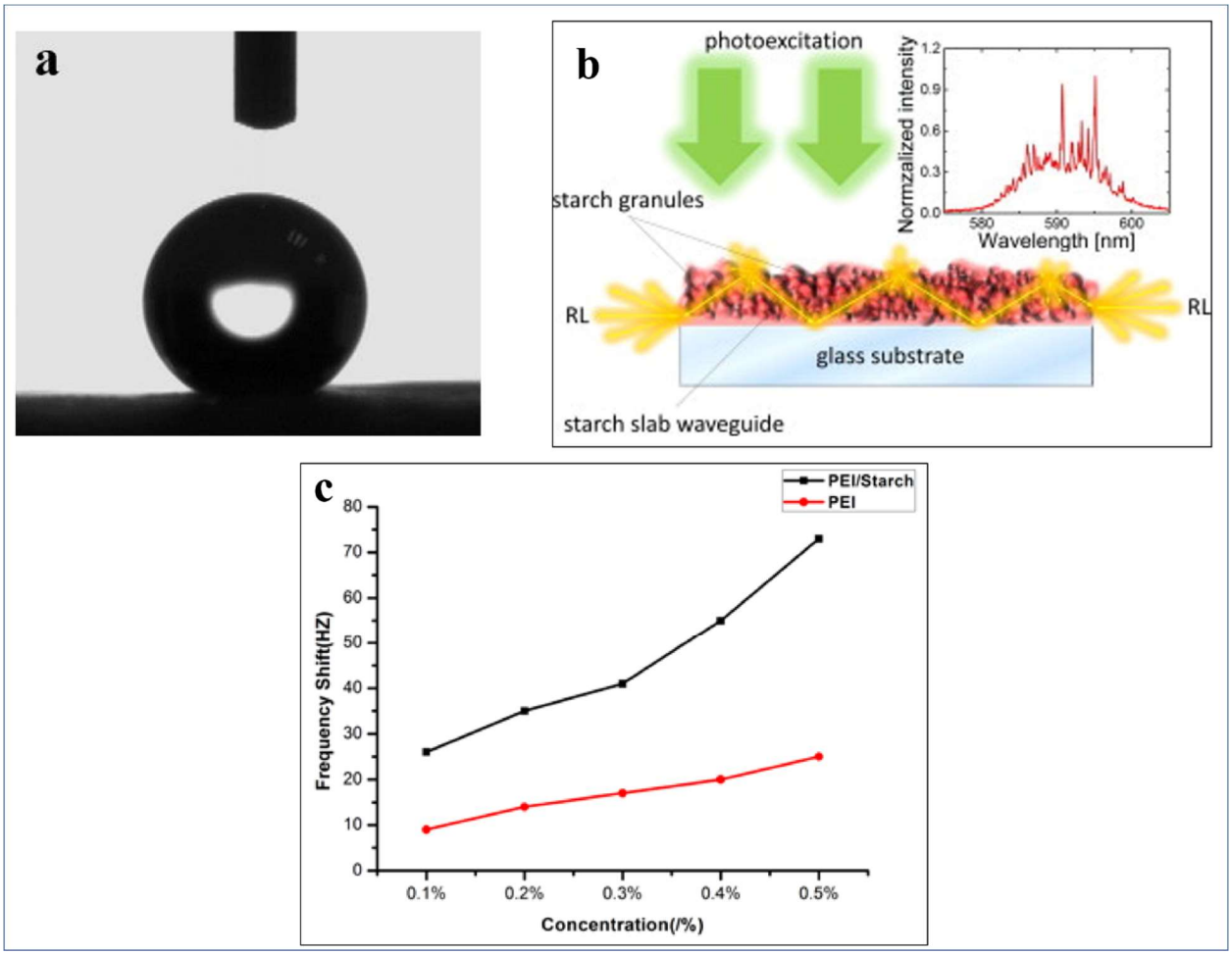

Figure 0.7. (a) Contact angle test of superhydrophobic paper modified with starch composites. Adapted with permission [126]. Copyright 2017. Elsevier, (b) Schematic representation of random lasing of modified starch on glass substrate after photoexcitation is applied. Adapted with permission [127]. Copyright 2017. Elsevier, and (c) The effect of frequency changes of PEI and PEI/starch film sensors materials as a function of carbon dioxide concentration. Adapted with permission [128]. Copyright 2011. Elsevier.

With the rate of carbon dioxide emissions from our ever-growing industries around the world, we have seen great significance in climate change. One of the areas starch has been used is in research and development of sensors for carbon dioxide. In a study by Sun *et al* [128], polyethylenimine (PEI) and polyethylenimine-starch composite films were spin coated on quartz crystal microbalance sensors. Carbon dioxide and nitrogen gases were pumped alternatively and the sensitivity through frequency changes were observed. It was noted that the PEI/starch composite exhibited significantly higher sensitivity to the carbon dioxide. Figure 2.7c shows the effect of carbon dioxide gas concentration on the frequency changes of both PEI and PEI/starch films. Both films showed an increase with increasing carbon dioxide concentrations while the PEI/starch film showed significantly greater frequency changes in comparison to that of the PEI film. It was postulated that the greater sensitivity to carbon dioxide was due to the more protonation of the amino groups within the PEI polymer thereby increasing recognition of carbon dioxide at the polymer layer. The mechanism through which this occurred was deduced to come from the presence of starch attracting moisture to the surface of the film and subsequently interacting with carbon dioxide to form carbonates and bicarbonate ions. This study shows that starch is a versatile material and with fundamental understanding of its properties, it can be geared towards specific applications.

2.4. Outlooks, Prospects and Conclusions

The environmental concerns from the utilization of non-sustainable, non-biodegradable and toxic feedstock in industrial applications have created an increased interest for the need to research and develop biomaterials with starch being a sort after and potential candidate because of the many benefits it brings. The environmentally friendliness and ease of chemical modification such as gelatinization and blending of starch with other materials such as polymers have been shown to

produce desirable properties suited to specific end use. By varying the type, level and degree of modification in modified starch, the physicochemical properties of the final material based on starch can be varied. Utilization of starch as healant in self-healing thermoset resins have shown to be a viable alternative material to currently used highly reactive and toxic chemicals [68]. Drug delivery systems require carriers and materials that can easily be modified and used as carriers for dosage of active drugs at specific sites. Starch has shown great promise for use in drug delivery system especially because of its biocompatibility and degradability within the subject after effective release of the drug. Likewise, it is less-expensive and readily found across the globe. Properties of starch such as bindability, and gel-ability has found many uses in the pharmaceutical industry to act as disintegrants, binders, dispersants and lubricants. They have also found utilization in the production of porous metallic and ceramic media for applications such as filtration and tissue engineering. With the world focused on moving towards sustainability, starch has found itself as one of the for front runners in the development of functional materials for advanced applications. While starch can complement efforts towards the development of renewable polymers, perceived competition with food production could limit its extensive utilization in commodity applications. However, its use in functional and advanced material application is expected to attract more attention.

Chapter 3. Hydrophobic and Melt Processable Starch-Laurate Esters: Synthesis, Structure – Property Correlations[2]

3.1. Introduction

Plastics are used in a variety of applications such as automobiles, textiles, packaging, construction, cosmetics, electronics and medicine[129]. However, the largest application of plastics remained food packaging and containment applications (e.g bags, cups etc.) whose growth is attributed to a shift in product lifetime from multiple to single use due to the low cost and ease of processing these polymers. Such single use of plastics led to municipal solid wastes that consist of a high percentage of these plastics creating a serious environmental challenge. Common plastics used in such commodity applications are polyethylene (LDPE and HDPE), polystyrene, polypropylene, polyethylene terephthalate etc[4]. Unfortunately, these plastics are sourced from fossil fuel, and are resistant to biodegradation. Thus, after their useful lifetime, they accumulate in the natural environment, and in most occasions, end up in water bodies thereby posing potential harm to aquatic life[130]. These shortcomings have prompted research interest in alternative bio-resourced feedstock. This is because natural polymers are renewable and typically degrade in the natural environment by the actions of microorganisms.

Starch is among the most promising natural polymers because of its renewability, biodegradability, abundance, low cost, film-forming properties and ease of modification [131,132]. Nevertheless, native starch without modification is not suitable for most polymer applications. This is partly because the hydroxyl groups of starch readily associate with moisture via hydrogen

[2] A version of this chapter has been published. E. Ojogbo, R. Blanchard, T. Mekonnen, Hydrophobic and Melt Processable Starch-Laurate Graft Polymers: Synthesis, Structure – Property Correlations, J. Polym. Sci. Part A-Polymer Chem. (2018). doi:10.1002/pola.29237.

bonds leading to high moisture sensitivity. Moreover, the amylose and amylopectin fractions form inter- and intramolecular hydrogen bonds that raise its melting temperature beyond its degradation temperature[132]. Strategies to modify starch for material application can be: (a) conversion into low molecular weight hydroxylated compounds, such as dextrins and other glycolized products and their utilization as a monomer for polymer synthesis, (b) hydrolyze it into glucose and utilize the glucose in fermentation process for producing polylactic acid (PLA), polyhydroxyalkanoates (PHAs) etc., (c) thermoplastic modification that involves the addition of external plasticizers and high temperature processing in an extruder [133–135].

Among the various modifications, thermoplastic starch (TPS) has attracted the most attention because of the ease and low cost of the process. However, leaching out of external plasticizers, water sensitivity, premature aging caused by re-crystallization, brittleness, and too fast biodegradation [136–138] has limited it from achieving the touted potential. The direct blending of starch with other polymers has also been extensively investigated with some success [55,139]. An alternative approach to mitigate these challenges is to chemically modify starch (e.g etherification, esterification, crosslinking, acetylation, oxidation etc.) that involves replacement of the –OH groups with other suitable functionalities while maintaining the backbone chain intact. Each anhydroglucose unit (AGU) of starch has three -OH groups that could allow substitution of other chains to a maximum degree of substitution (DS) of three that paved a way for several types of modifications. Esterification of starch is among the several chemical modification efforts that are extensively reported in the literature. For instance, esterification with organic acids such as acid anhydrides and fatty acids introduces both hydrophobicity and thermoplasticity in starch[140].

The incorporation of short-chain fatty acids (C_2 to C_5) on the structure of starch has been studied by some groups[141–143]. Although the water vapor permeability of the modified starch has improved, the resulting materials were brittle and required external plasticizers[141–143]. Attaching medium (C_6 – C_{12}), and long chain (C_{13} – C_{21}) fatty acids could offer better processability, and mechanical properties. However, the increase in the chain length could result in limited substitution efficiency (low DS) because of steric hindrance and unfavorable side reactions [140,144].

In this research, a robust and single stage modification of starch with fatty acid is investigated to produce a renewable and biodegradable plastic alternative to polyolefins and other bio-based polyesters. An activated fatty acid with a medium chain length (C_{12}), lauroyl chloride, was selected here to replace the hydroxyl groups of starch and produce starch – fatty acid esters. Lauroyl chloride is prepared from lauric acid that is typically derived from coconut oil in the presence of thionyl chloride. The level of modification, estimated here as the degree of substitution (DS), was controlled by varying the mole ratio concentration of the lauroyl acid to the anhydrous glucose unit (AGU) of starch. Pyridine was selected as the solvent for the reaction based on previous research reported in the literature[27]. Detailed structural studies of the fatty acid modified starch and correlation of the modification efficiency with the structure - properties of the material are elucidated in this study.

3.2. Materials and Methods

3.2.1. Materials

Cornstarch containing approximately 73% amylopectin and 27% amylose was obtained from Sigma-Aldrich. All starch samples were dried to a moisture content of below 1% prior to use.

The drying was conducted at a temperature of 70 °C for 24 h under reduced pressure and stored in an airtight container. Lauroyl chloride (98%, 0.946 g/mL), pyridine (≥ 99%, ACS grade), chloroform (≥ 99.8%, for HPLC), toluene, dimethyl sulfoxide (DMSO), tetrahydrofuran (THF) (≥ 99%, ACS grade) were also supplied by Sigma Aldrich. Acetone (≥ 99%, lab grade), and ethanol (≥ 99%, lab grade) were obtained from VWR.

3.2.2. Methods

3.2.2.1. Esterification of starch with fatty acids

The esterification reaction of starch with lauroyl chloride was carried out in accordance with the method of Winkler *et al*[27]. Dried starch was first dispersed in pyridine at 10% (w/v) ratio using a homogenizer and transferred to a three neck round bottom flask equipped with a magnetic stir bar and thermometer. It was then assembled in a silicone oil bath under reflux condition and under agitation. A calculated amount of lauroyl chloride (1 mol, 1.5 mol, 2 mol and 4 mol ratio corresponding to the anhydrous glucose unit (AGU) of starch) was added dropwise to the starch dispersion using a burette. The reaction was then conducted at 110 °C for 1h under constant stirring (~400 rpm), after which it was cooled and precipitated in 150mL of ethanol. The precipitate was isolated using vacuum filtration, and solubilized in warm chloroform or THF for purification. It was then precipitated in ethanol and centrifuged to remove the raffinate, and washed twice in ethanol and twice in acetone. The product was then dried overnight under reduced vacuum.

3.2.2.2. Degree of substitution

Elemental Analysis

The carbon content in our samples was determined by combustion conversion into gas, using a 4010 Elemental Analyzer (Costech Instruments, Italy) coupled with a Delta Plus XL (Thermo-Finnigan, Germany) continuous flow isotope ratio mass spectrometer (CFIR-MS). For this, samples were prepared by milling a dried material into a fine powder using a mortar and pestle, followed by drying overnight at 110ºC. The degree of substitution (DS) of the -OH groups of starch with the laurate was calculated in accordance with Vaca-Garcia *et al* (2001)[145], using the relationship between % C obtained from elemental analysis and the DS as shown in equation (3.1) and (3.2):

$$\%\mathrm{C} = \frac{12.011(6+12\quad)}{12.011[6+12\mathrm{DS}]+1.008(10+22\quad)+15.999(5+\mathrm{DS})} \tag{3.1}$$

$$DS = \frac{\%C(0.01)(162.141)-72.066}{144.132-(\%C)(0.01)(182.307)} \tag{3.2}$$

Fourier transform infrared spectroscopy (FTIR)

FTIR analysis was conducted using a Nicolett 6700 by Thermo Scientific FTIR, in which 16 scans were collected and averaged. Sample pellets were prepared by first crushing the individual samples of the modified starch and KBr with a mortar and pestle. The powdered samples were then mixed (5 mg of the samples and 200 mg KBr), dried at 80 ºC for 1h under vacuum, and pressed into pellets at 10,000 psi for 2 minutes using a Carver Press. In the case of the most modified starch sample (using 4 mol lauroyl chloride), the sample was dried, and a thin film was cut from the material for direct scanning. A pellet made of just 200 mg KBr was used as the background when scanning all powder samples, and air was used for the most modified starch

sample. For comparison purpose, the intensities of the graphs were adjusted by normalizing the starch reference peak at approximately 1000 cm^{-1}.

Nuclear magnetic resonance (^{1}H-NMR)

Proton NMR was carried out using a Bruker 500 MHz high-resolution spectrometer. The spectra were acquired on samples dissolved in either DMSO-d_6, C_5D_5N (pyridine-d), or $CDCl_3$ at a frequency of 500MHz at room temperature. The solutions were prepared using 10mg of samples in 0.7mL of solvent, then heating overnight at approximately 80ºC (pyridine and DMSO solubilized samples) and 50ºC (Chloroform solubilized samples).

3.2.2.3. Morphology

X-ray diffractometry (XRD)

X-ray patterns of native starch and modified starch were collected using a Bruker D-8 focus powder x-ray diffractometer operated at 40 kV and 40 mA with Cu Kα. Data was acquired between 2θ of 5º and 50º at a scan speed of 1s/step and increment of 0.02. Powdered samples were used for all XRD analysis except for the highly modified sample. In the case of the highly modified starch (with 4 mol lauroyl chloride), the sample was pressed into a plastic sheet because the resultant product after the reaction was a plastic lump.

Scanning electron microscopy (SEM)

The morphology of starch and modified samples were observed using an Oxford instruments Quanta FEG 250 Environmental microscope. The environmental SEM was used due to the non-

conductive nature of samples. The samples were placed on a stub with double-sided adhesive tape, and photomicrographs were then recorded at various magnifications.

3.2.2.4. Thermal properties and structural analysis

Thermogravimetric analysis (TGA) was carried out using Q500 TGA equipment from TA instruments. 5-10 mg of samples were placed on platinum pans and heated from 25 ºC to 500 ºC with a heating rate of 5 °C/min under nitrogen atmosphere. Differential scanning calorimetry (DSC) was conducted using DSC (TA Instruments, Q-200) in a nitrogen atmosphere. For this test, an accurately weighed sample between 5 and 10 mg was placed on hermetic aluminum pans and loaded onto the instrument. Samples were then scanned from room temperature (25°C) to 220 °C with a heating rate of 20 °C/min to clear the thermal history of the samples. The sample was then cooled to -50 °C, followed by a second heating from -50 °C to 220 °C at the same heating rate as the first heating. The second heating cycle was used to investigate the thermal transitions of the specimens.

Dynamic mechanical analysis (DMA) measurements were conducted using a (TA instrument, DMA Q800), in tension mode on specimens with free dimensions of 0.14 × 12 × 55 mm^3. The tests were carried out by heating the samples from -40 °C to 120 °C with 1 Hz oscillating stress. The storage (E') and loss (E'') moduli and damping factor ($tan\ \delta = E''/E'$) were determined. The glass transition temperature was assigned to the temperature of the maximum loss factor peak combined with the E' drop and the peak of E''.

3.2.2.5. Contact angle measurements

Contact angle measurements were carried out using a custom-built optical sessile drop system equipped with new era pump systems. For this test, the modified starch samples were solubilized

in an appropriate solvent and casted on glass plates. Triplicates of solution casted films were then allowed to dry overnight prior to testing. About 3µL of deionized water droplet was dropped on the surface of the samples, and images were captured using a video camera. These images were taken at 0, 45 s and 90 s after dropping the water to study the interaction of water with the specimens over time, and a Matlab software was used to measure the contact angle.

3.2.2.6. Solubility in organic solvents

The solubility of the starch – fatty acid esters were studied in water, DMSO, THF, chloroform, and toluene to observe how the samples interacted with solvents of different polarities and how solubility changes with the increase in the substitution level.10 mg of each sample was placed in each of the five solvents and homogenized. They were then heated to temperatures below the boiling points of each of the respective solvents for 24 hours while being mixed periodically. The homogenized suspensions or solutions were then kept for 12h undisturbed, and solubility was observed visually.

3.3. Results and Discussion

3.3.1. Esterification of starch

The esterification of starch with fatty acids was conducted in a one-step homogenous process using an activated fatty acid. The activated fatty acid, lauroyl chloride, was a medium chain length fatty acid chloride usually prepared by the action of an excess thionyl chloride on lauric acid that was derived from coconut oil. While the esterification of starch using acid chlorides has been reported in some literatures,[27,146] a controlled esterification that ranges from low degree to complete substitution of the –OH group with laurates to render the starch –fatty acid ester melt

processable, coupled with the structural characterization of the modified material was rather scarce. The reaction in this study was conducted at a constant temperature, agitation and reaction time, while varying the concentration of laurate to the anhydrous glucose unit (AGU) of starch to obtain various levels of substitution.

It was observed that the modified starch stayed suspended in the pyridine solvent despite a high degree of modification. These results were attributed to the effectiveness of using pyridine as the reaction media. The nucleophile pyridine acted here as a reaction media, catalyst and scavenger for the acid (HCl) that could form from the reaction of lauroyl chloride with bound moisture in starch, which otherwise could hydrolyze starch[147]. Figure 3.1 illustrated pyridine's involvement in the reaction as a catalyst, as it initially forms a complex with the reactants (a), then breaks off unchanged (b). This mechanism (a) was proposed by Koivu *et al* (2016)[148]. However, it was expanded to include the proceeding steps (b) where the pyridinium salt is produced, as seen in literature [27]. This is a very important step, because it prevents the production of undesirable HCl from the hydrogen and chlorine ions (in addition to moisture) that can potentially hydrolyze starch into dextrins or glycolized monomers. The formation of a pyridinium chloride by scavenging free Cl^- coming from the acid chlorides was reported before [149].

Furthermore, pyridine worked well as a reaction media due to the increased solubility of the product as the reaction takes place, thereby leaving the product in solution during reaction. Despite the fact that native starch was not soluble in pyridine, the intense homogenization mixing dispersed starch well that resulted in a reactive gel at high temperature (110 °C) during the reaction. As the reaction proceeded, the modified starch stayed as a stable gel in the pyridine that assisted the continuation of the esterification till a complete substitution of the –OH

functional groups with lauric acid[27]. This was much more effective than using traditional starch solvents (e.g. DMSO), as the esterified starch product could experience reduced solubility and perhaps precipitation with an increase in the level of modification, which could limit the extent of modification[27].

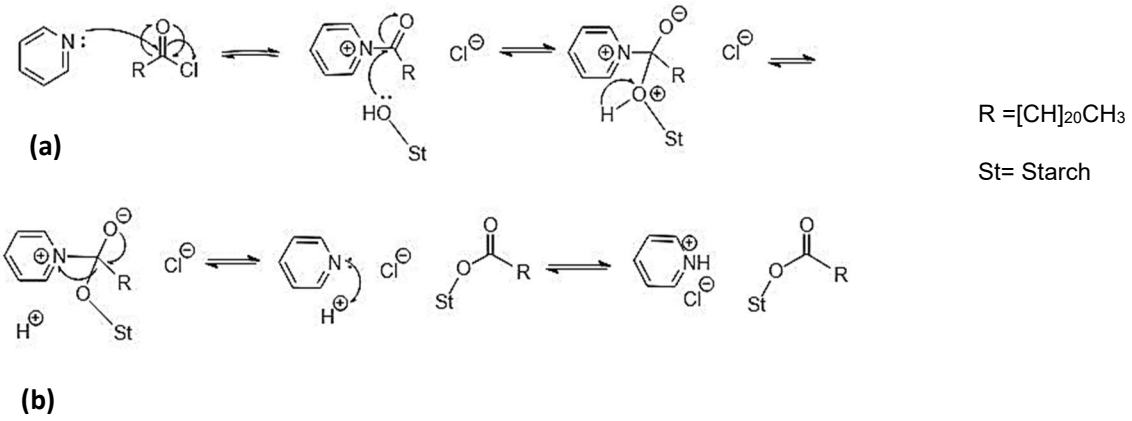

Figure 0.1. Scheme for (a) activation of lauryl chloride with pyridine, (b) esterification reaction of activated lauroyl chloride with starch in the presence of pyridine and Cl-scavenging of pyridine.

The starch – laurate ester products obtained from the reaction were all white powders, excluding the reaction that was carried out using a 4 mol lauroyl chloride/mol AGU ratio. This product was soft and sticky prior to drying. The dried material was a fairly clear, flexible and squishy material. It appeared that the modification that substituted about three laurate chains per glucose monomer (assuming complete substitution) completely transformed the starch into a different material.

The solubility of the starch – laurate esters in certain solvents was also a sign of the product's changed properties. During the washing process, the starch esters with 2 mol and 4 mol ratio of lauroyl chloride (Lauroyl chloride: AGU) exhibited complete dissolution in chloroform. This

was an initial proof that the laurate chains had been introduced, since the addition of the laurate aliphatic groups increased its affinity for solvents with lower solubility parameters. The solubility parameters of DMSO and water, which both solubilize native starch, are 26.4MPa$^{1/2}$ and 48MPa$^{1/2}$ respectively; whereas chloroform has a lower solubility parameter of 18.7 MPa$^{1/2}$ [150]. The sample modified with 1 mol lauroyl chloride was soluble in THF, indicating low degree of modification [27]. However, an excess of THF solvent was needed for such dissolution. On the contrary, it was noted that pyridine could completely dissolve this material at concentrations as high as 1.4% (w/v) pointing out that, there was some degree of modification as starch is only dispersible in pyridine. Starch – laurate esters prepared with 1.5 mol ratio lauroyl chloride exhibited an enhanced solubility, indicating a higher degree of modification in comparison to the use of 1 mol ratio of lauroyl chloride. The solubility observations here were in agreement with Winkler *et al*[27].

3.3.2. Degree of substitution (DS) analysis using elemental analysis (EA) and ^{1}H-NMR

The degree of substitution of –OH groups with lauric acid as a result of the esterification was estimated using elemental analysis (EA) and ^{1}H-NMR techniques. The mass percentages of carbon determined via elemental analysis are presented in Table 3.1. The EA degree of substitution was then calculated based on these carbon percentages using Equation (3.2). The results showed that the degree of substitution increased with an increase in the concentration of the mole ratio of lauroyl chloride to the starch in the reaction while keeping other reaction conditions (e.g. temperature, mixing rate, time) constant. It was interesting to note that the use of 4 mol ratio of lauroyl chloride resulted in an almost complete –OH substitution (DS 2.9 from a possible DS of 3).

Table 0.1. Percent carbon, degree of substitution calculated using elemental analysis (DS_{EA}) and DS calculated form 1H-$_{NMR}$

Sample	% C (average from EA)	*DS_{EA}	*DS_{NMR}
Starch	44.64 ± 3.1	-	-
1 mol ratio	55.79 ± 4.2	0.46 ± 0.01	0.45 ± 0.01
1.5 mol ratio	64.49 ± 2.1	1.21 ± 0.01	1.31± 0.03
2 mol ratio	68.77 ± 3.9	2.10 ± 0.17	1.96 ± 0.02
4 mol ratio	70.90 ± 5.1	2.88 ± 0.19	2.92 ± 0.07

* Values are average ± standard deviation.

^{1}H-NMR spectra were collected for native starch and modified samples, and results are presented in Figure 3-2. This was to verify the degree of substitution obtained from the elemental analysis. From the native starch spectra, it was evident that the protons showed up starting from about 3ppm. Contrarily, peaks appeared starting from the three terminal hydrogens of the laurate chain (0.85 ppm) on the starch – laurate esters. This included the first methylene group beside the carbonyl group (2.1-2.4ppm), the next methylene group (1.5ppm), and all other methylene groups on the chain (1.2ppm)[140]. The peaks had slightly shifted upwards for the starch – laurate esters with DS 0.5 and DS 1.2, where the corresponding peaks occur at about 0.95 ppm, 2.5ppm, 1.8ppm, and 1.3 ppm, respectively. This shift could be attributed to the use of a different solvent.

Pyridine was used for the low DS esters as opposed to chloroform that was used for the high DS (2.1 and 2.9) esters, as the solubility of these esters were limited to chloroform.

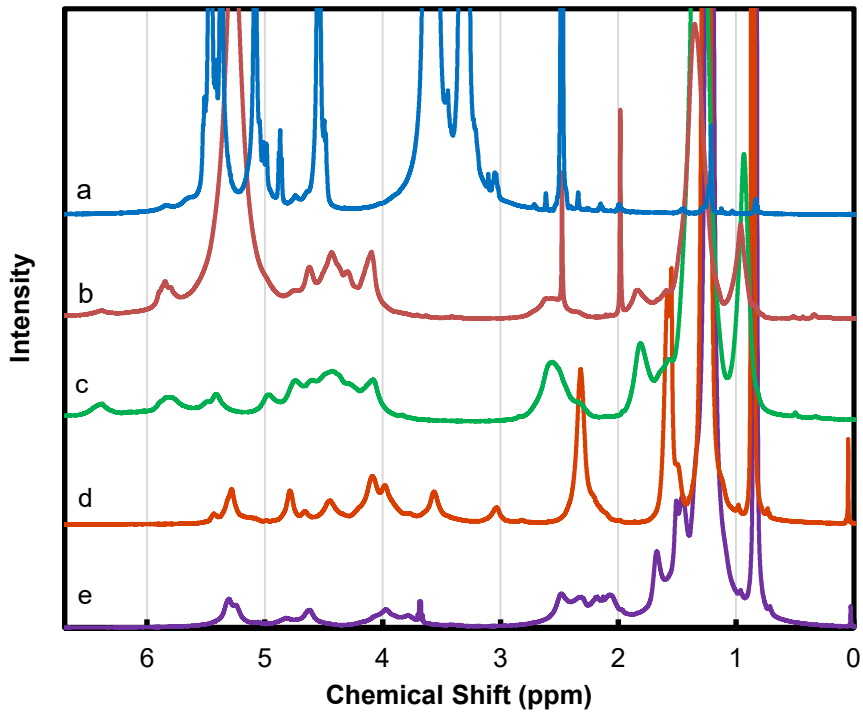

Figure 0.2. ^{1}H-NMR spectra of (a) native starch in DMSO, (b) 0.5 DS ester in pyridine, (c) 1.2 DS ester in pyridine, (d) 2.1 DS ester in $CDCl_3$, and (e) 2.9 DS ester in $CDCl_3$

In both esters that were solubilized in chloroform (DS 2.1 and 2.9), proton signals were observed at 3.6-4.3ppm, 4.5-5ppm, and 5-5.4ppm, corresponding to the three peaks outlined in Figure 3.2. Due to the large peak area compared to the other peaks, it was assumed here that the last peak consisted of overlapping protons. Also, there were three peaks at 4.4ppm, 3.5ppm and 3ppm on the DS 2.1 starch ester that were here assigned to the protons of the hydroxyl groups due to their disappearance in the 2.9DS ester, as shown in Figure 3.3. For the calculations of the degree of substitution, the signal from methyl group of laurate (0.85ppm) was compared to the signals of starch observed at 3.6-4.3ppm, 4.5-5ppm, and 5-5.4ppm. This was similar to the method reported

by Namazi *et al* [140], where the signals of protons from 4.58-5.5ppm were used as the reference corresponding to starch. The spectra of the lower DS esters contained several overlapping peaks, so the signals from the hydroxyl groups could not be distinguished from the hydrogen peaks. For these samples, it was assumed that the number of hydroxyl groups of starch did not change much after the modification, as the degree of substitution was lower. Therefore, the signals from the hydroxyl groups were included in the starch reference signals.

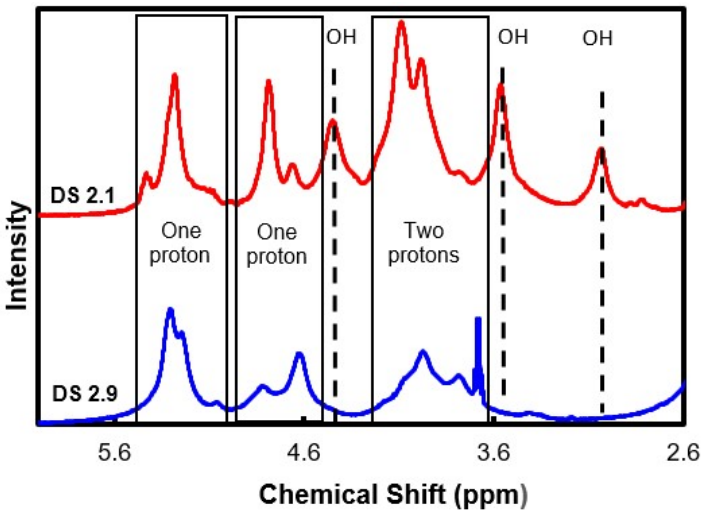

Figure 0.3. ^{1}H-NMR spectra of the proton signals of the starch backbone, for the 2.1DS and 2.9 DS esters dissolved in $CDCl_3$.

The DS values were then calculated in accordance with Equation (3.3) for the DS 2.1 and 2.9DS samples, and in accordance with Equation (3.4) for the 0.5 and 1.2 DS esters, and results are presented in Table 3.1.

$$DS = \frac{\frac{I_{Signal1}}{3}}{\frac{I_{AGU1}}{4}} \tag{3.3}$$

$$\mathrm{DS} = \frac{\frac{\mathrm{I_{Signal2}}}{3}}{\frac{\mathrm{I_{AGU2}}}{7}} \tag{3.4}$$

where I_{Signa} refers to the integral the methylene signal at 0.85 ppm and, I_{AGU1} refers to the integral of the four protons at 3.6-4.3ppm, 4.5-5ppm, and 5-5.4ppm on the higher DS samples. $I_{Signal2}$ refers to the integral of the methylene signal at 0.95ppm and I_{AGU1} refers to the integral of the four signals from the starch backbone and the three from hydroxyl groups, which appeared between 4-6.4ppm on the lower DS samples. Comparison of the degree of substitution obtained from EA and ^{1}H-NMR exhibited good agreement as shown in Table 3.1.

3.3.3. Structural evolution due to esterification by FTIR spectroscopy

A comparative structural study between the native starch and the corresponding starch-laurate esters were monitored by FTIR spectroscopy (Figure 3.4). IR results revealed clear structural changes as a result of the esterification. The broad peak between 3000-3600 cm^{-1}on Figure 3.4 (a and b) was attributed to the vibrational stretching of hydrogen-bonded OH groups [27]. The peak intensity reduced with an increase in the degree of esterification (Figure 4 c, d, and e) due to the substitution of the starch -OH groups with laurate chains. A strong and sharp peak within the OH band was also noted at approximately 3565 cm^{-1} in the samples with a DS ≥2. This was most likely due to the occurrence of free OH groups with limited hydrogen bond forming capability. When many of the starch -OH groups were replaced, the remaining ones became more isolated and had no adjacent -OH groups with which they could form inter- or intramolecular hydrogen bonds [151], resulting in a diminished peak.

The peak that loomed at approximately 1740 cm^{-1} in the starch– laurate samples was attributed to the vibration of an ester -C=O bond that was formed as a result of the esterification modification. The ester peak intensity increased with the the degree of substitution, elucidating the increased

ester formation connecting laurate chains to the starch molecule. The peaks at 2925 cm^{-1} and 2852cm^{-1} were attributed to the -CH vibrations[27]. As expected, the esterification of aliphatic fatty acid caused a gradual increase with the increase in the degree of esterification. This peak was prominent with the most esterified starch (DS 2.9). Because this sample was not prepared in the conventional way with a similar concentration to the other samples (as shown in the methods section), the peaks within the -CH signal could not be resolved. The peak around 2850 cm^{-1} was specifically representative of the aliphatic -CH bonds introduced by the substituted laurate [140]. This was an additional evidence of the substitution of the hydrocarbon chains, as this peak appeared only in the modified starches and exhibited an enhanced intensity with increasing DS, as noticed from Figure 3.4 (b, c, and d).

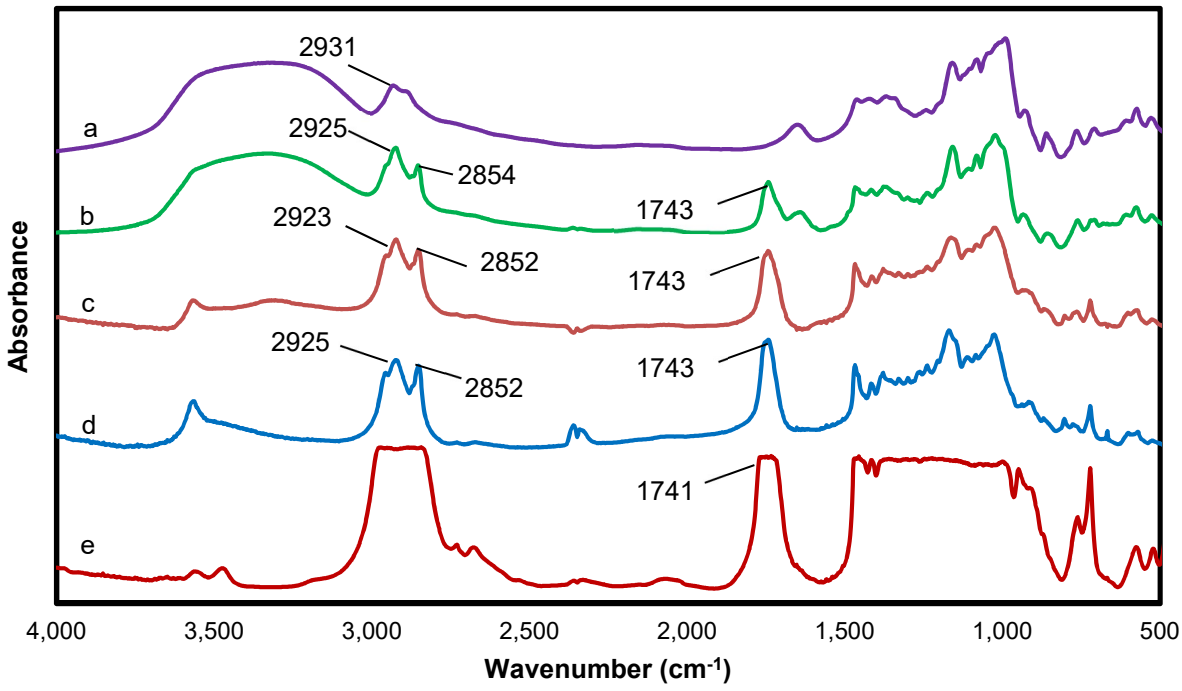

Figure 0.4. FTIR spectra of (a) starch, (b) Starch ester DS 0.5, (c) Starch ester DS 1.2, (d) Starch ester DS 2.1, and (e) Starch ester DS 2.9.

3.3.4. Effect of lauric acid esterification on the morphology of starch

X-ray diffractometry was used to analyze crystallization behavior of the native and esterified starch, and the diffraction patterns are laid out in Figure 3-5. The native starch exhibited type A crystalline structure that is typical of cereals starch, with two single peaks at 2θ of 15° and 22°, and a doublet at 17° and 18°. It is well established that starch is a semi-crystalline polymer with the branched amylopectin chains responsible for the crystallinity while the linear amylose responsible for the amorphous segments[152]. The formation of inter- and intramolecular hydrogen bonds is responsible for the highly ordered crystalline structure in starch. At low degree of esterification (DS 0.5), only a few hydroxyl groups have been replaced by the lauric acids, therefore the formation of intermolecular hydrogen bonding was possible. However, the diffraction results exposed that the granular crystal has been damaged, and a broad peak was noted even with this low DS. This loss in crystallinity indicates that modification took place not only in the amorphous region, but also in the crystalline region. This was because the starch has swollen enough via the pyridine at the reaction temperature that provided access for the substitution of –OH with lauric acid to occur in regions that are not otherwise accessible. Additionally, a small new peak emerged at 2θ of 8° that could be attributed to the crystallization of laurate. Kong *et al.*[153] reported similar crystallization of lauric acid in polyurethane (PU) conjugates as a result of a combination of peaks of PU and lauric acid substituent.

As the DS increased, the crystal peaks became narrower and narrower owing to the incorporation of an increased number of medium chain laurates that pushed the starch molecules apart. This gave rise to an increased mobility of the substituted chains and more free volume causing limited crystal formation. At a high degree of modification (DS 2.9), the crystalline structure was

completely lost and the starch- laurate provided a broad and low-intensity diffraction pattern indicating that this material was completely amorphous. This has resulted from an almost complete replacement of the hydroxyl groups with the laurate. Such replacements would not allow re-establishment of hydrogen bonds that are accountable for the formation and stabilization of starch crystals.

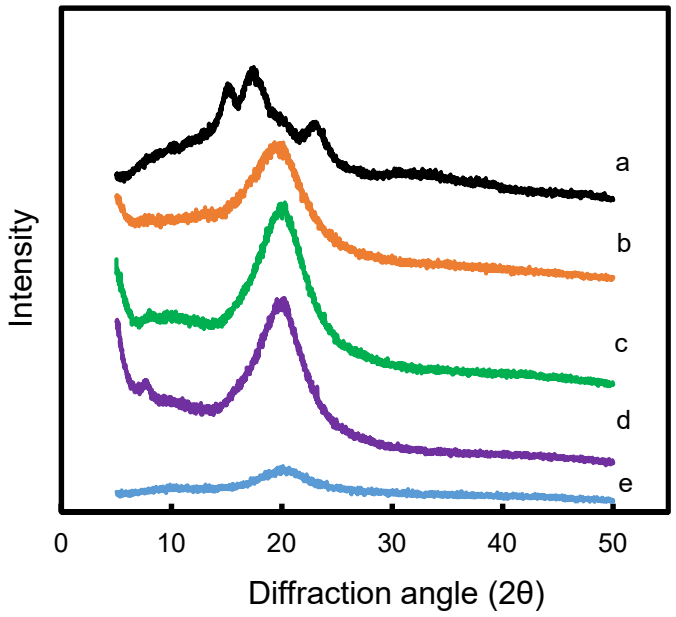

Figure 0.5. XRD pattern of (a) native starch, (b) DS 0.5 modified starch, (c) DS 1.2 modified starch, (d) DS 2.1 modified starch, and (e) DS 2.9 modified starch.

The effect of esterification on the morphology of starch was further investigated using scanning electron microscopy (SEM), and images are illustrated in Figure 3.6. Upon the incorporation of laurates, the round and smooth granules of the native starch (Figure 3-6a) started to change. A low degree of laurate substitution (DS 0.5) maintained the granules with minor surface deformation and roughness as shown in Figure 3.6b. As the substitution density increased, a significant deformation of the granules was observed. For instance, the esterification with a DS

of 2.9 resulted in complete disruption of the granules resulting in a porous and amorphous structure. In summary, the XRD and SEM morphology study clearly illustrated that the incorporation of laurate to starch transformed it into a novel material with no tendency of crystallization. This has been a limiting factor in many starch modification efforts for bio-plastic applications.

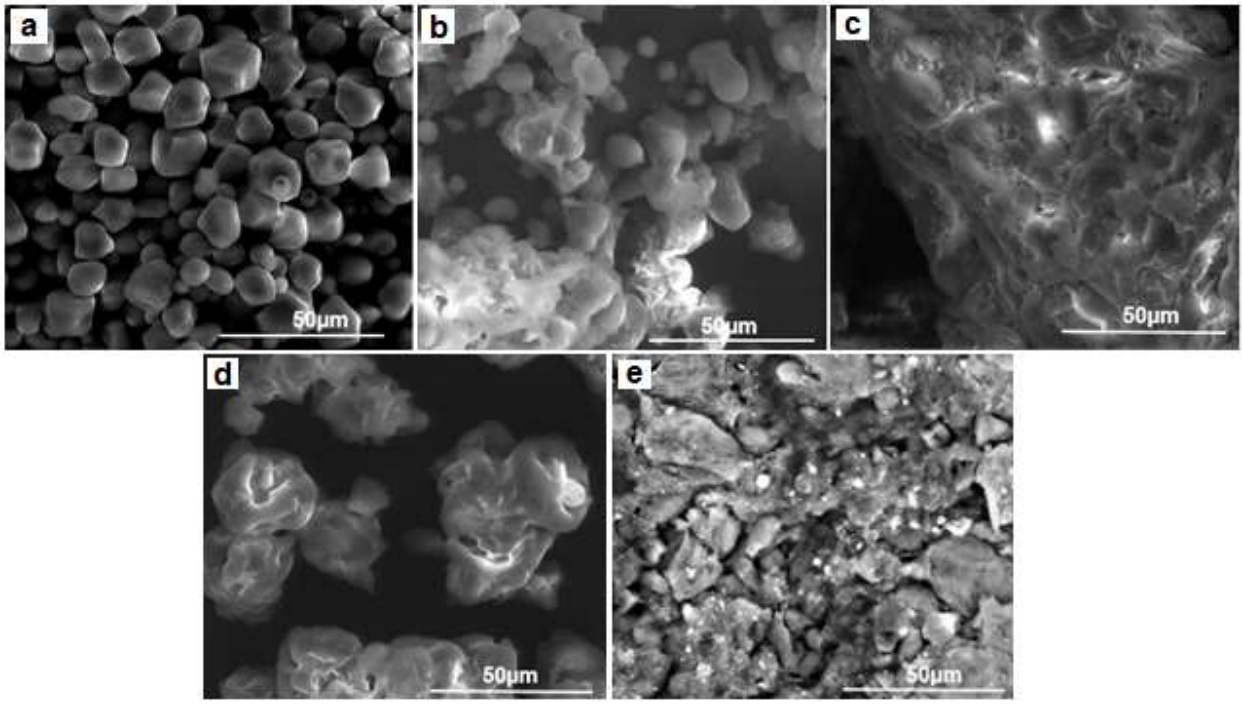

Figure 0.6. SEM images at magnification 1000x of (a) starch (b) Starch ester DS 0.5, (c) Starch ester DS 1.2 (d) Starch ester DS 2.1, and (e) Starch ester DS 2.9

3.3.5. Thermal stability of the starch- laurate ester structures

The thermal stability of the starch ester polymers is an important attribute for their use in thermoplastics, as most plastic processing operations require high temperature. Studies[154–156] have shown the thermal degradation of starch involves the dehydration of the –OH from the glucose monomers followed by main chain secession to produce volatile compounds. The –OH

significantly participate in thermal condensation reactions, and are responsible for thermal degradation below 300 ^{o}C [157]. Thus, the replacement of the starch –OH moieties via laurates could improve the thermal stability. TGA study was conducted over a temperature range of 25 ^{o}C to 600 ^{o}C and results of weight loss are presented in Figure 3.7 (a and b).

The lauric acid incorporation invariably altered the thermal degradation behavior. A higher degree of lauric acid substitution (DS 2.1 and 2.9) resulted in a remarkable improvement in both the onset and peak degradation temperatures, illustrating the suppression of the starch degradation via –OH dehydration. However, the onset degradation temperature of the low DS esters was slightly lower than the native starch despite the overall thermal stability improvements. Similar results were reported by Elomaa *et al*[63] in their study of acetylated starch, where the degradation of lower DS starches occurred in two stages: one below and the other above the onset degradation of starch.

The reduction in the onset of degradation was more evident in the DS 0.5 sample where two degradation stages occurred, as seen by the two apparent equal peaks in the weight % derivative curve of Figure 3.7b. The first peak began at lower temperatures compared to starch but followed the same peak degradation and endpoint. The first peak was most likely from the –OH groups of the unmodified portion of starch within the low DS sample. The reduced initial degradation temperature compared to starch was possibly due to the disruption of the crystal structure of starch as a result of the modification. The loss of crystallinity as such increased the number of exposed hydroxyl groups available for thermal dehydration as compared to the semi-crystalline structure of native starch where some of this –OH groups are hidden in the crystal structure. The second peak, similar to starch, could be attributed to the degradation of the main polymer chain.

The peak degradation temperatures of native starch and starch –laurate esters are listed in Table 3.2. It was observed that the most thermally stable material was the highly modified starch-laurate (DS 2.9), which exhibited a peak degradation that is 68 ºC above that of native starch. Though the onset degradation temperatures of the low DS starch esters were generally below that of starch, it was evident from the plots that such weight loss in the early stages was minor. A marked thermal stability enhancement was noticed as a result of high fatty acid substitution density as observed from the DS 2.1 and DS 2.9 starch esters. Moreover, a single stage and sharp derivative degradation peak were observed in the esters that were indicative of a great structural uniformity as a result of the modification. This was quite a contrast with native starch, where the amylose and amylopectin display varying levels of thermal stability and as a result non-uniformity as a biomolecule. While the thermal stability of pure lauric acid is not specifically impressive (197°C)[158], the starch – laurate ester network generally showed good stability. In summary, the incorporation of fatty acids on starch positively affected the thermal stability and structural uniformity of starch. Highly modified starch with a DS of 2.1 and 2.9 exhibited a peak degradation temperature of 362 °C and 364 °C, respectively. These degradation temperature ranges point out that they are amenable for thermoplastic processing as a sole bio-polymer, or to be melt blended with other traditional polymers. This is because most commodity polymers (e.g. PLA, PHB, PE, EVA, PPC)[132,159,160] that can potentially be blended with the starch – laurate are processed within a temperature range of 120 to 220 °C.

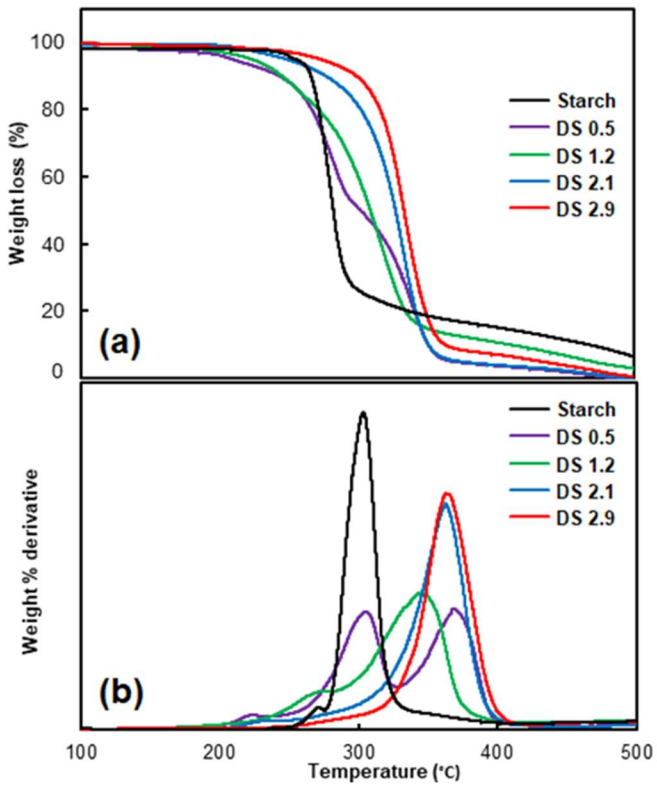

Figure 0.7. (a)TGA plot of native starch and modified starch esters, and (b) weight loss derivative.

Table 0.2. List of maximum degradation temperatures obtained from TGA.

Sample (DS)	Peak Degradation Temperature (°C)	10 % weight loss Temperature (°C)
Native starch	303	290
0.5	305 (1st stage) 368 (2nd stage)	267
1.2	343	267
2.1	362	305
2.9	364	330

3.3.6. Surface wettability behavior

The use of contact angle measurements to study the surface wettability and other surface properties is well established. Typically, the surface wettability behavior of polymers is expressed using a contact angle formed between the solvent droplet and the polymer that comes in contact, and how they interact with time. In this study, deionized water was used as the solvent to study the water wettability of native and modified starch films. The water droplet spread on native starch films as shown in figure 3.8a forming a small contact angle. This was due to the strong interaction of water with the hydrophilic native starch. As expected, the water kept spreading and got absorbed by the native starch film with time. As laid out in Figure 3.8b, about 34% reduction in the contact angle was observed within the 90 s observation time for native starch films.

On the contrary, the lauric acid modified starch films exhibited hydrophobicity with contact angles greater than 90°. The increase in contact angle resulted from the replacement of the hydrophilic hydroxyl group in starch by the hydrophobic aliphatic chains of the lauric acid. The water resistance of modified samples improved significantly even with the DS 0.5 starch – laurate depicted by the high contact angle (>90) formed. The images presented in Figure 8a also revealed no visual change in the size of the droplet at 0, 45 and 90 s for modified materials, indicating very minimal or no water absorption by the starch- laurate samples as opposed to the native starch. Thitisomboon *et al*[144] noted similar results for octanoyl and dodecanoyl modified starch esters. Their study showed a contact angle of 80.5° at a DS of only 0.32. The plot of the

measured contact angle against time (Figure 3-8b) validated the minor interaction between water and the modified films, represented by a rather slight reduction in contact angles over time.

An increasing trend of hydrophobicity with an increase in the DS of the starch was expected in the study. However, discrepancies to this notion was observed in our study. This was due to the variation in the surface smoothness/roughness of the sample films, as this method does not consider surface roughness. It is generally recommended to evaluate the surface roughness of the sample using atomic force microscopy or other methods prior to contact angle measurements for more accurate results. Overall, the introduction of such hydrophobic substituent in starch, that clearly reduced the surface energy, is expected to increase its compatibility with other non-polymers in a blend formulations[4,161].

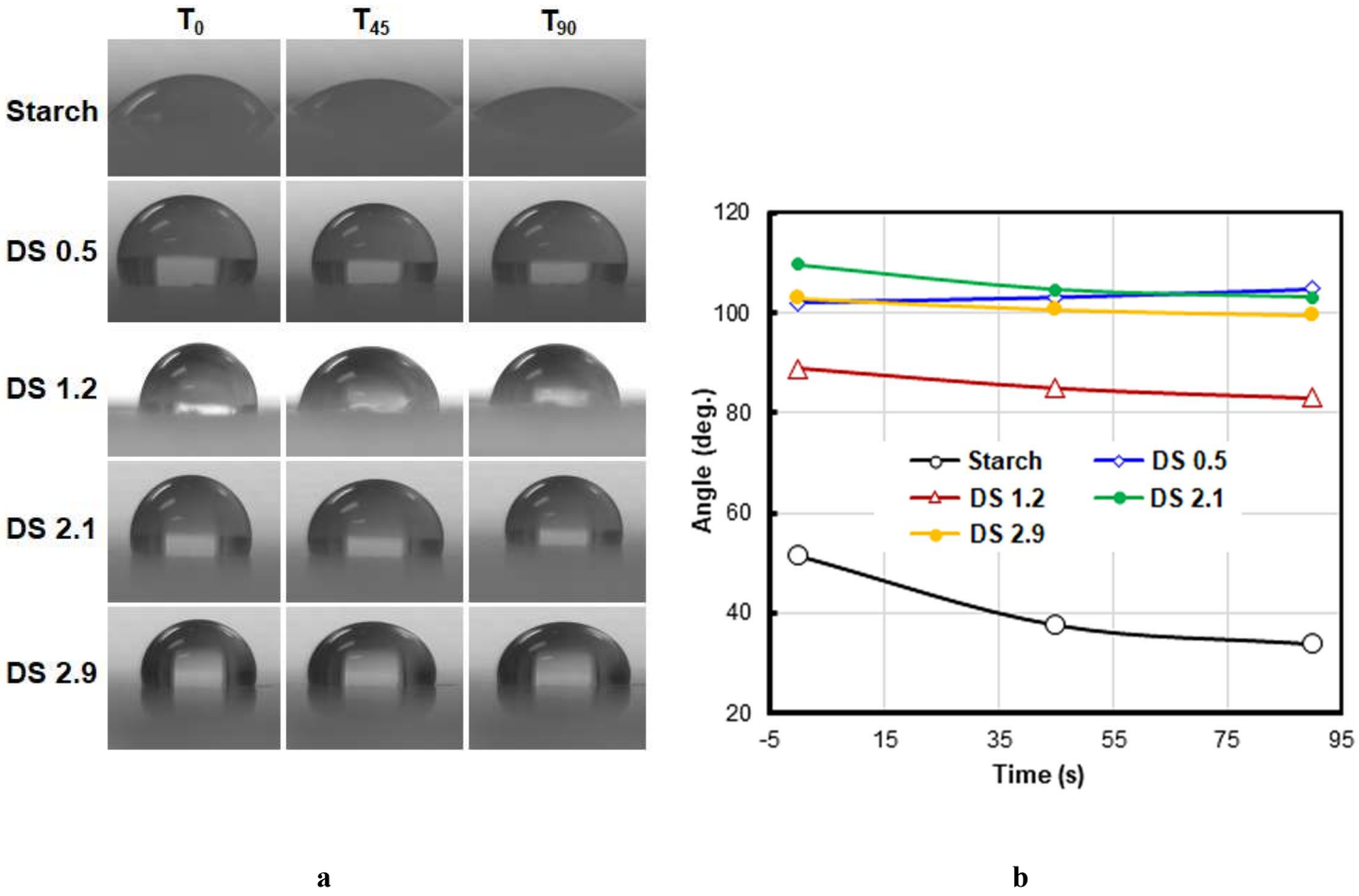

Figure 0.8. (a) Contact angle images of native and modified starch as a function of time, (b) Plot of contact angle values of starch and modified starch at varied times.

3.3.7. Solubility studies

Examination of the solubility behavior of polymers in solvents is essential to understand the solvent tolerance of the polymer, to conduct structural characterizations (e.g. NMR, or gel permeation chromatography), and to prepare solution cast films. The solubility behavior of native starch and starch – laurate samples were inspected in a range of solvents with various polarities (water, DMSO, THF, chloroform, pyridine, and toluene), and results are shown in figure 3-9. The solubility or lack of solubility of these polymers in various solvents illustrated

how the incorporation of fatty acid has changed the polarity of the molecule. An increased hydrophobicity of the lauric acid modified starch samples was observed from their poor interaction and sedimentation in water, as opposed to native starch that formed a soluble homogenous gel. Similar solubility examination in DMSO exhibited that native starch swelled and solubilized. Contrarily, the modified starch samples did not solubilize in the DMSO solvent, as particles were evidently visible. This was because DMSO is polar and a good starch solvent. The fatty acid modification clearly reduced their polarity making them less soluble [27].

Pyridine was proved the best solvent for the starch- laurate esters with DS 0.5, 1.2, and 2.1. The DS 0.5 esters solubilized almost completely and the other two solubilized completely. The two low DS esters (DS 0.5 and DS 1.2) were insoluble in the less polar solvents (THF, chloroform, and toluene) due to their relatively lower hydrophobicity. The solubility of the DS 2.1 modified material was also improved in these solvents, as noted from its solubility in chloroform and toluene. As expected, the DS 2.9 starch- laurate ester became more soluble in the more non-polar solvents, with its best solubilization in toluene.

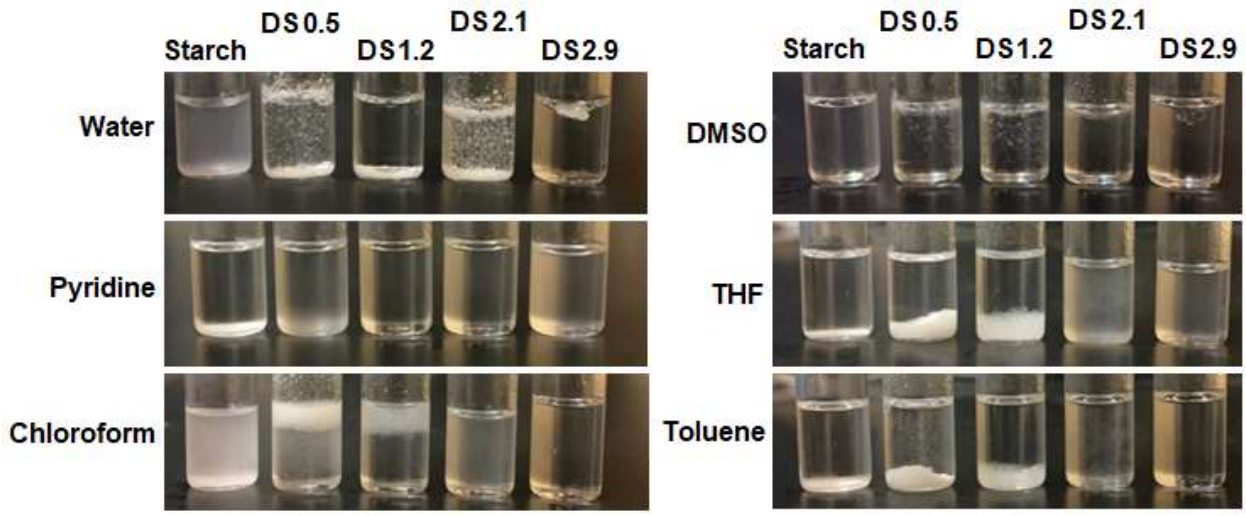

Figure 0.9. Solubility of native starch, and fatty acid modified starch at various levels (DS 0.5, DS 1.2, DS 2.1, and DS 2.9) in solvents with a range of polarities.

3.3.8. Starch- laurate material characterization: Structure – property relationships

The molecular dynamics of polymers as a result of absorption or release of heat can be conveyed as localized and cooperative chain motions, expressed as α, β, and γ relaxations in the order of decreasing temperature. Because of these relaxations or free volume changes, polymers have viscoelastic behavior, *i.e*. the material has properties between an elastic solid and a viscous liquid. Dynamic mechanical analysis (DMA) was used here to evaluate the viscoelastic behavior of starch- laurate as a function of temperature. Because of the high degree of modification, starch- laurate with DS 2.1 and 2.9 forms continuous, and transparent films via a solvent casting process as shown in Figure 2.10a. Native starch and starch- laurate with low DS (DS 0.5 and 1.2) could not form a continuous film without an external plasticizer, thus they were not included in the DMA study.

At low temperature, the polymer chains are tightly packed and as such, the specimens were stiff. As the temperature increases, the packed chains started to relax and expand resulting in an increase in free volume. The free volume increase allows localized bond movements that include bending and stretching (T_α) [162]. With further heating, polymer chains in the amorphous region started to exhibit a coordinated large-scale motion. The temperature at which the amorphous region displays such motion is the glass transition temperature (T_g). The T_g of the specimens, as determined from the peak of *tan δ*, was 47 °C and 97 °C for the starch- laurate ester samples with DS of 2.9 and 2.1, respectively. Determination of *Tg* from the peak of the loss modulus displayed a lower value (24 °C for DS 2.9, and 65 °C for the DS 2.1 starch- laurate). The storage modulus curve (Figure 3.10b) of the starch – laurate modified plastics illustrated a continuous loss of modulus with an increase in temperature, and neither samples showed a plateau within the studied temperature range. A peak in loss modulus and tan δ accompanied the change. The lack of plateau was because the glassy state of these plastics were below the studied temperature range (< -45 °C), and the samples were already in the rubbery region above -45 °C. Overall, the storage modulus was significantly affected by the variation in the degree of substitution. As the substitution of the –OH with lauric acid increased from a DS of 2.1 to DS 2.9, the storage modulus displayed orders of magnitude reduction. The DS 2.1 and DS 2.9 modified starch specimens displayed a modulus (*E′*) of 26 MPa and 229 MPa at room temperature (23°C), indicating of the flexibility of the materials in line with the visual observation (Figure 3-10a).

The intensity of *tan δ* peak reflects the extent of mobility of the polymer chain segments at the glass transition temperature [163,164] While the higher intensity of *tan δ* peak is indicative of higher energy dissipation and thus more viscous behavior, lower *tan δ* intensities point out less viscous

and higher elastic behavior. The high degree of starch modification (DS 2.9) exhibited about five-fold peak intensity as compared to the DS 2.1 materials (Figure 3.10d), indicating its enhanced viscous behavior. Moreover, the highly modified starch (DS 2.9) exhibited a narrow *tan δ* peak, indicating structural homogeneity as compared to the DS 2.1 starch – laurate material. This was in agreement with the structural uniformity that was observed on the TGA of these samples. The observed structural changes here indicated that the incorporation of fatty acid on starch polymer chains acted as an internal plasticizer. This assertion was supported by the observed reduction in the glass transition temperature, and the enhanced flexibility (reduction in modulus) with the increase in DS. The fatty acid chains incorporated on the starch prohibited inter and intramolecular hydrogen bond interaction among starch chains that was responsible for starches crystallinity and lack of flexibility (Figure 3.11).

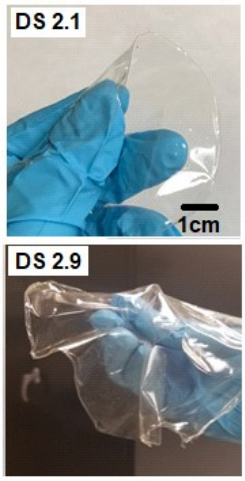

a

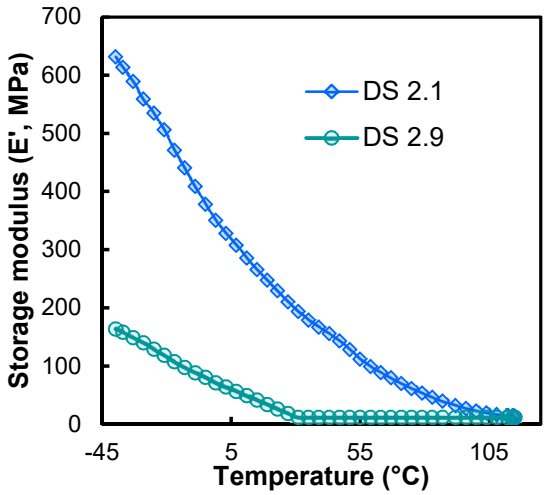

b

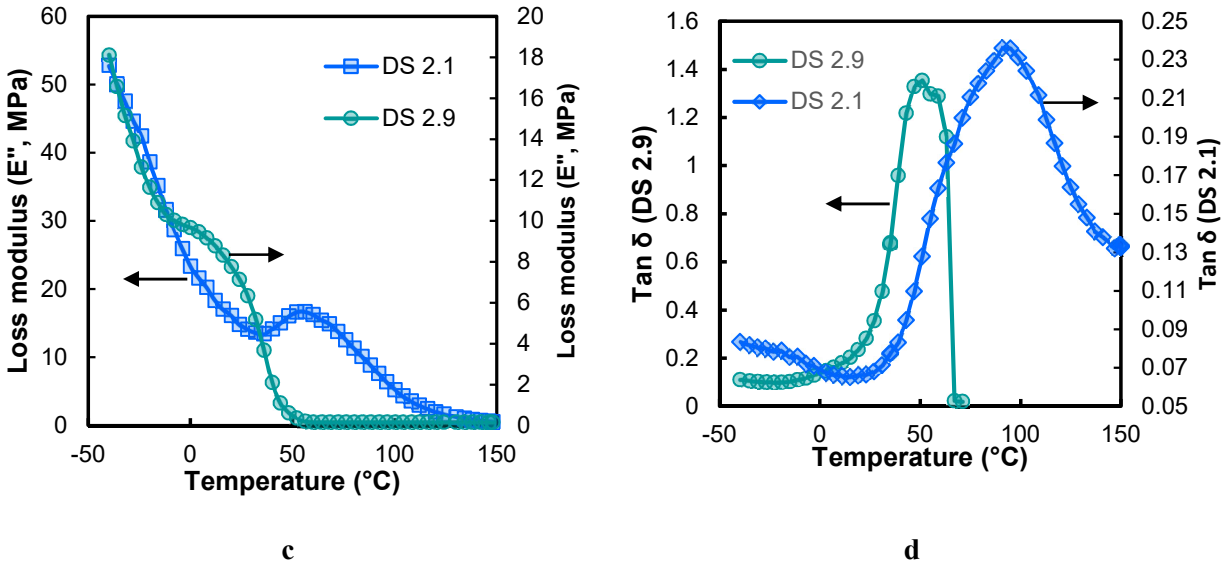

c d

Figure 0.10. (a) Image of highly modified starch films (DS 2.1 and 2.9); DMA plot of the films (a) Storage modulus (E′), (b) Loss modulus (E″), (c) Loss factor (tan δ).

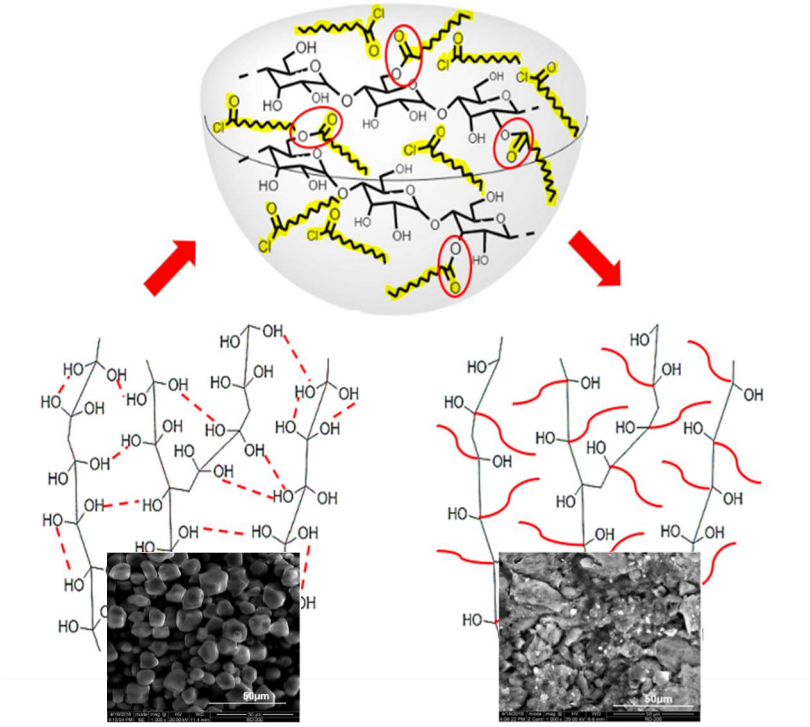

Figure 0.11. Schematics illustrating the substitution of hydroxyl group of starch with fatty acid, resulting in blocking of hydrogen bonds and amorphous morphology.

3.3.9. Structural characterization using DSC

DSC was employed to further elucidate the thermal events, and phase transitions (e.g. glass transition, crystallization, and melting) in the starch – laurate esters. DSC thermograms of the materials are illustrated in Figure 3.12. It is known that native starch polymer does not exhibit melting temperature upon heating owing to the inherent strong hydrogen bonds that pushes the melting temperature beyond the decomposition temperature. Thus, it typically degrades before melting temperature event is observed making it unsuitable for melt processing. Modifications, such as the esterification with fatty acids, could render it melt processable by blocking hydrogen bonds that result in packed structure. The thermal behavior of fatty acid modified starches depends on the length of the attached acyl group[49]. Winkler *et al*[26] classified short chain carbon fatty acid (C_6-C_{10}) starch esters as completely amorphous materials because no melting endotherms were observed in their thermograms. The degree of esterification also plays a significant role on the thermal behavior of modified starch as noted from the DMA study.

A summary of the T_g and melting temperature (T_m) of native and the lauric acid modified starch samples observed from DSC study (Figure 3.12) are presented in Table 3.3. The T_g of native starch occurred at 72 ºC. Upon incorporation of the lauric acid (C_{12}) on the starch structure, a reduction in T_g was observed. The reduction trend was proportional to the degree of substitution substantiated by the downward shift of T_g with higher DS as a result of enhanced chain mobility. This was in agreement with the DMA observation that was conducted for DS 2.1 and 2.9. Similar results were obtained by Winkler *et al*[26] and Vanmarcke *et al*[49]. Melting endotherms were observed at 156 ºC, 126 ºC and 108 ºC for DS 1.2, DS 2.1 and DS 2.9, respectively. No melting endotherm was observed for DS 0.5 modified starch. This was because such a low

degree of lauric acid substitution did not inhibit the hydrogen bonds and the material can still form packed crystals as observed from the XRD study.

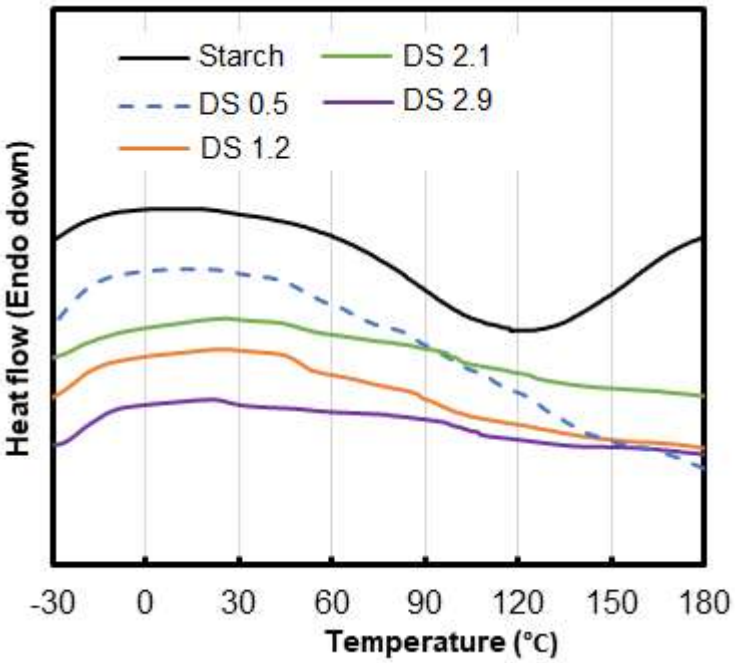

Figure 0.12. Second heating DSC curves of starch and modified starches

Table 0.3: Glass transition and melting temperatures of native and modified starch with various DS

Sample (DS)	T_g (°C)	T_m (°C)
Starch	72	-
0.5	60	-
1.2	53	156

2.1	49	126
2.9	28	108

3.4. Conclusions

In this study, the incorporation of lauric acid (C_{12}) via the replacement of the –OH functional groups of the glucose on starch chains was demonstrated using a one-step homogeneous process. The mole ratio of the activated fatty acid, lauroyl chloride, to the starch was varied in the reaction to obtain starch esters with various levels of substitution. Overall, the incorporation of lauric acid on the starch chain altered the thermal stability, polarity and thus the water affinity at various degrees depending on the level of modification. Interestingly, an almost complete substitution of the –OH groups of starch was achieved with the use of 4 mol ratio of lauroyl chloride per AGU. This was validated by FTIR, EA and proton NMR. A higher level of fatty acid incorporation on starch resulted in a complete disruption of the crystalline structure of starch with no re-crystallization behavior. This was well supported by the SEM and XRD studies. The observed hydrophobicity and melt processability of the starch- laurate esters were clear indicators of the potential of such materials to be used as a bio-plastic without the need of an external plasticizer or other modifiers. Also, the reduction in surface energy would make it more compatible with other aliphatic polymers (e.g. PLA, PHB, EVA etc) to produce blends. Overall, the starch- laurate ester polymers produced in this research exhibited melting behavior, thermal stability, excellent clarity, and promising mechanical properties pointing out that it can be melt processed via typical polymer processing tools as observed from the structural investigations. Since the backbone chain (glycosidic bond) was maintained in the esterification process, we

expect that it will be biodegradable. Synthesized starch – laurate ester polymers exhibit mechanical and thermal performance ranges comparable to some ethylene vinyl acetate (EVA) copolymers and are therefore promising as a renewable alternative. Possible applications of these polymers include packaging, toys, coating, grocery bags, drug delivery, agricultural mulch films and other advanced material applications.

Chapter 4. Functionalized Starch Microparticles for Antimicrobial Polymer Surfaces[3]

4.1. Introduction

The growing concern of illnesses caused by pathogenic microorganisms has triggered an increased need for innovative antimicrobial materials which are able to kill or inhibit the growth of pathogenic microorganisms. These materials find use in healthcare, personal care, and food management sectors[165,166] such as packaging materials, sanitary products, gloves, biomedical devices and surfaces which are very susceptible to microbial attack and contamination leading to health-related illnesses. Antimicrobial food packaging materials, for instance, can extend the shelf life of food by minimizing microbial spoilage.[167–169] This could reduce or eliminate the need for preservatives or other additives, which are currently used to assure product safety.[170,171] Biomedical applications of antimicrobial materials as medical device packaging or as materials in contact with the human body such as implants or biomedical devices (e.g. valves, catheters, vascular grafts etc.) is of great interest.[166,172] While antibiotics have long been used to prevent and treat infectious microbial diseases, increasing prevalence of antibiotic resistance in pathogenic microorganisms[173] has spurred interest in the development of materials to control the spread of microorganisms.

Antimicrobial materials can be divided into two general categories based on their mode of action. First, surface coatings or surface modifications can be applied which prevent microbial

[3] A version of this chapter has been submitted for peer-reviewed publications. Ojogbo, E., Ward, V., Mekonnen, T. Functionalized Starch Microparticles for Contact-Active Antimicrobial Polymer Surfaces (Under review).

growth by either leaching of an antimicrobial agent from the surface, or by deactivating bacteria upon contact. Surface modifications can be polymeric (e.g. chitosan), or involve the addition of natural (plants, animals, and essential oils), or synthetic products (silver nanoparticles, peptides, and quaternary ammonium salts),[170] Leaching occurs by diffusion which causes the movement of antimicrobial agent out of the surface material resulting in a change in its concentration in the packaging, and eventually loss of its antimicrobial efficacy when it falls below the minimum inhibitory concentration.[174] On the other hand, the 'on-contact' mode of action deactivates the microorganism when it comes in contact with a surface containing the antimicrobial agent. This is typically achieved by immobilizing the antimicrobial agent on the surface through a covalent bond or through strong mechanical interlocking. As a result, these surfaces do not lose their antimicrobial efficiency like leaching materials. For permanent sterile surfaces however, the build-up of dead bacteria coating on surfaces over time should be considered as this could prevent further contact with bacteria and a reduction in overall antimicrobial efficiency.[175]

This study focuses on grafting of a modified guanidine polymer onto starch using a coupling agent for antimicrobial polymer surface applications. Polyhexamethylene guanidine (PHGH), was selected because of its known ability to inhibit Gram-positive and Gram-negative bacteria.[176] PHGH is a cationic antimicrobial oligomer that is typically synthesized by a polycondensation reaction between hexamethylene diamine and guanidine hydrochloride. Previous studies have shown that it has excellent antimicrobial activity against a wide spectrum of microorganisms (bacteria, virus, parasite, yeast, molds and antibiotic resistant bacteria).[177] Additionally, it is chemically stable, inexpensive, relatively non-toxic to human and animal cells, and less detrimental to the environment.[178,179] However, the direct incorporation of PHGH into

polymers for antimicrobial material applications has been limited because its low molecular weight and high solubility in polar solvents including water causes rapid leaching of PHGH out of the polymer, which then loses its antimicrobial activity. Chemical grafting of PHGH onto carrier polymers (e.g. starch) before incorporating it into other polymers could circumvent these challenges. Starch was selected as the carrier polymer because it is renewable, biocompatible, biodegradable, inexpensive, and abundant.[180] Moreover, the anhydroglucose units (AGU) of starch are rich in hydroxyl (–OH) functional groups that are chemically accessible for grafting via coupling reactions.[53,119,181–183] Polylactic acid (PLA) was selected as a model matrix polymer to test the antimicrobial properties of the PHGH grafted starch. PLA is of particular interest for packaging and biomedical applications due to the fact that it is biocompatible, compostable, and produced from renewable resources.[132]

The objective of this study was to chemically graft antimicrobial PHGH molecule onto a starch carrier and incorporate it into PLA polymers to produce a contact active antimicrobial material. Isophorone isocyanate (IPDI) was selected as the coupling agent because of the differentiated reactivity of its two isocyanate groups (-NCO), and the grafting reactions were investigated using various qualitative and quantitative analytical tools as described in the methodology section. The antimicrobial materials were then processed into microparticles and incorporated into PLA at various concentration ranges, and their antimicrobial efficiency was elucidated.

4.2. Materials and Methods

4.2.1. Materials

Cornstarch with 73% amylopectin and 27% amylose was purchased from Sigma Aldrich. A sample was dried overnight at 110ºC and stored in an air tight container prior to use. Isophorone diisocyanate (IPDI), dimethyl sulphoxide (DMSO), chloroform, hexamethylene diamine, guanidine hydrochloride, toluene, ethanol, and dibutylin dilaurate (DBTDL) were purchased from Sigma Aldrich and used as received. Film grade polylactic acid (PLA) (4043D) was provided by Nature Works (USA), Luria-bertani (LB) broth was purchased from BD Difco, Agar was purchased from VWR. All chemicals were analytical grade and used a received.

4.2.2. Methods

4.2.2.1. Synthesis of Polyhexamethylene guanidine hydrochloride (PHGH)

PHGH was synthesized by the condensation of guanidine hydrochloride and hexamethylene diamine in accordance with the method described by Zhang *et al*[184] Equal moles of 1,6-hexamethylene diamine and guanidine hydrochloride were added to a three neck round bottom flask equipped with a stirrer, thermometer and reflux condenser. The condensation reaction was then carried out at 120ºC for 1 h until complete liberation of ammonia and at 150ºC for 4 h. The viscous polyhexamethylene guanidine hydrochloride product solidified upon cooling at room temperature.

4.2.2.2. Modification of starch with polyhexamethylene guanidine hydrochloride

For the modification of starch with PHGH, 10% (w/v) of dry starch was first dispersed (Homogenizer, PowerGen 700) in DMSO at 80ºC until a clear viscous paste was obtained.

Concurrently, a separate round bottom flask containing a 1 to 6 mole ratio of starch to IPDI equipped with a stirrer and thermometer was placed in an oil bath at 60°C in an inert atmosphere. 1 mole percent of dibutylin dilaurate (DBTDL) catalyst was then added and allowed to stir for 5 min. 6 mole ratio of PHGH corresponding to the starch previously solubilized in DMSO was then added to the IPDI/DBTDL mixture and allowed to react for 1 h. The reaction product was then washed three times with toluene and the viscous product was separated from toluene each time using a separatory funnel. The solubilized starch was then added to the viscous IPDI-PHGH product and transferred to a round bottom flask in an oil bath. The reaction proceeded while stirring at 60°C for 3 h. The final product, a slightly viscous clear liquid was precipitated in ethanol to produce starch microparticles (average particle size 39 μm, from dynamic light scattering measurement). The precipitated starch microparticles in ethanol were centrifuged (4000 rpm for 3 min) to remove the unreacted reagents and repeated three times, dried at 70°C overnight, and characterized.

4.2.3. Characterization of modified starch microparticles

4.2.3.1. Fourier transform infrared spectroscopy (FTIR)

FTIR spectra of starch, PHGH, IPDI and PHGH-starch were obtained using infrared spectroscopy (Nicolett 6700, Thermo scientific). For this, powder samples were prepared by pressing a mixture of 5 mg of the sample and 200 mg of KBr into pellets using a Carver press. For the liquid and gelled samples, an aliquot of the sample was spread on a NaCl salt plate and scanned. A total of 16 scans were collected and averaged.

4.2.3.2. Nuclear magnetic resonance (^{1}H-NMR)

The proton NMR spectra of the samples were recorded using a Bruker 500 MHz high-resolution NMR spectrophotometer (Bruker-electrospin 500 MHz Ultrashield, Bruker Corporation, MA). The samples were prepared by dissolving 10 mg in deuterated DMSO and the spectra were obtained at 500 MHz at room temperature.

4.2.3.3. Elemental Analysis

The samples were dried at 70ºC overnight prior to analysis. The elements C, H, and N were quantified using a 4010 elemental analyzer (Costech instruments, Italy) equipped with a Delta Plus XL continuous flow isotope ratio mass spectrometer (Thermo-Finnigan, Germany). The coupling efficiency (CE) was calculated in accordance with Guan *et al*[119] based on the % N of the final product obtained from C/N elemental analysis as shown in the following equations.

$$CE = \frac{Wm-}{Wp} \times 100 \quad (4.1)$$

W_s, W_m and W_p are the weights of native starch, starch – PHGH microparticle and PHGH, respectively.

$$W_m = \frac{1}{1-G} \times W_s \quad (4.2)$$

$$G = \frac{177.5}{3 \times 14} \times \% N \quad (4.3)$$

G is the weight of PHGH in the starch-PHGH microparticle, % N is the nitrogen weight percent in the starch-PHGH microparticle obtained from elemental analysis, and 177.5 is the molar mass of the repeating unit of the PHGH oligomer.

4.2.3.4. Thermogravimetric Analysis (TGA)

The thermal stability of starch-PHGH microparticles in comparison with native starch and PHGH was analyzed using TGA (Q500 TGA equipment, TA instruments). Samples weighing between 3-5 mg were placed on platinum pans and heated at a rate of 5°C/min from 25°C to 100°C, then kept isothermal at 100°C for 3 min and heated again at 5°C/min until 600°C under a nitrogen atmosphere.

4.2.4. Preparation of starch-PHGH microparticles - PLA composite films

The baseline control PLA films and starch–PHGH microparticles referred to as antimicrobial starch (AMS) were prepared by a solvent casting method. These were carried out by dissolution of PLA pellets in chloroform (5 wt. %), followed by addition of AMS in the amounts of 1, 5, 10 and 20 wt. %. The blends were then homogenized, degassed under vacuum, and casted on glass molds at room temperature for 24 h.

4.2.5. Antimicrobial Activity Evaluation

The antimicrobial efficacy of AMS was tested against Gram-negative *E. coli* (NEB5α, New England Biolabs) and Gram-positive *B. subtilis* (BGSC 1A1[185]) bacteria. Two methods were used to investigate the antimicrobial activity of AMS-PLA composite films under static and dynamic contact conditions. Liquid culture on film test (static) was used to quantify the percent inhibition of bacterial growth and a shaking flask method revealed the growth kinetics of the bacteria. The procedures are outlined below.

4.2.5.1. Shaking flask method (dynamic contact)

All broths, agar, buffers, tubes, and tools used in this study were sterilized by autoclaving for 20 min at 120°C. Bacterial starter cultures were prepared by inoculating each strain into sterilized LB broth (25 g/L LB powder) and incubating overnight at 37°C and 180 rpm.

Flasks containing LB broth (22 mL) were inoculated with 0.9 mL of the starter culture and films measuring 5.4 cm in diameter were then added (to give a surface area to volume ratio of 1 cm^2/mL). The flasks were incubated at 37°C and 150 rpm overnight. A 1 mL sample was then collected from each flask at 2 h intervals for the first 8 h and at 24 h afterwards to measure the growth by optical density at 600 nm.

4.2.5.2. Plate count Assay (static contact)

Baseline PLA films (control samples), and PLA – AMS composite film specimens were cut to 2.54 cm in diameter and sterilized by soaking in 70% ethanol for 30 min followed drying in a sterile environment. For the static tests (culture on film), an aliquot of the overnight innoculum culture was added to sterile LB to obtain an optical density between 0.07 and 0.08 at 600 nm using a UV/Vis spectrophotometer (Beckman coulter, DU 530 life science). The films were placed in a sterile aluminum dish and 0.15 mL of bacteria culture was deposited on the surfaces of the sterile films and incubated for 24h at room temperature. As a positive control, an equivalent amount of culture was placed in a sterile centrifuge tube and left under the same conditions as the films. A 50 µL sample of the culture was retrieved from the film surface and serially diluted with sterile phosphate buffered saline (PBS, pH 7.3) with dilution factors (DF) between 10^{-1} to 10^{-9}. Then, 0.1 mL of each dilution was seeded onto an agar plate. Plates were incubated at 37°C for 24 h. The number of colonies for each plate were counted if they fell in the

range of 20 and 200 colonies. All experiments were performed in triplicate and the mean values are reported. The percent inhibition of bacteria cell growth defined as the number of live bacteria cells compared to the corresponding film containing AMS was then calculated according to equation (4.4) below:

$$\text{Growth inhibition of cell (\%)} = \frac{(A-B)}{A} \times 100 \quad (4.4)$$

Where A and B are the number of colonies from the positive control and film sample, respectively.

4.2.6. Leaching Evaluation

FTIR was used to investigate the possibility of PHGH, starch or AMS microparticle leaching from the polymer matrix films. For this analysis, films measuring 2.54 cm in diameter were cut and placed in a beaker containing 25 mL deionized (DI) water. Samples of the soaking water were then collected at 24, 48 and 72h and scanned using an FTIR to check for the presence of PHGH. A scan of DI water was used as a background.

4.3. Results and Discussion

4.3.1. Grafting of PHGH on Starch

Starch was used as a carrier of PHGH to ensure retention of PHGH within the PLA films because covalently bonding an oligomer to a long chain, high molecular weight polymer can prevent the leaching of the oligomer.[186] The grafting was executed in a two-step homogenous reaction process using IPDI as coupling agent to immobilize PHGH on starch via a covalent bond. IPDI was selected as a coupling agent because of the differential reactivity of the two -NCO groups to allow a controlled grafting of the PHGH antimicrobial agent and starch. DBTDL was used as a catalyst to activate the secondary NCO end-group. Girouard *et al*[187] performed a similar reaction with cellulose by reacting IPDI with the hydroxyl functional group in cellulose in the first reaction step. However, we chose the reverse route by first reacting IPDI with the amine group of PHGH for 1 h in the first reaction step, followed by the hydroxyl group in starch for 3 h. This reaction route was chosen because slower reaction rates have been reported between aliphatic isocyanates and hydroxyl groups compared to amines.[188] Hence, the secondary -NCO end group was first activated using the catalyst and the second step reaction proceeded for 3 h to compensate for the slow reaction rates.

The reaction between PHGH and starch is represented in Figure 4.1 (a, b and c). Figure 4-1(a) illustrates the copolymerisation reaction of hexamethylene diamine and guanidine hydrochloride to synthesize PHGH and 4.1(b) illustrates the DBTDL-catalyzed reaction pathway of IPDI and PHGH. The reaction mechanism between PHGH and starch has been previously proposed.[189] The reaction occurs when the active hydrogen atom of PHGH attacks the electrophilic carbon atom, resulting to the addition of the active hydrogen to the nitrogen atom.

The reaction with starch (Figure 4.1b) proceeds in a similar mechanism. The grafting was confirmed via elemental analysis (EA), FTIR and ^{1}H NMR.

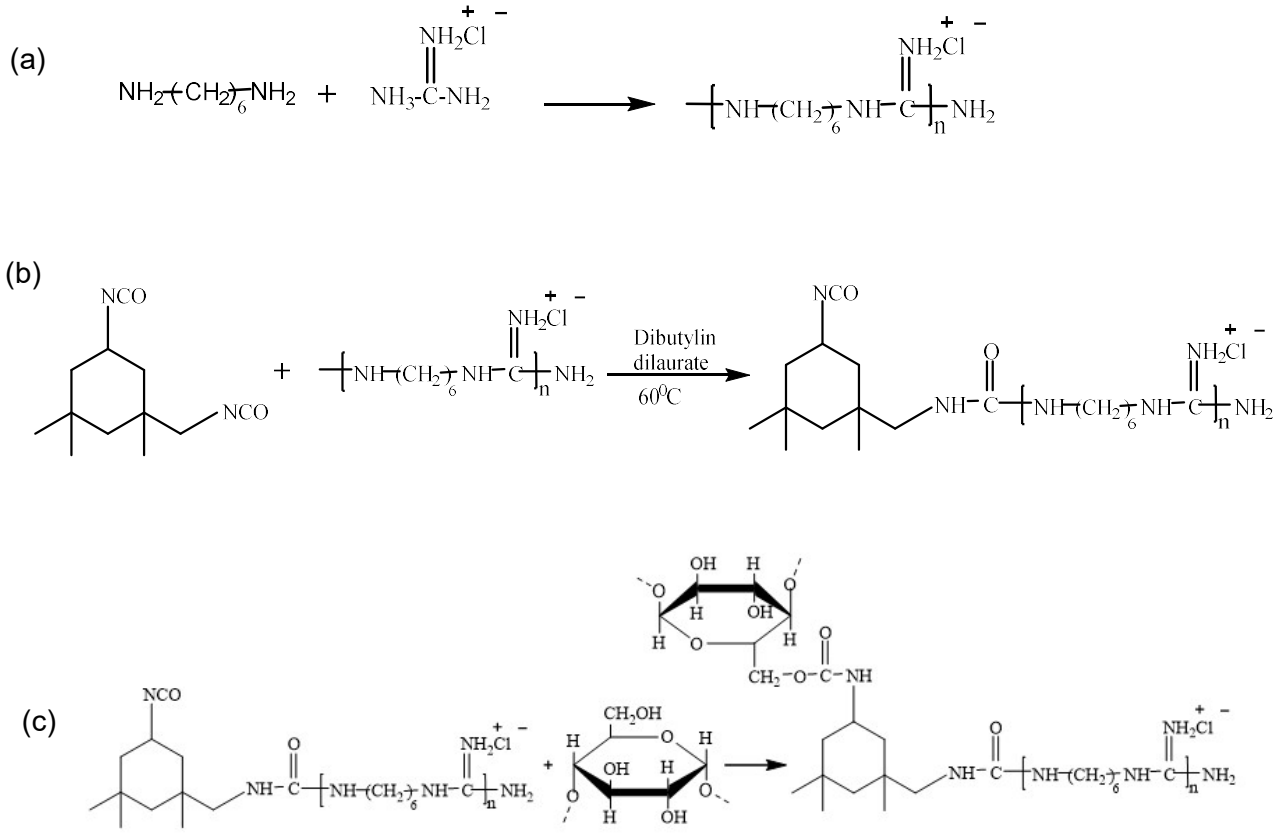

Figure 0.1. Reaction scheme for (a) copolymerisation of hexamethylene diamine and guanidine hydrochloride, (b) coupling reaction between IPDI and PHGH, and (c) reaction of coupled PHGH with starch

4.3.1.1. Grafting investigation via FTIR and ^{1}H NMR

The structural changes during the grafting of PHGH on starch to produce AMS microparticles was analyzed using FTIR and ^{1}H NMR as represented in Figure 4.2 and Figure 4.3, respectively. The reduction in the isocyanate peak (-N=C=O) at 2266 cm^{-1} as a result of the reaction of IPDI with PHGH was indicative of covalent bonding between the –NH_2 group of

PHGH and the – N=C=O of IPDI coupling agent. The PHGH–IPDI (Figure 4-2C) conjugate had a strong carbonyl band from the urea linkage from the reaction between the isocynate groups of IPDI and the amine group of PHGH (Figure 4.1). A shoulder amine functionality was also observed at 1580 cm^{-1}. Isocyanate functional groups are very reactive with compounds that contain active hydrogen group (e.g. $–NH_2$, -OH) as a result of nucleophilic attack by their electrophilic carbon.[190,191] The residual isocyanate peak observed at 2266 cm^{-1} on the PHGH–IPDI spectrum was indicative of unreacted isocyanate functional groups (Figure 4.1), as a result of the differentiated reactivity of the IPDI functional groups. This was quite beneficial as it avoids crosslinking among the PHGH groups, making isocyanate functional groups available for reaction with the –OH groups of starch. The native starch (4.2d) displayed a broad peak between 3000 and 3600 cm^{-1} resulting from the vibrational stretching of the O-H groups, a band at 2923 cm^{-1} attributed to the stretching of the C-H groups, and at 1629 cm^{-1} associated with a bound water in starch.[192] The IR spectra of the reaction product between PHGH–IPDI intermediate product and starch is shown in 4.2E. The isocyanate peak (2266 cm^{-1}) observed in the PHGH–IPDI intermediate product was completely consumed in the PHGH–IPDI-starch final product. In addition, the broad peak of starch between 3200 – 3450 cm^{-1} associated with anhydroglucose unit –OH functional groups have shifted to a lower wavenumber and a relatively sharp peak was observed at 3350 cm^{-1} that was attributed to secondary amine group formation. Moreover, a substantial increase in the absorbance of carbonyl (-C=O) in urethane groups, and a prominent amine peak were observed at 1627 cm^{-1} and at 1580 cm^{-1}, respectively. These results suggested that there was a covalent grafting between the PHGH–IPDI and the –OH functional group of starch to produce a PHGH–IPDI–starch.

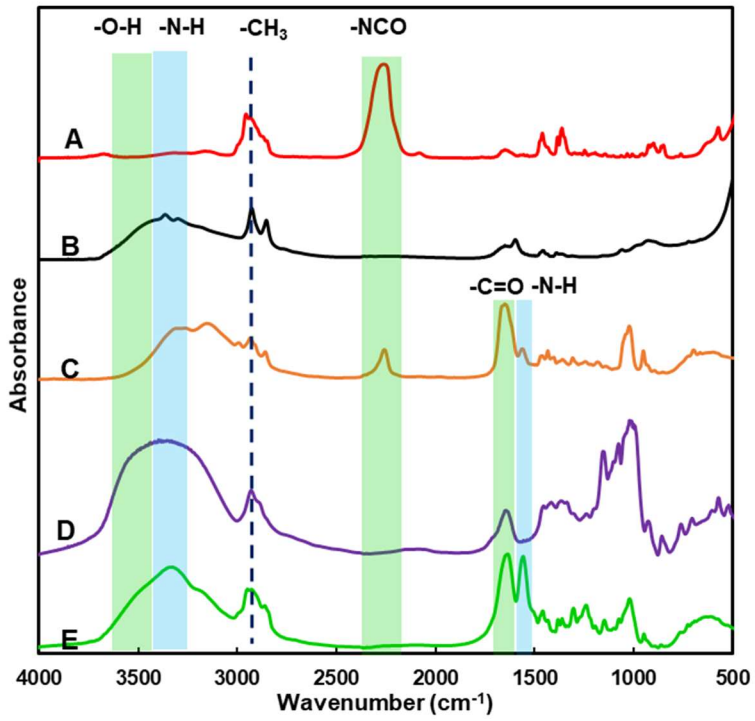

Figure 0.2. FTIR spectra of (A) IPDI, (B) PHGH, (C) IPDI - PHGH, (D) starch, and (E) PHGH-IPDI-Starch or Antimicrobial Modified Starch (AMS)

The grafting of PHGH onto starch using the IPDI coupling agent was further investigated with ^{1}H NMR spectroscopy and results are presented in Figure 4.3. Signals at δ 3.33 ppm and at 2.51 ppm correspond to residual moisture and DMSO in the samples, respectively. ^{1}H NMR spectrum of native starch (Figure 4.3a) exhibited characteristic signals at δ 5.47 ppm (OH-3), 5.39 (OH-2), 5.11 (H-1), and 4.56 (OH-6). Signals at δ 3.30 - 3.66 ppm were assigned to H-2 to H-6 of anhydroglucose units in line with other reports.[193,194] The PHGH displayed sharp ^{1}H NMR peaks at δ 3.12, 1.52 and 1.29 ppm that were attributed to –methylene groups (-CH_2).[195] Peaks at δ 2.61 – 2.66 ppm, δ 3.13 – 3.22 ppm, and δ 4.74 – 4.83 ppm were attributed to –NH_2, -CH_2, –H, and –NH-, respectively.[196]

On the other hand, the PHGH-IPDI-starch graft AMS microparticles (4.3c) showed peaks between δ 0.7 and 1.48 ppm from four methylene groups associated with PHGH. The peaks between 3 and 4 ppm were assigned to the first and last methylene group of PHGH and the equatorial starch proton while the peaks between 7 and 8 ppm were assigned to proton from the amine group of PHGH. The results obtained here verify the covalent grafting of PHGH onto starch observed from the IR characterization, and is in agreement with results reported by Guan *et al*[119] in their study of starch modifications for paper applications.

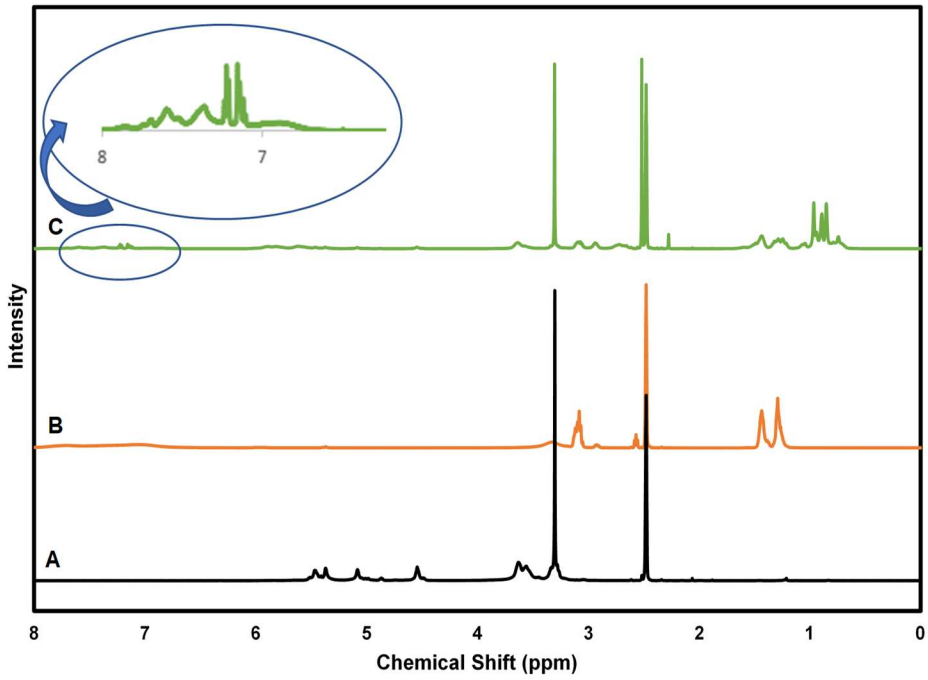

Figure 0.3. Proton NMR spectra of (A) Starch, (B) PHGH, and (C) PHGH - IPDI- Starch, in DMSO at room temperature.

4.3.1.2. Coupling efficiency analysis via Elemental Analysis

The grafting of PHGH on starch using IPDI coupling agent was quantitatively confirmed by elemental analysis (EA). The weight percent of PHGH in the modified starch was used to estimate the coupling efficiency (CE). This was determined by using the weight percent of nitrogen in the modified starch obtained from carbon and nitrogen analysis via EA. The weight percentages of nitrogen and the calculated coupling efficiency are presented in Table 4.1. The results showed a coupling efficiency of 17.37 % at our reaction conditions. Guan *et al*[119] reported similar starch modification levels by using glycerol diglycidyl ether (GDE) coupling agent. While the results obtained here clearly showed that significant grafting of PHGH to the starch was achieved by using the IPDI coupling agent, there is still room for the optimization of the reaction conditions, as well as selection of the coupling agent. It is anticipated that higher levels of PHGH grafting onto starch could lead to higher antimicrobial efficiency of the AMS microparticles.

Table 0.1. Elemental analysis results of starch, and PHGH – starch graft microparticles

Sample	% N	CE (%)
Starch	ND	ND
PHGH modified starch	13.48 ± 0.09	17.37 ± 0.29

4.3.1.3. Thermal Stability of the Antimicrobial Starch Microparticles

To utilize AMS microparticles as an additive in other polymers, its thermal stability at the processing conditions of polymers (typically 120–200°C) is an important factor to consider to

prevent degradation during processing. In this case, the TGA thermal stability analysis provided a range of temperatures for which the AMS can be processed without being degraded. The thermal degradation mechanism of starch has been reported and involves the dehydration of the hydroxyl groups by thermal condensation reactions at low temperatures, followed by the cleavage of the chemical bonds in the main chain.[156,181] Although reducing the number of hydroxyl groups on starch by chemical modification can improve its thermal stability, the disruption of the crystal structure during modification can expose a significant number of the hydroxyl groups, leading to a lower degradation onset temperature (T_{onset}).

The grafting of PHGH onto starch altered its overall thermal degradation behavior as shown in Figure 4.4. There was a reduction in the onset of degradation of the AMS microparticles (T_{onset} of 240ºC) as compared to for starch (T_{onset} of 269ºC). This reduction can be attributed to the thermal dehydration from increased exposure of hydroxyl groups. Native starch showed a two-stage peak degradation; the first, a minor peak at 287°C with 11 % weight loss has been reported to be associated with the amylose fraction of starch and a major peak at 318°C with 42 % weight loss associated with the branched amylopectin.[197] Following the major peak, the weight loss continued steadily up to 347°C. In contrast, the AMS microparticles revealed a single degradation peak at 273°C where it lost 32 % of its weight and followed the same degradation pattern as starch thereafter. Additionally, the temperature range between the onset and final degradation temperatures in AMS broadened compared to that of starch. This observed trend can be attributed to the consistency of the AMS structure as a result of modification in contrast to the structure of starch composed of amylose and amylopectin polymers with different thermal degradation behaviours within the same molecule.[181] Although the modified starch had

a reduced onset of degradation, it still falls within a suitable temperature range for processing with most thermoplastic or thermosetting polymers, which are typically processed below 220°C.[181,198]

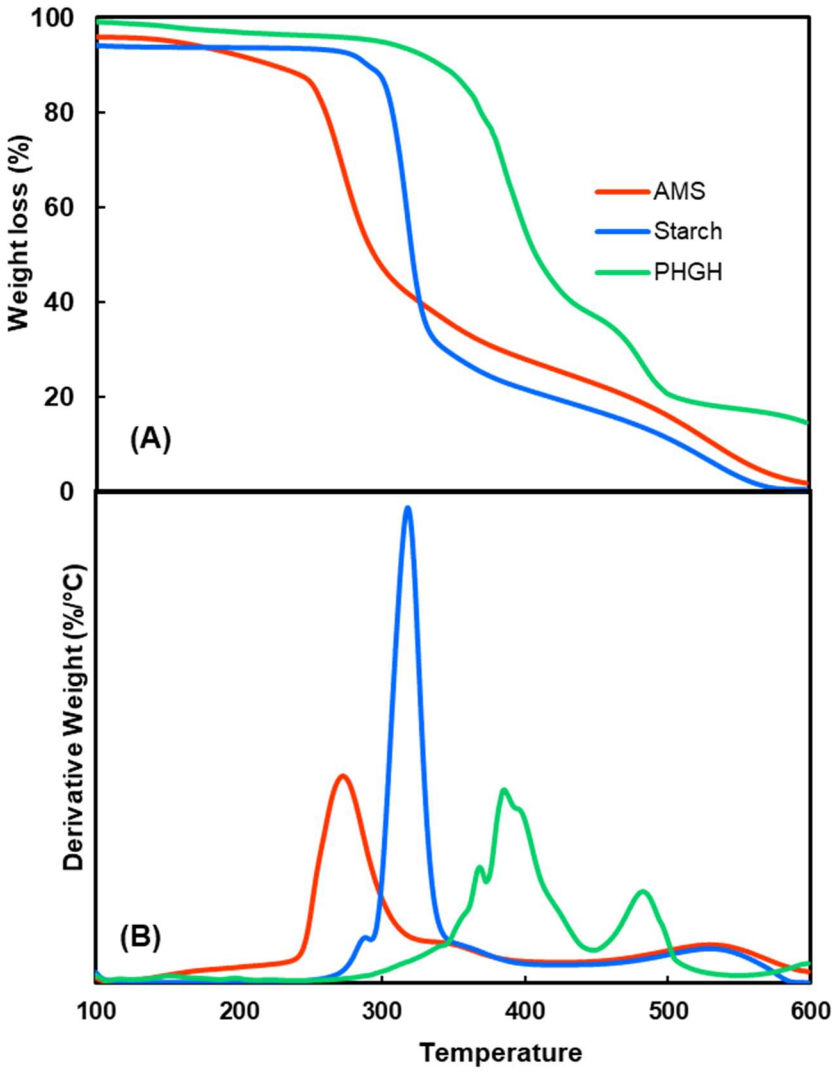

Figure 0.4. (A) TGA weight loss plot of starch, PHGH and AMS, and (B) Weight loss derivative starch, PHGH, and AMS microparticles.

4.3.2. Antimicrobial activity assessment

PHGH is an excellent cationic biocidal agent that has a wide spectrum of activity against bacteria, fungi, virus, and molds.[199] The amphipathic nature of PHGH, is responsible for antimicrobial inhibition. Typically, guanidine-based polymers contain cationic charge density, which enhances adhesion to the anionic phospholipids of the bacterial cell membranes by electrostatic association. The long molecular chain of PHGH permeates the cell membrane as a result of hydrophobic interactions; thereby, forming pores and allowing leakage of intracellular contents and as a result, cell death.[200–202] This deactivation mechanism is illustrated in Figure 4.5, which shows the contact barrier provided by polymer surfaces used in packaging, the surface modifications performed in this study, and the deactivation of bacteria cells on contact with the polymer surface. In this work, we compared the antimicrobial activity of various concentrations of PHGH–starch grafted microparticles, referred here AMS microparticles, in PLA films against Gram-negative *E. coli* and Gram-positive *B. subtilis*.

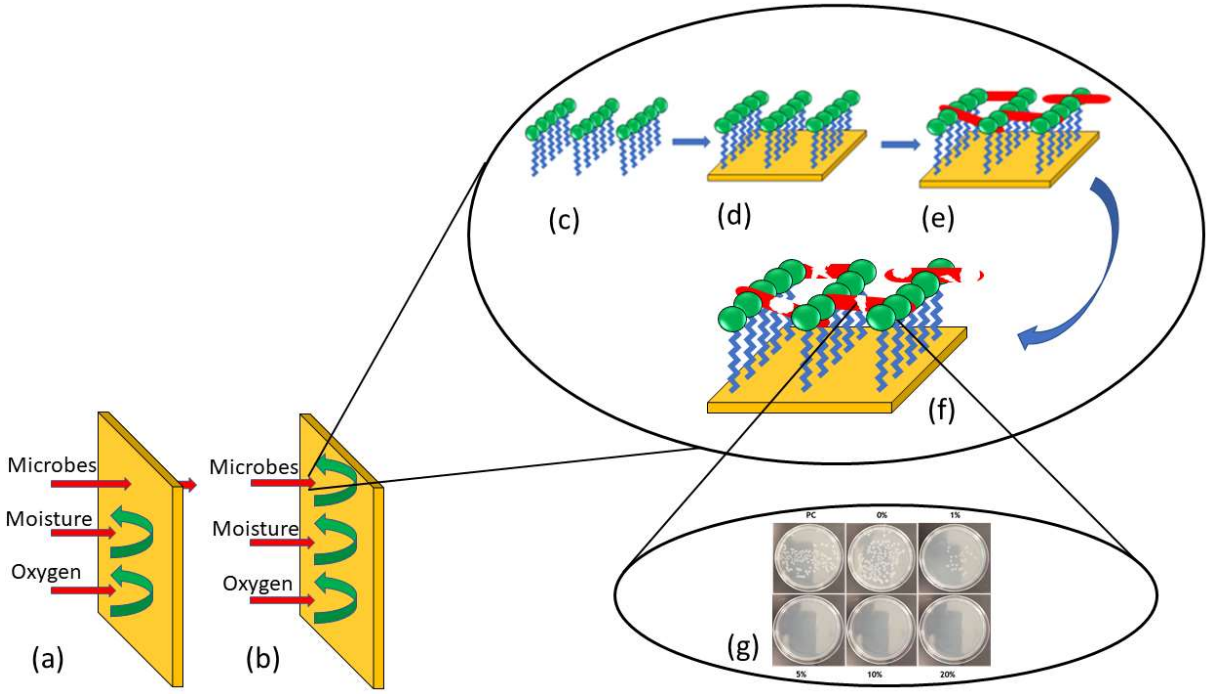

Figure 0.5. Pictorial representation illustrating surfaces provided by (a) conventional polymer surfaces, and (b) contact-active antimicrobial polymer surfaces (c) PHGH grafted onto starch, (d) AMS on PLA surface (yellow), (e) bacteria "on contact" with antimicrobial polymer surface, (f) rupture of bacteria cell membrane by AMS on polymer surface, and (g) Agar plate assay showing viability of bacteria cells after contacting antimicrobial surface.

The shaking flask method (dynamic test) shows the effect of AMS microparticles concentration on bacteria growth and results are represented in Figure 4.6 (a & b). This method provided information on microbial kinetics and was qualitatively used to assess antimicrobial activity. Aside from the extent of bacteria contact with the films and the concentration and dispersion of AMS within the films, it is important to consider the ratio of the film surface area to the volume (S/V) of media when conducting this test using polymer films. Soares and Hotchkiss[203] showed that increasing the surface to volume ratio increases the activity of antimicrobial materials. Thus, to avoid discrepancies resulting from variation in S/V ratio, a value of 1 cm^2/mL was selected and used for all PLA films containing AMS microparticles.

Analyzing the results obtained for *E. coli*, the positive control (PC) containing no film showed a typical cell growth pattern of lag, growth, stationary, and death phases. The 1% and 5% AMS containing films followed the same growth pattern as the PC with a steep growth phase up to 6 h followed by a stationary phase. On the other hand, the films containing 10% and above of AMS showed a very slow rise in the optical density indicating excellent growth inhibition. However, after 8 h, a reduction in the UV absorbance was observed. This reduction in the UV absorbance could be indicative of the death, cell lysis, and release of cytoplasm from the cell membrane resulting from contact with the AMS-PLA films. The cytoplasm content that leached out of the cell tends to precipitate, thereby, reducing the particle population and light scattering, and consequently, lower optical density measurements.

B. subitilis followed a similar growth pattern as that of the *E. coli* when in contact with the PLA–AMS surfaces. However, AMS-PLA showed enhanced antimicrobial performance of against *B. subitilis* compared to *E. coli* (Figure 4.6b). The sample with 1% AMS revealed a slight growth inhibition compared to the PC due to the presence of the low concentration AMS in the polymer film. With AMS-PLA of 5% and above a very small rise in optical density over 24 h was observed indicating excellent growth inhibition.

To physically examine the growth or inhibition of the bacteria, the turbidity difference in the growth media as a result of AMS were evaluated (Figure 4.7a & b). For both *E. coli* and *B. subtilis*, the turbidity of the media decreased with increasing AMS concentration. The media containing control samples PC and 0 % showed cloudiness which is a visual indication of bacterial growth. As AMS-PLA films were introduced starting from a concentration of 1 wt. %, the cloudiness reduced compared to the PC and further decreased as the concentration increased.

This indicated that introducing AMS-PLA films in the growth media inhibits the growth of bacteria for the lower concentration samples and completely prevents the same in the higher concentration samples. These results agree with the growth curve of the shaking flask method where the bacteria growth inhibition began at 5 wt. % AMS concentration.

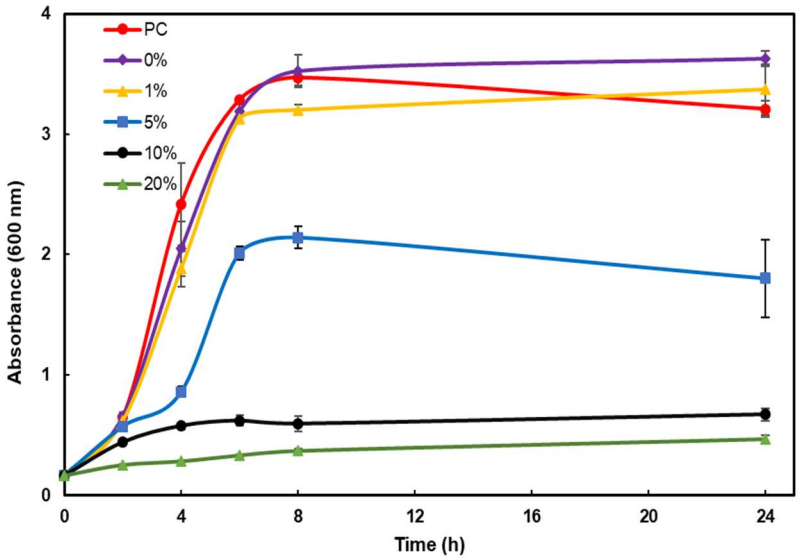

(A)

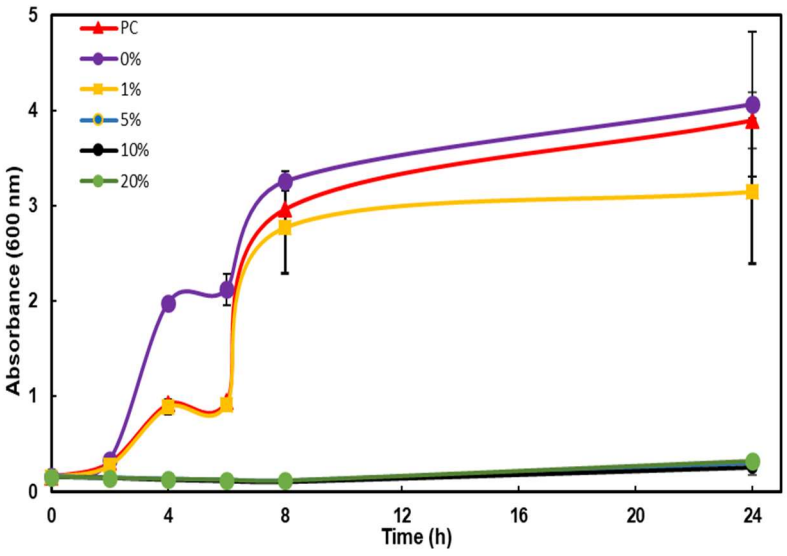

(B)

Figure 0.6. Growth curves of *E. coli* (A) and B. Subtilis (B) cultures containing AMS-PLA films with the indicated loading density of AMS (% weight) and a positive control (PC) containing no film.

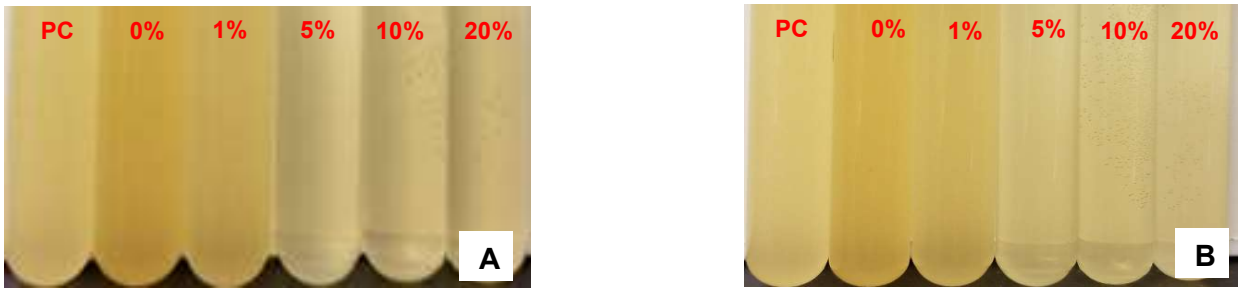

Figure 0.7. Images showing the turbidity of the growth media of bacteria grown in the presence of antimicrobial PLA-AMS films with the indicated AMS concentrations. (A) *B. subtilis* and (B) *E. coli*

One shortcoming of studying bacteria growth activity using optical density measurements was that it cannot distinguish viable from non-viable cells, limiting its utility as a measurement of antimicrobial efficacy.[204] Hence, to verify and quantify bacteria growth inhibition, a static agar plate count assay was performed. This method simulates wrapping used in food packaging applications and can provide information regarding the interaction of films with bacteria. Colony forming units (CFU) per mL of culture is calculated from the number of colonies grown on agar plates after treatment which represents the number of viable bacterial. This can then be compared to the CFU/mL of the PC and expressed as a percentage of inhibition. Figures 4.8 and 4.9 represent results obtained for *E. coli* and *B. subtilis,* respectively and Figure 4.10 shows the calculated percent growth inhibition per sample. For *E. coli*, a decrease in the average CFU/mL was observed for the 1 and 5% AMS containing films, corresponding to a growth inhibition of 42 and 71%, respectively. Additionally, starting at 10 % AMS concentration, the growth inhibition reached 99.94 %, indicating almost all the bacteria were destroyed. These results

verify that at the appropriate concentration, the AMS–polymer surface kills the bacteria cells on contact.

A noticeable increase in the growth of *B. subtilis* cells in the culture media containing 0 % AMS (PLA baseline film) as compared to PC was observed. This was rather unexpected and one plausible explanation for the observation could be the presence of residual lactic acid in PLA which could have served as additional carbon source for the *B. subtilis* cells, hence the increase in growth.

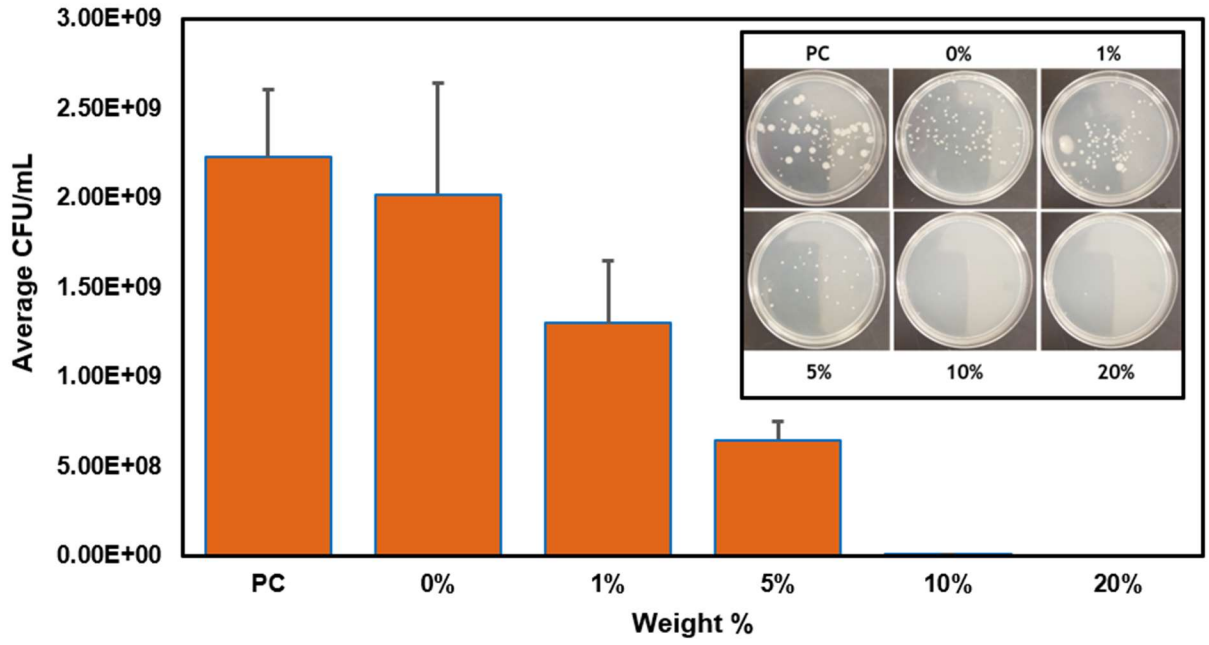

Figure 0.8. Average colony plate count for *E. coli* showing the number of viable cell for each film.

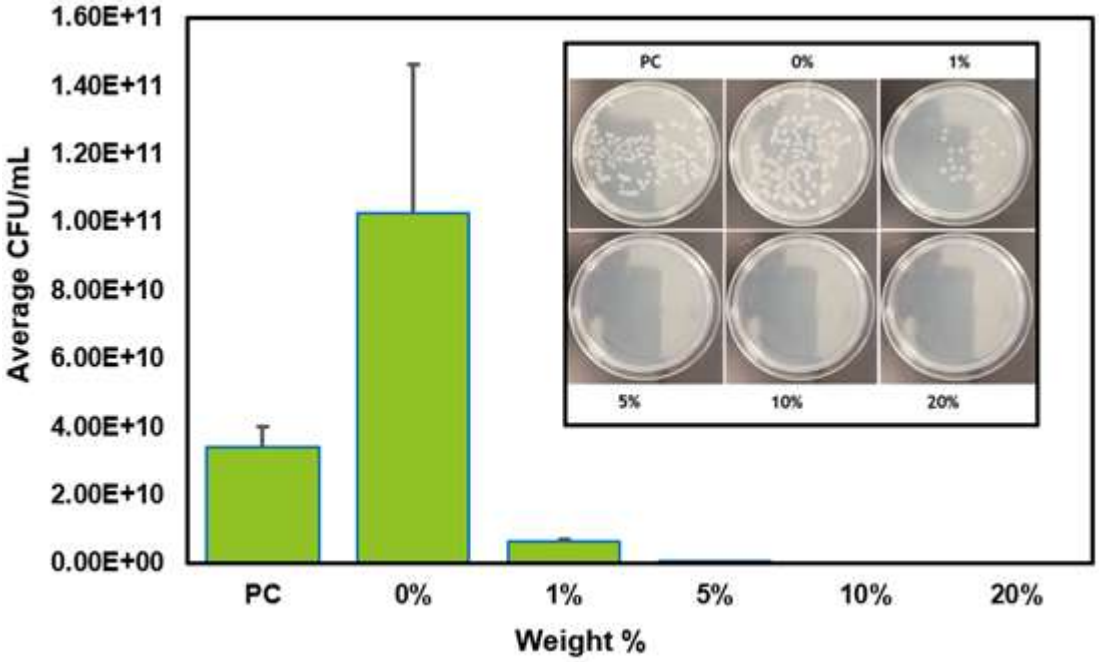

Figure 0.9. Average colony plate count for *B. subtilis* showing the number of viable cell for each film.

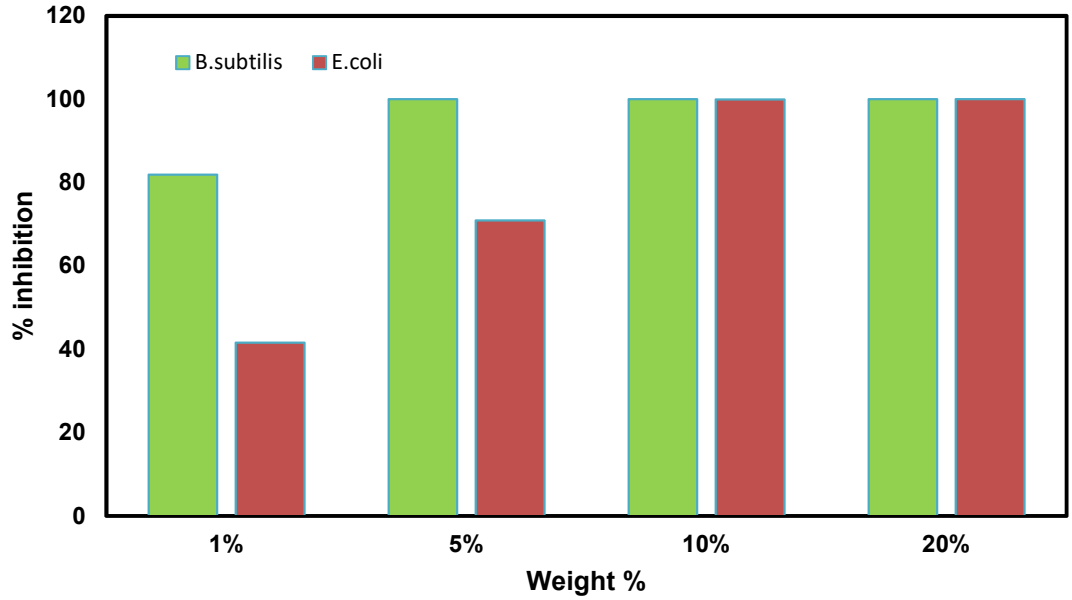

Figure 0.10. Percent growth inhibition of AMS-PLA films against *E. coli* and *B. subtilis.*

Overall, the antimicrobial activity of the polymer surfaces against the tested bacterial strains indicated a better efficacy against *B. subtilis* than *E.coli* using both experimental methods. Zhou et al[202] suggested that the efficacy of PHGH depends on the following: concentration, exposure time, and bacteria starting concentration. They showed micrographic images resulting from antimicrobial treatment which revealed that on contact with bacteria, PHGH first destroys the outer membrane of cell followed by damage to the cell wall only at higher concentrations. Our results agree with their proposition as the activity of PHGH was higher on *B. subtilis* which lacks an outer membrane unlike *E.coli* which contains both a plasma membrane and an outer membrane[202]. It is important to highlight that the AMS microparticles were embedded in the polymer matrix, and only a fraction of the AMS were exposed on the surface of the polymer film. Nonetheless, highly effective antimicrobial properties were observed when the concentration of AMS was close to 10% in the total film. Based on the thickness of the film (~1 mm), the average particles size of AMS microparticles (39 μm), and assuming a uniform distribution of the AMS microparticles over the area and thickness of the films, the quantity of AMS on the surface of the films was computed. The calculations indicate that the 10 % AMS loading in the PLA films was equivalent to about 0.39 % AMS on the surface of the film, which caused the observed antimicrobial effect upon contact. This demonstrates that by employing other methods for the incorporation of these antimicrobial materials (e.g. spray coating), a similar bacterial inactivation could be achieved with a significantly lower antimicrobial material use.

4.3.3. Leaching analysis of PHGH from PLA Film

PHGH is an oligomer with molecular weight ranging between 300 and 2500. Although it has shown excellent antimicrobial properties, one known challenge of introducing this biocide directly into polymers surfaces was its leaching out due to its low molecular weight. In addition, PHGH is soluble in polar solvents including water, consequently, it may diffuse out of the polymer matrix when exposed to moisture. Thus, starch was used as a carrier to immobilize PHGH, in an attempt to mitigate the leaching and loss of this biocide. To confirm that PHGH grafted onto starch was not lost by leaching, this was tested by soaking 20% AMS-PLA films in water for 72 h and the IR spectra of the soaking water sample was collected (Figure 4.11) while using deionized water as a background. In comparison to a PHGH and starch spectrum, the 20% AMS based film displayed no peaks, indicating that the biocide did not leach out of the film. This was also an indication that PHGH was successfully attached to starch via a covalent graft. This implies that the antimicrobial PLA can be used on surfaces requiring the deactivation of bacteria on contact without diffusing into the material and losing its antimicrobial activity.

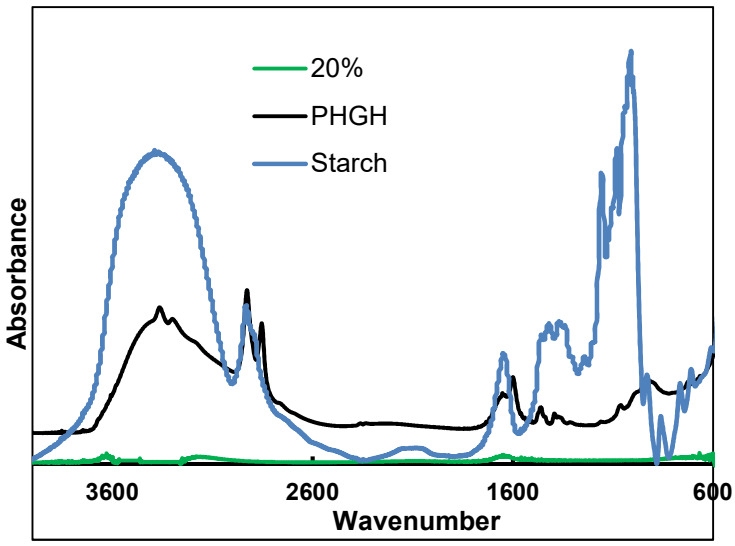

Figure 0.11. FTIR spectra of 20% AMS-PLA film soaked in water for 72 h to test for leaching of PHGH from polymer film.

4.4. Conclusion

Antimicrobial starch microparticles were prepared by grafting PHGH onto starch in a two-step homogenous reaction using IPDI as coupling agent. The grafting reaction was confirmed by FTIR, EA and proton NMR analysis. The starch – PHGH microparticles (AMS) exhibited thermal stability that is amenable to polymer melt processing as observed from TGA studies. The AMS microparticles were then incorporated into PLA films at varied weight percent and cast into films to produce antimicrobial polymer surfaces. The films showed antimicrobial activity when tested against Gram-positive *B. subtilis* and Gram-negative *E. coli* demonstrating that the PHGH maintained its antimicrobial property not only in the graft AMS microparticles, but also embedded in the polymer matrix. The antimicrobial activity of the polymer films increased with an increase in the concentration of AMS. The observed bacterial deactivation occurs when bacteria contact the surface of films and not by diffusion of the antimicrobial agent as observed by FTIR spectra of the starch films soaked in water for 72 h which revealed the non-leaching behavior of PHGH from the graft films. The "grafting onto" approach using coupling agents with differentiated reactivity could serve as a general surface modification platform for the development of contact active antimicrobial surfaces.

Chapter 5. Concluding Remarks and Recommendations

The expansion of material applications using starch as a feedstock has seen a lot of interest because of its biodegradability, low cost, and abundance. In view of this, the objective of this thesis was to modify starch to incorporate functional properties via the replacement of –OH functional groups of the anhydroglucose units of the starch chains in a chemical reaction process. The end use of the modified material informs the type and extent of modification to be carried out. This research demonstrated chemical modification platforms for sustainable bio-plastic applications and functional materials.

The incorporation of lauric acid on the starch chain altered the thermal stability, polarity and thus the water affinity at various degrees depending on the level of modification. Interestingly, an almost complete substitution of the –OH groups of starch was achieved with the use of 4 mol ratio of lauroyl chloride per AGU. This was validated by FTIR, EA and proton NMR. Such high level of fatty acid incorporation on starch resulted in a complete disruption of the crystalline structure with no re-crystallization behavior. This was well supported by SEM and XRD studies. The observed hydrophobicity and melt processability of the starch- laurate esters were clear indicators of the potential of such materials to be used as a bio-plastic without the need of an external plasticizer or other modifiers. Also, the reduction in surface energy would make it more compatible with other aliphatic polymers (e.g. PLA, PHB, EVA etc) to produce blends. Overall, the starch-laurate ester polymers produced in this research exhibited melting behavior, thermal stability, excellent clarity, and promising mechanical properties pointing out that it can be melt processed via typical hot melt processing tools as observed from the structural investigations.

Antimicrobial starch microparticles were also prepared by grafting PHGH onto starch in a two-step homogenous reaction using IPDI as coupling agent. The grafting reaction was confirmed by FTIR, EA and proton NMR analysis. The starch – PHGH microparticles (AMS) exhibited thermal stability that is amenable to polymer melt processing as observed from TGA studies. The AMS microparticles were then incorporated into PLA films at varied weight percent and cast into films to produce antimicrobial polymer surfaces. The films showed antimicrobial activity when tested against Gram-positive *B. subtilis* and Gram-negative *E. coli* demonstrating that the PHGH maintained its antimicrobial property not only in the graft AMS microparticles, but also embedded in the polymer matrix. The antimicrobial activity of the polymer films increased with an increase in the concentration of AMS. The observed bacterial deactivation occurs when bacteria contact the surface of films and not by diffusion of the antimicrobial agent as observed by FTIR spectra of the starch films soaked in water for 72 h which revealed the non-leaching behavior of PHGH from the graft films. The "grafting onto" approach using coupling agents with differentiated reactivity could serve as a general surface modification platform for the development of contact active antimicrobial surfaces.

Chemical modification established here is not limited to starch. Taking advantage of the rich –OH groups and introducing side chains (functional groups) on the main chain of polysaccharides can provide endless material application possibilities. For instance, if the intended applications require polymer feedstock with excellent mechanical properties, cellulose nanocrystals could be explored. In addition, the backbone structure of polysaccharides is susceptible to scission by the actions of microorganism. Introducing desirable properties by chemical modification with other materials can extend their applications making them suitable alternative feedstock to synthetic polymers.

Exploring these alternatives could be a solution to the environmental concerns caused by non-degradable plastic waste.

References

1. Lin, C. S. K. *et al.* Food waste as a valuable resource for the production of chemicals, materials and fuels. Current situation and global perspective. *Energy Environ. Sci.* **6**, 426 (2013).
2. Mekonnen, T., Mussone, P. & Bressler, D. Valorization of rendering industry wastes and co-products for industrial chemicals, materials and energy: review. *Crit. Rev. Biotechnol.* **36**, 120–131 (2016).
3. Mekonnen, T. & M. Fermented Soymeals and Their Reactive Blends with Poly(butylene adipate-co-terephthalate) in Engineering Biodegradable Cast Films for Sustainable Packaging. *Acs Sustain. Chem. Eng.* **4**, 782–793 (2016).
4. Muthuraj, R. & Mekonnen, T. Recent progress in carbon dioxide (CO 2) as feedstock for sustainable materials development: Co-polymers and polymer blends. *Polymer (Guildf).* **145**, 348–373 (2018).
5. Muthuraj, R. & Mekonnen, T. Carbon dioxide derived poly (propylene carbonate) polymer for composites and nanocomposites: performance, biodegradation and applications. *Macromol. Mater. Eng.* (2018). doi:10.1002/mame.201800366
6. Domingos De Sousa, F. *et al.* Physicochemical Properties of Edible Seed Hemicelluloses. *Open Access Libr. J.* **4**, (2017).
7. Ojogbo, E., Blanchard, R. & Mekonnen, T. Hydrophobic and Melt Processable Starch-Laurate Graft Polymers: Synthesis, Structure – Property Correlations. *J. Polym. Sci. Part A-Polymer Chem.* (2018).
8. Copeland, L., Blazek, J., Salman, H. & Tang, M. C. Form and functionality of starch. *Food Hydrocoll.* **23**, 1527–1534 (2009).
9. Zia-ud-Din, Xiong, H. & Fei, P. Physical and chemical modification of starches: A review. *Critical Reviews in Food Science and Nutrition* (2017). doi:10.1080/10408398.2015.1087379
10. Masina, N. *et al.* A review of the chemical modification techniques of starch. *Carbohydr. Polym.* **157**, 1226–1236 (2017).
11. Šárka, E. & Dvořáček, V. Waxy starch as a perspective raw material (a review). *Food*

Hydrocoll. **69**, 402–409 (2017).

12. Ahmed, J. *Starch-based polymeric materials and nanocomposites : chemistry, processing, and applications*. (CRC, 2012).
13. Gao, J., Luo, Z.-G. & Luo, F.-X. Ionic liquids as solvents for dissolution of corn starch and homogeneous synthesis of fatty-acid starch esters without catalysts. *Carbohydr. Polym.* **89**, 1215–1221 (2012).
14. Villar, M. A. *Starch-based materials in food packaging : processing, characterization and applications*.
15. Zhang, Y., Rempel, C. & Liu, Q. Thermoplastic Starch Processing and Characteristics—A Review. *Crit. Rev. Food Sci. Nutr.* **54**, 1353–1370 (2014).
16. Belgacem, M. N. & Gandini, A. *Monomers, polymers and composites from renewable resources*. (Elsevier, 2008).
17. Singh, N., Singh, J., Kaur, L., Singh Sodhi, N. & Singh Gill, B. Morphological, thermal and rheological properties of starches from different botanical sources. *Food Chem.* **81**, 219–231 (2003).
18. Mutungi, C., Rost, F., Onyango, C., Jaros, D. & Rohm, H. Crystallinity, Thermal and Morphological Characteristics of Resistant Starch Type III Produced by Hydrothermal Treatment of Debranched Cassava Starch. *Starch - StÃ¤rke* **61**, 634–645 (2009).
19. Rolland-Sabaté, A. *et al.* Structural characterization of novel cassava starches with low and high-amylose contents in comparison with other commercial sources. *Food Hydrocoll.* **27**, 161–174 (2012).
20. Muller, J., González-Martínez, C. & Chiralt, A. Combination of Poly(lactic) Acid and Starch for Biodegradable Food Packaging. *Materials (Basel).* **10**, 952 (2017).
21. Boudries, N. *et al.* Physicochemical and functional properties of starches from sorghum cultivated in the Sahara of Algeria. *Carbohydr. Polym.* **78**, 475–480 (2009).
22. Ebnesajjad, S. *Handbook of Biopolymers and Biodegradable Plastics : Properties, Processing, and Applications*.
23. Wang, K. *et al.* Mechanical properties and solubility in water of corn starch-collagen composite films: Effect of starch type and concentrations. *Food Chem.* **216**, 209–216 (2017).

24. Liu, H., Xie, F., Yu, L., Chen, L. & Li, L. Thermal processing of starch-based polymers. *Prog. Polym. Sci.* **34**, 1348–1368 (2009).
25. Le Corre, D. & Angellier-Coussy, H. Preparation and application of starch nanoparticles for nanocomposites: A review. *React. Funct. Polym.* **85**, 97–120 (2014).
26. Winkler, H., Vorwerg, W. & Rihm, R. Thermal and mechanical properties of fatty acid starch esters. *Carbohydr. Polym.* **102**, 941–949 (2014).
27. Winkler, H., Vorwerg, W. & Wetzel, H. Synthesis and properties of fatty acid starch esters. *Carbohydr. Polym.* **98**, 208–216 (2013).
28. Chi, H. *et al.* Effect of acetylation on the properties of corn starch. *Food Chem.* **106**, 923–928 (2008).
29. López, O. V., García, M. A. & Zaritzky, N. E. Film forming capacity of chemically modified corn starches. *Carbohydr. Polym.* **73**, 573–581 (2008).
30. Sasaki, T., Yasui, T. & Matsuki, J. Effect of Amylose Content on Gelatinization, Retrogradation, and Pasting Properties of Starches from Waxy and Nonwaxy Wheat and Their Seeds. *Cereal Chem. J.* **77**, 58–63 (2000).
31. Simi, C. K. & Abraham, T. E. Physicochemical Rheological and Thermal Properties of Njavara Rice (Oryza sativa) Starch. *J. Agric. Food Chem.* **56**, 12105–12113 (2008).
32. Fujita, S. & Fujiyama, G. The Study of Melting Temperature and Enthalpy of Starch from Rice, Barley, Wheat, Foxtail- and Proso-millets. *Starch - Stärke* **45**, 436–441 (1993).
33. Waliszewski, K. N., Aparicio, M. A., Bello, L. A. & Monroy, J. A. Changes of banana starch by chemical and physical modification. *Carbohydr. Polym.* **52**, 237–242 (2003).
34. Vanier, N. L., El Halal, S. L. M., Dias, A. R. G. & da Rosa Zavareze, E. Molecular structure, functionality and applications of oxidized starches: A review. *Food Chem.* **221**, 1546–1559 (2017).
35. Miyazaki, M., Van Hung, P., Maeda, T. & Morita, N. Recent advances in application of modified starches for breadmaking. *Trends Food Sci. Technol.* **17**, 591–599 (2006).
36. Chen, Q. *et al.* Recent progress in chemical modification of starch and its applications. *RSC Adv.* **5**, 67459–67474 (2015).
37. Haroon, M. *et al.* Chemical modification of starch and its application as an adsorbent material. *RSC Adv.* **6**, 78264–78285 (2016).

38. Rajan, A. & Abraham, T. E. Enzymatic modification of cassava starch by bacterial lipase. *Bioprocess Biosyst. Eng.* **29**, 65–71 (2006).
39. Rajan, A., Sudha, J. D. & Abraham, T. E. Enzymatic modification of cassava starch by fungal lipase. *Ind. Crops Prod.* **27**, 50–59 (2008).
40. Arijaje, E. O., Wang, Y.-J., Shinn, S., Shah, U. & Proctor, A. Effects of Chemical and Enzymatic Modifications on Starch–Stearic Acid Complex Formation. *J. Agric. Food Chem.* **62**, 2963–2972 (2014).
41. Heinze, T., Haack, V. & Rensing, S. Starch Derivatives of High Degree of Functionalization. 7. Preparation of Cationic 2-Hydroxypropyltrimethylammonium Chloride Starches. *Starch - Stärke* **56**, 288–296 (2004).
42. Tomasik, P., Wang, Y. J. & Jane, J.-L. Facile Route to Anionic Starches. Succinylation, Maleination and Phthalation of Corn Starch on Extrusion.
43. López, O. V., Castillo, L. A., Ninago, M. D., Ciolino, A. E. & Villar, M. A. Modified Starches Used as Additives in Enhanced Oil Recovery (EOR). in *Industrial Applications of Renewable Biomass Products* 227–248 (Springer International Publishing, 2017). doi:10.1007/978-3-319-61288-1_9
44. Vanier, N. L. *et al.* Physicochemical, crystallinity, pasting and morphological properties of bean starch oxidised by different concentrations of sodium hypochlorite. *Food Chem.* **131**, 1255–1262 (2012).
45. Simsek, S., Ovando-Martínez, M., Whitney, K. & Bello-Pérez, L. A. Effect of acetylation, oxidation and annealing on physicochemical properties of bean starch. *Food Chem.* **134**, 1796–1803 (2012).
46. Huneault, M. A. & Li, H. Morphology and properties of compatibilized polylactide/thermoplastic starch blends. *Polymer (Guildf).* **48**, 270–280 (2007).
47. Singh, J., Kaur, L. & Singh, N. Effect of Acetylation on Some Properties of Corn and Potato Starches. *STARCH - ST*[illegible]*RKE* **56**, 586–601 (2004).
48. Fang, J. ., Fowler, P. ., Sayers, C. & Williams, P. . The chemical modification of a range of starches under aqueous reaction conditions. *Carbohydr. Polym.* **55**, 283–289 (2004).
49. Vanmarcke, A. *et al.* Influence of fatty chain length and starch composition on structure and properties of fully substituted fatty acid starch esters. *Carbohydr. Polym.* **164**, 249–

257 (2017).

50. Thiebaud, S. *et al.* Properties of fatty-acid esters of starch and their blends with LDPE. *J. Appl. Polym. Sci.* **65**, 705–721 (1997).
51. Aburto, J. *et al.* Synthesis, characterization, and biodegradability of fatty-acid esters of amylose and starch. *J. Appl. Polym. Sci.* **74**, 1440–1451 (1999).
52. Fang, J. ., Fowler, P. ., Tomkinson, J. & Hill, C. A. . The preparation and characterisation of a series of chemically modified potato starches. *Carbohydr. Polym.* **47**, 245–252 (2002).
53. Avval, M. E., Moghaddam, P. N. & Fareghi, A. R. Modification of starch by graft copolymerization: A drug delivery system tested for cephalexin antibiotic. *Starch - Stärke* **65**, 572–583 (2013).
54. Worzakowska, M. Chemical Modification of Potato Starch by Graft Copolymerization with Citronellyl Methacrylate. *J. Polym. Environ.* **26**, 1613–1624 (2018).
55. Zuo, Y. *et al.* Synthesis and characterization of maleic anhydride esterified corn starch by the dry method. *Int. J. Biol. Macromol.* **62**, 241–247 (2013).
56. Zhou, J., Zhang, J., Ma, Y. & Tong, J. Surface photo-crosslinking of corn starch sheets. *Carbohydr. Polym.* **74**, 405–410 (2008).
57. Malafaya, P. B., Stappers, F. & Reis, R. L. Starch-based microspheres produced by emulsion crosslinking with a potential media dependent responsive behavior to be used as drug delivery carriers. *J. Mater. Sci. Mater. Med.* **17**, 371–377 (2006).
58. Petzold, K., Einfeldt, L., Gü, W., Stein, A. & Klemm, D. Regioselective Functionalization of Starch: Synthesis and 1 H NMR Characterization of 6-O-Silyl Ethers |. doi:10.1021/bm010067u
59. Wei, B. *et al.* Synthesis, characterization and hydrophobicity of silylated starch nanocrystal. *Carbohydr. Polym.* **136**, 1203–1208 (2016).
60. Petzold, K., Koschella, A., Klemm, D. & Heublein, B. Silylation of Cellulose and Starch – Selectivity, Structure Analysis, and Subsequent Reactions. *Cellulose* **10**, 251–269 (2003).
61. Wang, S. & Copeland, L. Effect of Acid Hydrolysis on Starch Structure and Functionality: A Review. *Crit. Rev. Food Sci. Nutr.* **55**, 1081–1097 (2015).
62. Wang, W. J., Powell, A. D. & Oaks, C. G. Effect of annealing on the hydrolysis of sago

starch granules. *Carbohydr. Polym.* **33**, 195–202 (1997).

63. Elomaa, M. *et al.* Determination of the degree of substitution of acetylated starch by hydrolysis,1H NMR and TGA/IR. *Carbohydr. Polym.* **57**, 261–267 (2004).
64. Ashogbon, A. O. & Akintayo, E. T. Recent trend in the physical and chemical modification of starches from different botanical sources: A review. *Starch/Staerke* (2014). doi:10.1002/star.201300106
65. Ahmed, S. & Jones, F. R. A review of particulate reinforcement theories for polymer composites. *J. Mater. Sci.* **25**, 4933–4942 (1990).
66. Cantwell, W. & Morton, J. The impact resistance of composite materials—a review. *Composites* **22**, 347–362 (1991).
67. Thakur, V. K. & Kessler, M. R. Self-healing polymer nanocomposite materials: A review. *Polymer (Guildf).* **69**, 369–383 (2015).
68. Kim, J. R. & Netravali, A. N. Self-healing starch-based 'green' thermoset resin. *Polymer (Guildf).* **117**, 150–159 (2017).
69. Kim, J. R. & Netravali, A. N. Parametric study of protein-encapsulated microcapsule formation and effect on self-healing efficiency of 'green' soy protein resin. *J. Mater. Sci.* **52**, 3028–3047 (2017).
70. Kessler, M. ., Sottos, N. . & White, S. . Self-healing structural composite materials. *Compos. Part A Appl. Sci. Manuf.* **34**, 743–753 (2003).
71. White, S. R. *et al.* Autonomic healing of polymer composites. *Nature* **409**, 794–797 (2001).
72. Sanada, K., Yasuda, I. & Shindo, Y. Transverse tensile strength of unidirectional fibre-reinforced polymers and self-healing of interfacial debonding. *Plast. Rubber Compos.* **35**, 67–72 (2006).
73. Rule, J. D., Brown, E. N., Sottos, N. R., White, S. R. & Moore, J. S. Wax-Protected Catalyst Microspheres for Efficient Self-Healing Materials. *Adv. Mater.* **17**, 205–208 (2005).
74. Lyckfeldt, O. & Ferreira, J. M. F. Processing of porous ceramics by 'starch consolidation'. *J. Eur. Ceram. Soc.* **18**, 131–140 (1998).
75. Davis, J. B., Kristoffersson, A., Carlström, E. & Clegg, W. J. Fabrication and Crack

Deflection in Ceramic Laminates with Porous Interlayers. *J. Am. Ceram. Soc.* **83**, 2369–2374 (2004).

76. Alves, H. ., Tarì, G., Fonseca, A. . & Ferreira, J. M. . Processing of porous cordierite bodies by starch consolidation. *Mater. Res. Bull.* **33**, 1439–1448 (1998).
77. Živcová, Z. *et al.* Thermal conductivity of porous alumina ceramics prepared using starch as a pore-forming agent. *J. Eur. Ceram. Soc.* **29**, 347–353 (2009).
78. Kim, J.-G., Sim, J.-H. & Cho, W.-S. Preparation of porous (Ba,Sr)TiO 3 by adding corn-starch. *J. Phys. Chem. Solids* **63**, 2079–2084 (2002).
79. Lemos, A. . & Ferreira, J. M. . Porous bioactive calcium carbonate implants processed by starch consolidation. *Mater. Sci. Eng. C* **11**, 35–40 (2000).
80. Peng, H. X., Fan, Z. & Evans, J. R. G. Factors affecting the microstructure of a fine ceramic foam. *Ceram. Int.* **26**, 887–895 (2000).
81. Peng, H. X., Fan, Z., Evans, J. R. G. & Busfield, J. J. C. Microstructure of ceramic foams. *J. Eur. Ceram. Soc.* **20**, 807–813 (2000).
82. Fadli, A. & Sopyan, I. Preparation of porous alumina for biomedical applications through protein foaming–consolidation method. *Mater. Res. Innov.* **13**, 327–329 (2009).
83. Ribeiro, C., Bressiani, J. C. & Bressiani, A. H. de A. A study of the consolidation method with albumin to obtain porous beta-TCP ceramics. *Mater. Res.* **10**, 307–310 (2007).
84. Mansourighasri, A., Muhamad, N. & Sulong, A. B. Processing titanium foams using tapioca starch as a space holder. *J. Mater. Process. Technol.* **212**, 83–89 (2012).
85. Lemos, A. F. & Ferreira, J. M. F. Combining Foaming and Starch Consolidation Methods to Develop Macroporous Hydroxyapatite Implants. *Key Eng. Mater.* **254**–**256**, 1041–1044 (2003).
86. Aussawasathien, D., Teerawattananon, C. & Vongachariya, A. Separation of micron to sub-micron particles from water: Electrospun nylon-6 nanofibrous membranes as pre-filters. *J. Memb. Sci.* **315**, 11–19 (2008).
87. Jackson, E. A. & Hillmyer, M. A. Nanoporous Membranes Derived from Block Copolymers: From Drug Delivery to Water Filtration. *ACS Nano* **4**, 3548–3553 (2010).
88. Raveendran, P., Fu, J. & Wallen, S. L. Completely “Green” Synthesis and Stabilization of Metal Nanoparticles. *J. Am. Chem. Soc.* **125**, 13940–13941 (2003).

89. He, F. & Zhao, D. Preparation and Characterization of a New Class of Starch-Stabilized Bimetallic Nanoparticles for Degradation of Chlorinated Hydrocarbons in Water. *Environ. Sci. Technol.* **39**, 3314–3320 (2005).
90. Wang, C.-B. & Zhang, W. Synthesizing Nanoscale Iron Particles for Rapid and Complete Dechlorination of TCE and PCBs. *Environ. Sci. Technol.* **31**, 2154–2156 (1997).
91. Wing, R. E. Dissolved heavy-metal removal by Insoluble Starch Xanthate (ISX). *Environ. Prog.* **2**, 269–272 (1983).
92. Kim, B. S. & Lim, S.-T. Removal of heavy metal ions from water by cross-linked carboxymethyl corn starch. *Carbohydr. Polym.* **39**, 217–223 (1999).
93. Delval, F. *et al.* The sorption of several types of dye on crosslinked polysaccharides derivatives. *Dye. Pigment.* **53**, 79–92 (2002).
94. Desai, P. M., Liew, C. V. & Heng, P. W. S. Review of Disintegrants and the Disintegration Phenomena. *J. Pharm. Sci.* **105**, 2545–2555 (2016).
95. Hartesi, B., Sriwidodo, Abdassah, M. & Chaerunisaa, A. Y. Starch as Pharmaceutical Excipient. *Int. J. Pharm. Sci. Rev. Res.* **2**, 59–64 (2016).
96. Faure, A., York, P. & Rowe, R. C. Process control and scale-up of pharmaceutical wet granulation processes: a review. *Eur. J. Pharm. Biopharm.* **52**, 269–277 (2001).
97. Builders, P. F. & Arhewoh, M. I. Pharmaceutical applications of native starch in conventional drug delivery. *Starch - Stärke* **68**, 864–873 (2016).
98. Adedokun, M. O. & Itiola, O. A. Disintegrant activities of natural and pregelatinized trifoliate yams, rice and corn starches in paracetamol tablets. *J. Appl. Pharm. Sci.* **1**, 200–206 (2011).
99. Ingram, J. T. & Lowenthal, W. Mechanism of Action of Starch as a Tablet Disintegrant I. *J. Pharm. Sci.* **55**, 614–617 (1966).
100. Hu, A. *et al.* Ultrasonic frequency effect on corn starch and its cavitation. *LWT - Food Sci. Technol.* **60**, 941–947 (2015).
101. Odeku, O. A. & Akinwande, B. L. Effect of the mode of incorporation on the disintegrant properties of acid modified water and white yam starches. *Saudi Pharm. J.* **20**, 171–175 (2012).
102. Odeku, O. A. & Picker-Freyer, K. M. Freeze-dried pregelatinized Dioscorea starches as

tablet matrix for sustained release. *J. Excipients Food Chem.* **1**, 21–32 (2010).

103. Odeku, O. A. & Picker-Freyer, K. M. Characterization of acid modified Dioscorea starches as direct compression excipient. *Pharm. Dev. Technol.* **14**, 259–270 (2009).
104. ODEKU, O., SCHMID, W. & PICKERFREYER, K. Material and tablet properties of pregelatinized (thermally modified) Dioscorea starches. *Eur. J. Pharm. Biopharm.* **70**, 357–371 (2008).
105. Odeku, O. A. & Picker-Freyer, K. M. Evaluation of the material and tablet formation properties of modified forms of Dioscorea starches. *Drug Dev. Ind. Pharm.* **35**, 1389–1406 (2009).
106. Alexiou, C. *et al.* Targeting cancer cells: magnetic nanoparticles as drug carriers. *Eur. Biophys. J.* **35**, 446–450 (2006).
107. Kockisch, S., Rees, G. D., Tsibouklis, J. & Smart, J. D. Mucoadhesive, triclosan-loaded polymer microspheres for application to the oral cavity: preparation and controlled release characteristics. *Eur. J. Pharm. Biopharm.* **59**, 207–216 (2005).
108. Ahmad, M. Z. *et al.* In vitro and in vivo evaluation of Assam Bora rice starch-based bioadhesive microsphere as a drug carrier for colon targeting. *Expert Opin. Drug Deliv.* **9**, 141–149 (2012).
109. Zaki Ahmad, M. *et al.* Development of Polysaccharide based Colon Targeted Drug Delivery System: Design and Evaluation of Assam Bora rice Starch based Matrix Tablet. *Curr. Drug Deliv.* **8**, 575–581 (2011).
110. Ju, B., Yan, D. & Zhang, S. Micelles self-assembled from thermoresponsive 2-hydroxy-3-butoxypropyl starches for drug delivery. *Carbohydr. Polym.* **87**, 1404–1409 (2012).
111. Rapoport, N. Physical stimuli-responsive polymeric micelles for anti-cancer drug delivery. *Prog. Polym. Sci.* **32**, 962–990 (2007).
112. Balmayor, E. R., Tuzlakoglu, K., Azevedo, H. S. & Reis, R. L. Preparation and characterization of starch-poly-ε-caprolactone microparticles incorporating bioactive agents for drug delivery and tissue engineering applications. *Acta Biomater.* **5**, 1035–1045 (2009).
113. Liu, C.-S., Desai, K. G. H., Meng, X.-H. & Chen, X.-G. Sweet Potato Starch Microparticles as Controlled Drug Release Carriers: Preparation and In Vitro Drug

Release. *Dry. Technol.* **25**, 689–693 (2007).

114. Szepes, A. *et al.* Characterization and drug delivery behaviour of starch-based hydrogels prepared via isostatic ultrahigh pressure. *Carbohydr. Polym.* **72**, 571–578 (2008).
115. Jaiturong, P. *et al.* Preparation of glutinous rice starch/polyvinyl alcohol copolymer electrospun fibers for using as a drug delivery carrier. *Asian J. Pharm. Sci.* **13**, 239–247 (2018).
116. Jain, A. K., Khar, R. K., Ahmed, F. J. & Diwan, P. V. Effective insulin delivery using starch nanoparticles as a potential trans-nasal mucoadhesive carrier. *Eur. J. Pharm. Biopharm.* **69**, 426–435 (2008).
117. Assefa, Z. & Admassu, S. Development and Characterization of Antimicrobial Packaging Films. (2013). doi:10.4172/2157
118. Ziaee, Z., Qian, L., Guan, Y., Fatehi, P. & Xiao, H. Antimicrobial/Antimold Polymer-Grafted Starches for Recycled Cellulose Fibers. *J. Biomater. Sci. Polym. Ed.* **21**, 1359–1370 (2010).
119. Guan, Y., Qian, L., Xiao, H. & Zheng, A. Preparation of novel antimicrobial-modified starch and its adsorption on cellulose fibers: Part I. Optimization of synthetic conditions and antimicrobial activities. *Cellulose* **15**, 609–618 (2008).
120. Liu, K., Lin, X., Chen, L. & Huang, L. Preparation of guanidine-modified starch for antimicrobial paper. *J. Bioresour. Bioprod.* **1**, 3–6 (2016).
121. Qian, L. Y., Guan, Y. & Xiao, H. N. Preparation of Guanidine Derivative Polymers as Novel Functional Additives for Value-Added Hygiene Paper. *Adv. Mater. Res.* **236**–**238**, 2993–2996 (2011).
122. Pelissari, F. M., Grossmann, M. V. E., Yamashita, F., Alfonso, E. & Pineda, G. Antimicrobial, Mechanical, and Barrier Properties of Cassava Starch-Chitosan Films Incorporated with Oregano Essential Oil. *J. Agric. Food Chem* **57**, 7499 (2009).
123. Shen, X. L., Wu, J. M., Chen, Y. & Zhao, G. Antimicrobial and physical properties of sweet potato starch films incorporated with potassium sorbate or chitosan. *Food Hydrocoll.* **24**, 285–290 (2010).
124. Vásconez, M. B., Flores, S. K., Campos, C. A., Alvarado, J. & Gerschenson, L. N. Antimicrobial activity and physical properties of chitosan–tapioca starch based edible

films and coatings. *Food Res. Int.* **42**, 762–769 (2009).

125. Salleh, E. *et al.* Starch-based Antimicrobial Films Incorporated with Lauric Acid and Chitosan. in *International Conference on Advancement of Materials and Nanotechnology: (ICAMN-2007). AIP Conference Proceedings, Volume 1217. AIP Conference Proceedings, Volume 1217, Issue 1, p.432-436* **1217**, 432–436 (2010).
126. Chen, G. *et al.* Durable superhydrophobic paper enabled by surface sizing of starch-based composite films. *Appl. Surf. Sci.* **409**, 45–51 (2017).
127. Cyprych, K., Sznitko, L. & Mysliwiec, J. Starch: Application of biopolymer in random lasing. *Org. Electron. physics, Mater. Appl.* **15**, 2218–2222 (2014).
128. Sun, B., Xie, G., Jiang, Y. & Li, X. Comparative CO2-Sensing Characteristic Studies of PEI and PEI/Starch Thin Film Sensors. *Energy Procedia* **12**, 726–732 (2011).
129. Zhu, Y., Romain, C. & Williams, C. K. Sustainable polymers from renewable resources. *Nature* **540**, 354–362 (2016).
130. Geyer, R., Jambeck, J. R. & Law, K. L. Production, use, and fate of all plastics ever made. *Sci. Adv.* **3**, e1700782 (2017).
131. Muneer, F. *et al.* Nanostructural Morphology of Plasticized Wheat Gluten and Modified Potato Starch Composites: Relationship to Mechanical and Barrier Properties. *Biomacromolecules* **16**, 695–705 (2015).
132. Mekonnen, T., Mussone, P., Khalil, H. & Bressler, D. Progress in bio-based plastics and plasticizing modifications. *J. Mater. Chem. A* **1**, 13379–13398 (2013).
133. Le Corre, D., Bras, J. & Dufresne, A. Starch Nanoparticles: A Review. *Biomacromolecules* **11**, 1139–1153 (2010).
134. Ma, X., Jian, R., Chang, P. R. & Yu, J. Fabrication and Characterization of Citric Acid-Modified Starch Nanoparticles/Plasticized-Starch Composites. *Biomacromolecules* **9**, 3314–3320 (2008).
135. Gandini, A., Lacerda, T. M., Carvalho, A. J. F. & Trovatti, E. Progress of Polymers from Renewable Resources: Furans, Vegetable Oils, and Polysaccharides. *Chem. Rev.* **116**, 1637–1669 (2016).
136. Viguié, J., Molina-Boisseau, S. & Dufresne, A. Processing and Characterization of Waxy Maize Starch Films Plasticized by Sorbitol and Reinforced with Starch Nanocrystals.

Macromol. Biosci. **7**, 1206–1216 (2007).

137. Peelman, N. *et al.* Application of bioplastics for food packaging. *Trends Food Sci. Technol.* **32**, 128–141 (2013).
138. Willett, J. L. & Finkenstadt, V. L. Comparison of Cationic and Unmodified Starches in Reactive Extrusion of Starch–Polyacrylamide Graft Copolymers. *J. Polym. Environ.* **17**, 248–253 (2009).
139. Averous, L., Moro, L., Dole, P. & Fringant, C. Properties of thermoplastic blends: starch–polycaprolactone.
140. Namazi, H., Fathi, F. & Dadkhah, A. Hydrophobically modified starch using long-chain fatty acids for preparation of nanosized starch particles. *Sci. Iran.* **18**, 439–445 (2011).
141. Fringant, C., Rinaudo, M., Foray, M. F. & Bardet, M. Preparation of mixed esters of starch or use of an external plasticizer: two different ways to change the properties of starch acetate films. *Carbohydr. Polym.* **35**, 97–106 (1998).
142. Mark, A. M. & Mehltretter, C. L. Facile Preparation of Starch Triacetates.
143. Sagar, A. D. & Merrill, E. W. Properties of fatty-acid esters of starch. *J. Appl. Polym. Sci.* **58**, 1647–1656 (1995).
144. Thitisomboon, W., Opaprakasit, P., Jaikaew, N. & Boonyarattanakalin, S. Characterizations of modified cassava starch with long chain fatty acid chlorides obtained from esterification under low reaction temperature and its PLA blending. *J. Macromol. Sci. Part A* **55**, 253–259 (2018).
145. Vaca-Garcia, C., Borredon, M. E. & Gaseta, A. Determination of the degree of substitution (DS) of mixed cellulose esters by elemental analysis.(Author abstract). *Cellulose* **8**, 225–231 (2001).
146. Mormann, W. & Al-Higari, M. Acylation of Starch with Vinyl Acetate in Water. *Starch - Stärke* **56**, 118–121 (2004).
147. R., S. A. Pyridine. *Encyclopedia of Reagents for Organic Synthesis* (2001). doi:doi:10.1002/047084289X.rp280
148. Koivu, K. A. Y., Sadeghifar, H., Nousiainen, P. A., Argyropoulos, D. S. & Sipilä, J. Effect of Fatty Acid Esterification on the Thermal Properties of Softwood Kraft Lignin. *ACS Sustain. Chem. Eng.* **4**, 5238–5247 (2016).

149. MATHEW, S. & ABRAHAM, T. Physico-chemical characterization of starch ferulates of different degrees of substitution. *Food Chem.* **105**, 579–589 (2007).
150. Dias, F., De Souza, R. & Lucas, E. Starch fatty esters for potential use in petroleum industry. *Chem. Chem. Technol.* **7**, 451–456 (2013).
151. KONDO, T. The assignment of IR absorption bands due to free hydroxyl groups in cellulose. *Cellulose* **4**, 281 (1997).
152. Hong, L.-F., Cheng, L.-H., Lee, C. Y. & Peh, K. K. Characterisation of Physicochemical Properties of Propionylated Corn Starch and Its Application as Stabiliser. *Food Technol. Biotechnol.* **53**, 278–285 (2015).
153. Kong, W., Fu, X., Yuan, Y., Liu, Z. & Lei, J. Preparation and thermal properties of crosslinked polyurethane/lauric acid composites as novel form stable phase change materials with a low degree of supercooling. *RSC Adv.* **7**, 29554–29562 (2017).
154. Simkovic, I. & Jakab, E. Thermogravimetry/mass spectrometry study of weakly basic starch-based ion exchanger. *Carbohydr. Polym.* **45**, 53–59 (2001).
155. Liu, X. *et al.* Thermal degradation and stability of starch under different processing conditions. *Starch - Stärke* **65**, 48–60 (2013).
156. Winkler, H., Vorwerg, W. & Rihm, R. Thermal and mechanical properties of fatty acid starch esters. *Carbohydr. Polym.* **102**, 941–949 (2014).
157. Rudnik, E., Matuschek, G., Milanov, N. & Kettrup, A. Thermal stability and degradation of starch derivatives. in *Journal of Thermal Analysis and Calorimetry* **85**, 267–270 (2006).
158. Wang, Z., Sun, J., Xie, S., Ma, G. & Jia, Y. Thermal Properties and Reliability of a Lauric Acid/Nonanoic Acid Binary Mixture as a Phase-Change Material for Thermal Energy Storage. *Energy Technol.* **5**, 2309–2316 (2017).
159. Mekonnen, T. & M. Fermented Soymeals and Their Reactive Blends with Poly(butylene adipate- co- terephthalate) in Engineering Biodegradable Cast Films for Sustainable Packaging. *Acs Sustain. Chem. Eng.* **4**, 782–793 (2016).
160. Sun, Q., Mekonnen, T., Misra, M. & Mohanty, A. Novel Biodegradable Cast Film from Carbon Dioxide Based Copolymer and Poly(Lactic Acid). *J. Polym. Environ.* **24**, 23–36 (2016).

161. Jane, J. Starch Properties, Modifications, and Applications. *J. Macromol. Sci. Part A* **32**, 751–757 (1995).
162. Menard, K. P. & Menard, N. R. Dynamic Mechanical Analysis in the Analysis of Polymers and Rubbers. in *Encyclopedia of Polymer Science and Technology* 1–33 (John Wiley & Sons, Inc, 2015).
163. Hill, D. J. T., Perera, M. C. S., Pomery, P. J. & Toh, H. K. Dynamic mechanical properties of networks prepared from siloxane modified divinyl benzene pre-polymers. *Polymer (Guildf).* **41**, 9131–9137 (2000).
164. Park, J., Eslick, J., Ye, Q., Misra, A. & Spencer, P. The influence of chemical structure on the properties in methacrylate-based dentin adhesives. *Dent. Mater.* **27**, 1086–1093 (2011).
165. Reilman, E., Hagting, J. G., Flipsen, T., Ulmer, H. & Van Dijl, J. M. Towards an antimicrobial 'microglove'. *Sci. Rep.* **5**, 1–11 (2015).
166. Aumsuwan, N., Heinhorst, S. & Urban, M. Antibacterial Surfaces on Expanded Polytetrafluoroethylene; Penicillin Attachment. *Biomacromolecules* **8**, 713–718 (2007).
167. Cutter, C. N., Willett, J. L. & Siragusa, G. R. Improved antimicrobial activity of nisin-incorporated polymer films by formulation change and addition of food grade chelator. *Lett. Appl. Microbiol.* **33**, 325–328 (2001).
168. Mauriello, G., De Luca, E., La Storia, A., Villani, F. & Ercolini, D. Antimicrobial activity of a nisin-activated plastic film for food packaging. *Lett. Appl. Microbiol.* **41**, 464–469 (2005).
169. Otero, V. *et al.* Evaluation of two antimicrobial packaging films against Escherichia coli O157:H7 strains in vitro and during storage of a Spanish ripened sheep cheese (Zamorano). *Food Control* **42**, 296–302 (2014).
170. Sung, S.-Y. *et al.* Antimicrobial agents for food packaging applications. *Trends Food Sci. Technol.* **33**, 110–123 (2013).
171. Ahvenainen, R. *Novel food packaging techniques*. (CRC Press, 2003).
172. Sun, D., Babar Shahzad, M., Li, M., Wang, G. & Xu, D. Antimicrobial materials with medical applications. *Mater. Technol.* **30**, B90–B95 (2015).
173. Ventola, C. L. The antibiotic resistance crisis: part 1: causes and threats. *P T* **40**, 277–83

(2015).

174. Li, Z., Lee, D., Sheng, X., Cohen, R. E. & Rubner, M. F. Two-Level Antibacterial Coating with Both Release-Killing and Contact-Killing Capabilities. *J. Polym. Sci., Part A Polym. Chem* **9**, 1467–1472 (2002).

175. Ferreira, L. & Zumbuehl, A. Non-leaching surfaces capable of killing microorganisms on contact. *J. Mater. Chem.* **19**, 7796 (2009).

176. Zhou, Z., Zheng, A. & Zhong, J. Interactions of biocidal guanidine hydrochloride polymer analogs with model membranes: a comparative biophysical study. *Acta Biochim. Biophys. Sin. (Shanghai).* **43**, 729–737 (2011).

177. Zhou, Z., Wei, D., Guan, Y., Zheng, A. & Zhong, J.-J. Extensive in vitro activity of guanidine hydrochloride polymer analogs against antibiotics-resistant clinically isolated strains. *Mater. Sci. Eng. C* **31**, 1836–1843 (2011).

178. de Paula, G. F., Netto, G. I. & Mattoso, L. H. C. Physical and chemical characterization of poly(hexamethylene biguanide) hydrochloride. *Polymers (Basel).* **3**, 928–941 (2011).

179. Zhang, C. *et al.* Poly(hexamethylene guanidine)-based hydrogels with long lasting antimicrobial activity and low toxicity. *J. Polym. Sci. Part A Polym. Chem.* **55**, 2027–2035 (2017).

180. Ogunsona, E., Ojogbo, E. & Mekonnen, T. Advanced material applications of starch and its derivatives. *Eur. Polym. J.* **108**, 570–581 (2018).

181. Ojogbo, E., Blanchard, R. & Mekonnen, T. Hydrophobic and Melt Processable Starch-Laurate Esters: Synthesis, Structure-Property Correlations. *J. Polym. Sci. Part A Polym. Chem.* (2018). doi:10.1002/pola.29237

182. Pedrosa, M. T. & Clerici, S. Physical and/or Chemical Modifications of Starch by Thermoplastic Extrusion.

183. Demirgöz, D. *et al.* Chemical modification of starch based biodegradable polymeric blends: effects on water uptake, degradation behaviour and mechanical properties. *Polym. Degrad. Stab.* **70**, 161–170 (2000).

184. Zhang, Y., Jiang, J. & Chen, Y. Synthesis and antimicrobial activity of polymeric guanidine and biguanidine salts. *Polymer (Guildf).* **40**, 6189–6198 (1999).

185. Westbrook, A. W., Moo-Young, M. & Chou, C. P. Development of a CRISPR-Cas9 Tool

Kit for Comprehensive Engineering of Bacillus subtilis. (2016). doi:10.1128/AEM.01159-16

186. Wei, D. *et al.* Non-leaching antimicrobial biodegradable PBAT films through a facile and novel approach. *Mater. Sci. Eng. C* **58**, 986–991 (2016).
187. Girouard, N. M., Xu, S., Schueneman, G. T., Shofner, M. L. & Meredith, J. C. Site-Selective Modification of Cellulose Nanocrystals with Isophorone Diisocyanate and Formation of Polyurethane-CNC Composites. *ACS Appl. Mater. Interfaces* **8**, 1458–1467 (2016).
188. Lu, Q.-W., Hoye, T. R. & Macosko, C. W. Reactivity of Common Functional Groups with Urethanes: Models for Reactive Compatibilization of Thermoplastic Polyurethane Blends. (2002). doi:10.1002/pola.10310
189. Sonnenschein, M. F. Introduction to Polyurethane Chemistry. in *Polyurethanes* 105–126 (John Wiley & Sons, Inc, 2014). doi:10.1002/9781118901274.ch3
190. Mekonnen, T. H., Mussone, P. G., Choi, P. & Bressler, D. C. Adhesives from Waste Protein Biomass for Oriented Strand Board Composites: Development and Performance. *Macromol. Mater. Eng.* **299**, 1003–1012 (2014).
191. Ozaki, S. & S. Recent Advances in Isocyanate Chemistry. *Chem. Rev.* **72**, 457–496 (1972).
192. J. H. Sung, †, D. P. Park, †, B. J. Park, †, H. J. Choi, *,† and & Jhon‡, M. S. Phosphorylation of Potato Starch and Its Electrorheological Suspension. (2005). doi:10.1021/BM050146W
193. Wen, Y., Ye, F., Zhu, J. & Zhao, G. Corn starch ferulates with antioxidant properties prepared by N,N′-carbonyldiimidazole-mediated grafting procedure. *Food Chem.* **208**, 1–9 (2016).
194. Liu, J. *et al.* Synthesis, characterization, and antioxidant activity of caffeic-acid-grafted corn starch. *Starch - Stärke* **70**, 1700141 (2018).
195. Sun, X. *et al.* Guanidine-based polymeric microspheres with a nonleaching, antibacterial performance. *J. Appl. Polym. Sci.* **134**, 44821 (2017).
196. Wei, D. *et al.* Structural characterization and antibacterial activity of oligoguanidine (polyhexamethylene guanidine hydrochloride). *Mater. Sci. Eng. C* **29**, 1776–1780 (2009).

197. Mano, J. F., Koniarova, D. & Reis, R. L. *Thermal properties of thermoplastic starch/ synthetic polymer blends with potential biomedical applicability*.
198. Trinh, B. & Mekonnen, T. Hydrophobic Esterification of Cellulose Nanocrystals for Epoxy Reinforcement. *Polymer (Guildf).* (2018). doi:10.1016/j.polymer.2018.08.076
199. Gilbert, P. & Moore, L. E. Cationic antiseptics: diversity of action under a common epithet. *J. Appl. Microbiol.* **99**, 703–715 (2005).
200. Qian, L., Xiao, H., Zhao, G. & He, B. Synthesis of Modified Guanidine-Based Polymers and their Antimicrobial Activities Revealed by AFM and CLSM. *ACS Appl. Mater. Interfaces* **3**, 1895–1901 (2011).
201. Hall, K., Mozsolits, H. & Aguilar, M.-I. *Surface plasmon resonance analysis of antimicrobial peptide-membrane interactions: affinity & mechanism of action*.
202. Zhou, Z. X., Wei, D. F., Guan, Y., Zheng, A. N. & Zhong, J. J. Damage of *Escherichia coli* membrane by bactericidal agent polyhexamethylene guanidine hydrochloride: micrographic evidences. *J. Appl. Microbiol.* **108**, 898–907 (2010).
203. Soares, N. F. F. & Hotchkiss, J. H. Bitterness reduction in grapefruit juice through active packaging. *Packag. Technol. Sci.* **11**, 9–18 (1998).
204. Hazan, R., Que, Y.-A., Maura, D. & Rahme, L. G. A method for high throughput determination of viable bacteria cell counts in 96-well plates. *BMC Microbiol.* **12**, 259 (2012).